Machine Detector Interface MDI

John T. Seeman
SLAC National Accelerator Laboratory

September 8, 2026

4th Annual Higgs Factory-Future Circular Collider Workshop at SLAC

U.S. DEPARTMENT OF ENERGY
Office of Science

SLAC NATIONAL ACCELERATOR LABORATORY

Machine Detector Interface (MDI) Tutorial

John Seeman (SLAC)

September 8, 2026

The Interaction Region IR in a high-current high-luminosity e^+e^- collider is compact and complex, combining many of the most difficult aspects of the accelerator and detector. MDI helps coordinate plans for the highly interconnected interface between detector and accelerator to facilitate that both are successful even at the highest luminosities, often at several center-of-mass energies, for example from the Z pole to the t-tbar threshold. The accelerator and detector layouts integrate accelerator components such as lightweight and actively cooled beampipes, superconducting IR-magnets, bellows, and remote vacuum connections with detector components of inner detectors, vertex chamber, diagnostics, luminosity detectors, and utilities (cables, cooling, power, supports). This tutorial will cover more than thirty interface topics (from SC magnets, shielding solenoids, vacuum chamber masks, and inner detector elements to IR beam physics, beam loss sources, various beam backgrounds, and irradiation protection shielding). Examples from past and present colliders (KEKB, PEP-II, SuperKEKB) and future colliders under design (FCCee, ILC) will be used. Attendee interactions are encouraged.

MDI inputs from these people and others.

Manuela Boscolo*[1], Fabrizio Palla*[2], Gherardo Ammirabile[2], Kevin D. J. Andre[3], Giorgio Baldinelli[4], Patricia Borges de Sousa[3], Filippo Bosi[2], Giacomo Broggi[1,3,5], Roderik Bruce[3], Helmut Burkhardt[3,6], Marco Calviani[3], Silvio Candido[3], Andrea Ciarma[1], Mogens Dam[7], Brieuc Francois[3], Rui Franqueira Ximenes[3], Francesco Fransesini[1], Alessandro Frasca[3,8], Andrea Gaddi[3], Armin Ilg[9], Robert Kieffer[3], Michael Koratzinos[10], Stefano Lauciani[1], Anton Lechner[3], Giuseppe Lerner[3], Giulia Nigrelli[1,3,5], Alexander Novokhatski[11], Katsunobu Oide[12], Antonio Perillo-Marcone[3], Brett Parker[13], Pantaleo Raimondi[14], John T. Seeman[11], Cristiano Turrioni[4], Leonard Watrelot[3], Frank Zimmermann[3].

[1] INFN, Laboratori Nazionali di Frascati, Italy
[2] INFN, Sezione di Pisa, Italy
[3] CERN, Switzerland
[4] INFN, Sezione di Perugia, Italy
[5] University of Rome "Sapienza", Italy
[6] University of Freiburg, Germany
[7] Niels Bohr Institute, Denmark
[8] University of Liverpool, UK
[9] University of Zurich, Switzerland
[10] Paul Scherrer Institute, Switzerland
[11] SLAC, USA
[12] University of Geneva, Switzerland
[13] Brookhaven National Laboratory, USA
[14] Fermilab National Laboratory, USA

*Corresponding authors: Manuela.Boscolo@cern.ch and Fabrizio.Palla@cern.ch

BNL:	B. Parker, V. Teotia,
FNAL:	P. Raimondi
CERN:	P. Borges de Sousa. A. Foussat, F. Zimmermann
KEK:	N. Ohuchi, Y. Funakoshi
SLAC:	S. DeBarger, A. Novokhatski, M. Sullivan
UniGen:	M. Koratzinos, K. Oide

T. Raubenheimer, S. Gessner, T. Montagne, C. Niebuhr, K. Suguitan, G. Kerr, L. Pollastrini

MDI Tutorial Topics

SLAC

1) General overview and IR layouts for various colliders
2) Main IR parameters
3) IR Comparison of various colliders
4) IP beta function versus L*
5) Detector requirements
6) Detector sub-components
7) IR accelerator requirements
8) Accelerator sub-components
9) Detector-Accelerator Interferences
- Main collider goal
- MDI compromises
- Detector end cap withdrawal
10) Luminosity measurement
- Lumi-Cal at 1.076 m

-11) Vacuum Chambers
- IR chamber design +/-0.5 m
- Y chamber 0.5-2 m
- Y chamber HOM issues and reduction
- Lumi-Cal at 1.8 m
- Remote flanges (e.g. CESR, SuperKEKB, SMA)
12) Magnet cryostat 2.4 to 7 m
- Cryostat cryogen feed
- lines and splice box
- Q1 magnet in 3 pieces
- Q2 magnet in 2 pieces
- Compensating and screening solenoids
- Correction magnet coils
13) Component assembly
14) Installation
15) Vibration control
16) Polarization
17) Background sources
- Beam background types
- Beam gas, Touschek, synchrotron radiation, non-Gaussian tails, luminosity,

FCCee Rings and IR beam lines

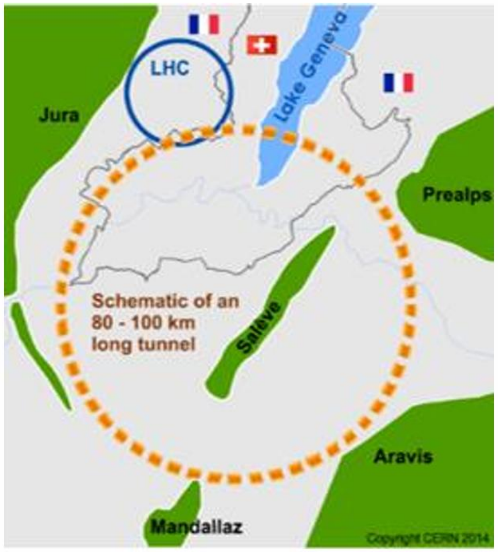

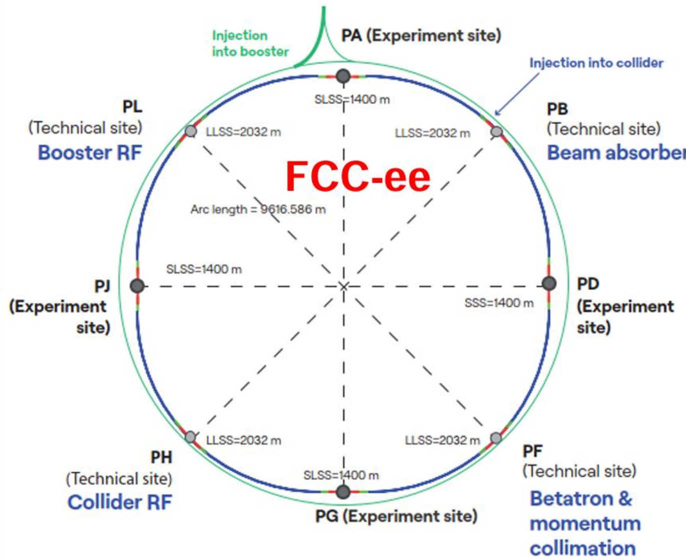

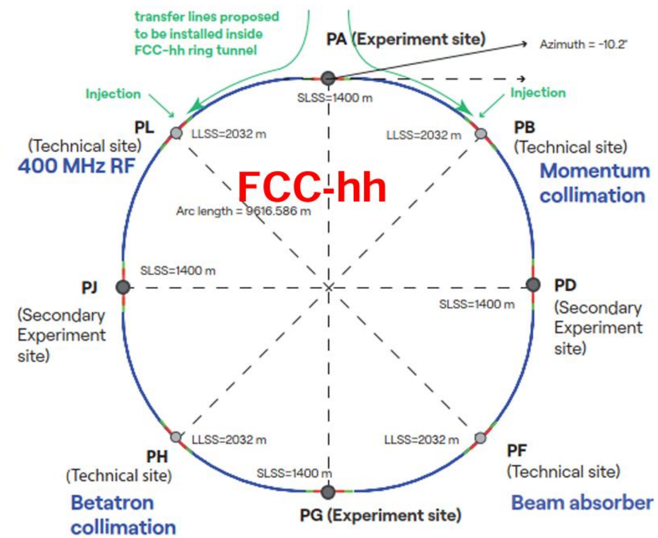

2020 - 2045 | 2048 - 2062 | ~2075 ?

Main Parameters for FCC at Jan 26 Lattice Review: LCC chosen.

Optics	GHC		LCC	
Mode	**Z**	**$t\bar{t}$**	**Z**	**$t\bar{t}$**
Beam energy E (GeV)	45.6	182.5	45.6	182.5
Circumference C (m)	90658.525		90644.816	
Arc-cell setup	90°/90° long	90°/90° short	52°/45°	99°/77°
Momentum compaction factor α_c (10^{-6})	28.5	7.3	28.6	9.5
Energy Loss per turn W_0 (GeV)	0.039	10.01	0.035	9.01
Beam Intensity N (10^{12} particles)	2400	9.405	2424	9.435
Bunch Intensity N_b (10^{11} particles)	2.02	1.85	2.02	2.20
Number of Bunches	12000	51	12000	43
Horizontal β-function at IP β_x^* (cm)	9	90	9	90
Vertical β-function at IP β_y^* (mm)	0.7	14	0.7	14
Horizontal emittance ε_x (nm)	0.74	1.74	0.70	2.10
Target vertical emittance in collision ε_y (pm)	1.48	1.75	1.40	2.11
Transverse tune Q_x/Q_y	214.16 / 214.20	394.19 / 390.27	194.16 / 170.20	346.19 / 262.27
Chromaticity Q_x'/Q_y'	12 / 5	0 / 0	12 / 5	0 / 0
Harmonic number h at 400 MHz	121200		121200	
Total RF voltage of 400 / 800 MHz (GV)	0.09	2.1 / 8.9	0.09	2.0 / 8.1
Synchrotron tune Q_s	0.031	0.086	0.031	0.111
RF momentum acceptance (%)	1	2	1	2
Bunch length σ_z (non coll./coll.) (mm)	5.4 / 16.3	1.9 / 2.7	5.1 / 16.7	1.9 / 2.8
Rel. mom. spread σ_p (non coll./coll.) (10^{-3})	0.40 / 1.29	1.58 / 2.21	0.39 / 1.34	1.52 / 2.33
Longitudinal damping time τ_z (turns)	1159	18	1297	20
Crab-waist ratio (%)	55	40	55	40
Beam-beam parameter ξ_x/ξ_y (10^{-3})	1.5 / 80	61.2 / 108.9	1.4 / 80	67.1 / 120
Luminosity $\mathscr{L}$ ($10^{34}\,s^{-1}/cm^2$)	151	1.54	150	1.45

Table 2.1: Parameter table for the GHC and LCC lattices at Z and $t\bar{t}$ mode.

General Detector-Collider Overviews (M. Boscolo)

FCC 6/6/2023 FCC WEEK 23 MDI OVERVIEW Manuela Boscolo INFN LNF

Interaction Region in two detectors

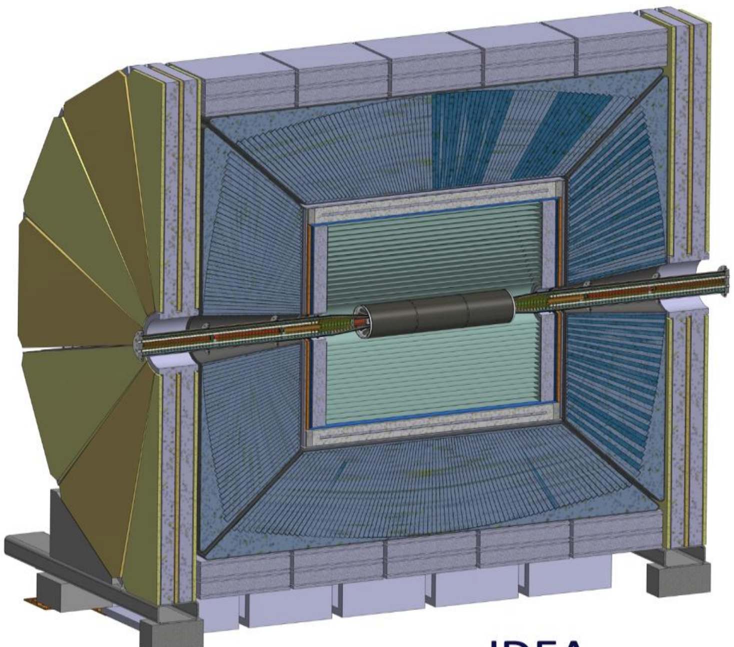

IDEA

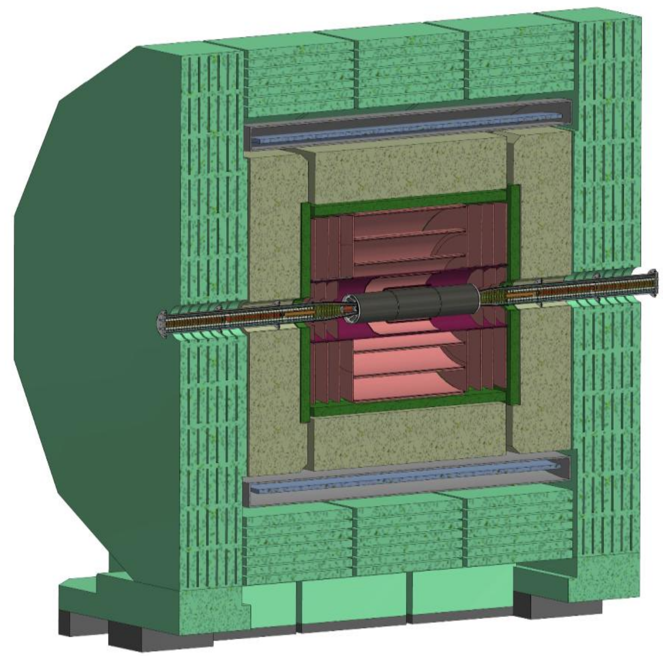

CLD

New: ALFA + two more!

FCC Detector Concepts (IR accelerator inside detector)

Integrated Physics

Integrated physics is (simplified)

$$Physics \sim \int L dt = L_{peak} \, X \, Run \, Time$$

Practical Integrated Physics

SLAC

Integrated Physics is

$Physics \sim L_{average}$ x Accel Colliding time x Det collection % x Det-fiducial-volume x (~Beam lifetime)

$L_{average} = L_{peak}$ x $(1-L_{decay})$-beam real-time lattice/coupling variations

Accel colliding time = colliding time – running down times - maintenance stops
(Maintenance time: PEP-II = 1 month/yr, CERN =3 months/yr (YETS)

Detector collection= (1 - recording deadtime) (1-injection deadtime)

Detector fiducial volume = ~0.99
To go to 0.995 → need to squeeze final quads out (L* x 2 distance) and will, thus, lower peak Lumi by ~1/2. Caution: a push for +5% could lose -50% in physics.

Beam lifetime ~ 10 min. Injection detector time veto is a few msec per injection.

SuperKEKB and Belle-II

Belle II @ SuperKEKB

- Luminosity frontier experiment to search for Physics beyond the Standard Model
    - e^+e^- asymmetric collision at the $\Upsilon(4S)$
    - High current / nano-beams, challenging background conditions
- Luminosity targets to achieve physics goals:
    - $\mathscr{L} = 6 \times 10^{35}\ \mathrm{cm}^{-2}\ \mathrm{s}^{-1}, \int \mathscr{L} dt = 50/\mathrm{ab}$

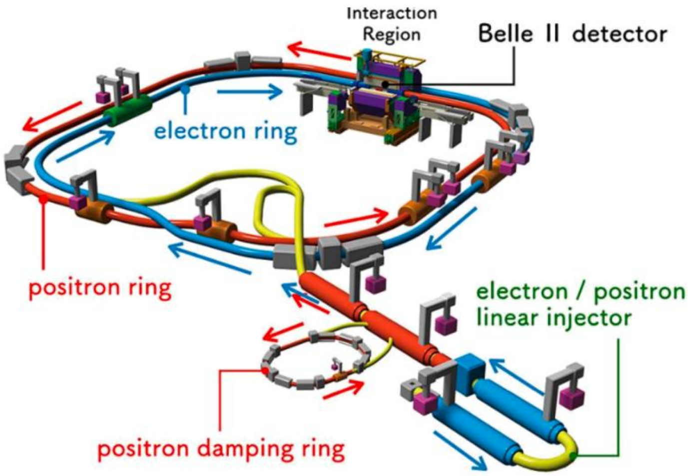

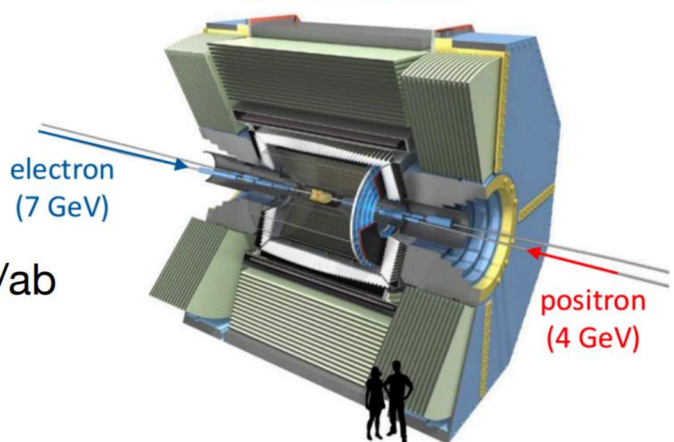

A new record of peak luminosity of 5.32x10^34 was achieved (Belle II HV off) and the integrated luminosity reached 914 /fb .

Example: SuperKEKB Operations (June 8, 2026) (courtesy KEK)

Top-up injection for both beams.

Lifetimes =
HER ~ 39 min
LER ~ 20 min
Luminosity lifetime ~13 min

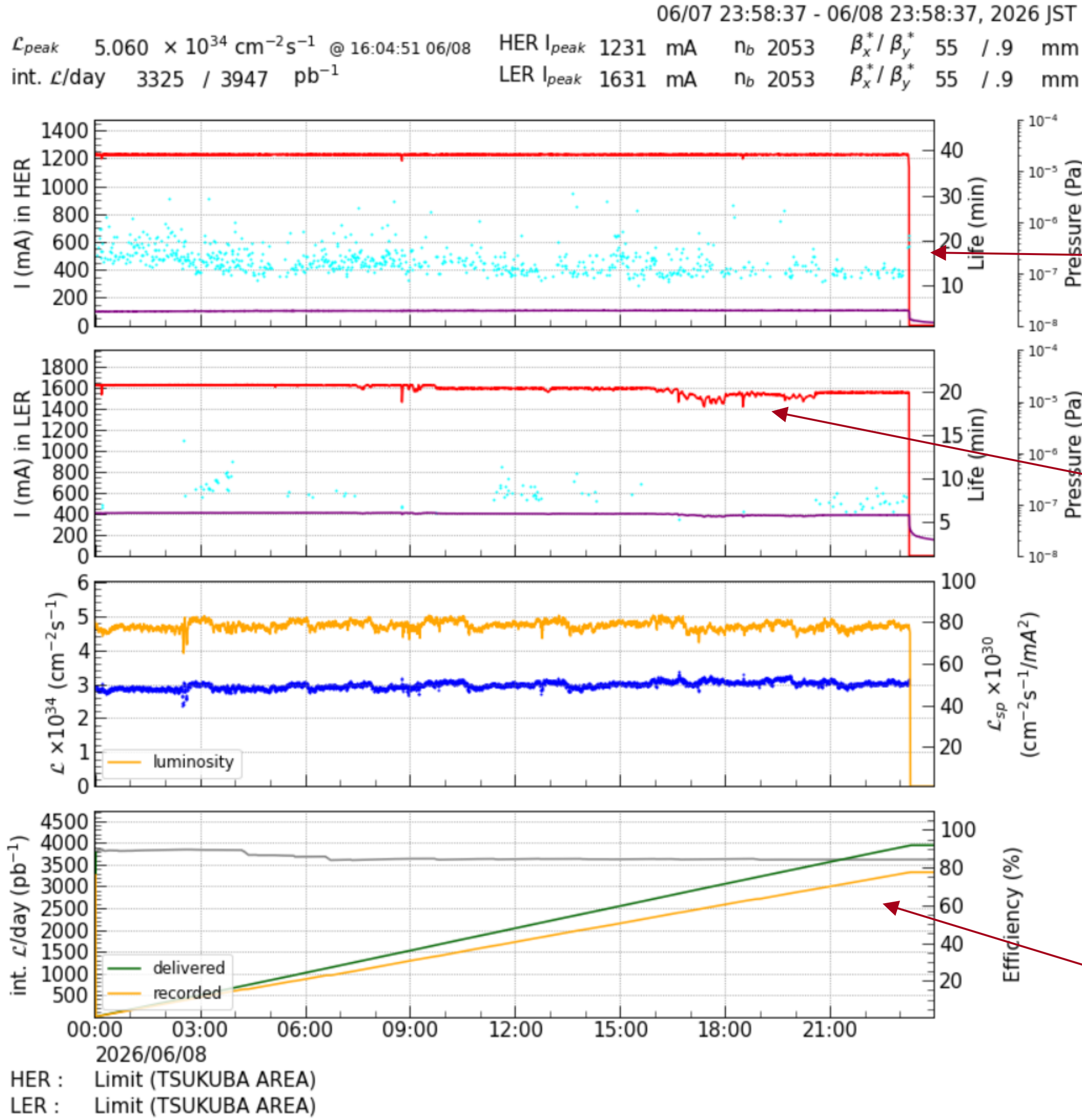

HER one beam trip

LER unstable current + one beam trip

Belle-II data collection is about 80%

SuperKEKB Parameters

SLAC

Machine Parameters

	December 27, 2024		Target at post-LS1 (1)		Target at post-LS1 (2)		Unit
Ring	LER	HER	LER	HER	LER	HER	
Emittance	4.0	4.6	4.0	4.6	4.0	4.6	nm
Beam Current	1632	1259	2080	1480	2750	2200	mA
Number of bunches	2346		2346		2346		
Bunch current	0.696	0.537	0.89	0.63	1.17	0.94	mA
Horizontal size σ_x*	15.5	16.6	17.9	16.6	17.9	16.6	μm
Vertical cap sigma Σ_y*	0.375		0.217		0.178		μm
Vertical size σ_y*	0.265		0.154		0.126		μm
Betatron tunes ν_x / ν_y	44.525 / 46.589	45.531 / 43.599	44.525 / 46.589	45.532 / 43.573	44.525 / 46.589	45.532 / 43.573	
β_x* / β_y*	**60 / 1.0**	60 / **1.0**	80 / **0.8**	60 / **0.8**	80 / **0.6**	60 / **0.6**	mm
σ_z	4.6 (6.0*)	5.1 (6.1*)	4.6 (6.5*)	5.1 (6.4*)	4.6 (6.5*)	5.1 (6.4*)	mm
Piwinski angle	**12.3**	**12.7**	10.7	12.7	10.7	12.7	
Crab waist ratio	80	60	80	80	80	80	%
Beam-Beam ξ_y	0.036	0.027	0.0444	0.0356	0.0604	0.0431	
Specific luminosity	5.8×10^{31}		7.62×10^{31}		9.31×10^{31}		$cm^{-2}s^{-1}/mA^2$
Luminosity	**5.1×10^{34}**		1×10^{35}		2.4×10^{35}		$cm^{-2}s^{-1}$

* Bunch lengthening is considered by using streak camera measurements. 4

Overall SuperKEKB IR Layout

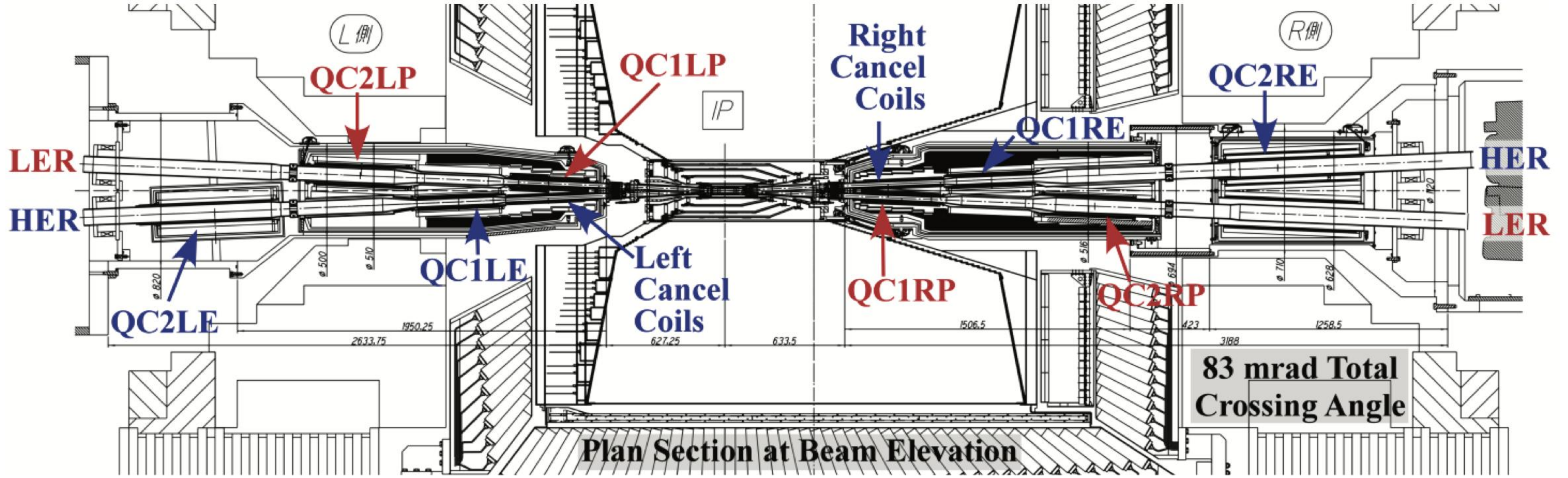

Figure 1:. SuperKEKB IR layout inside Belle-II with high energy, e^-, (HER) and low energy, e^+, (LER) rings indicated.

SuperKEKB IR Cryostats

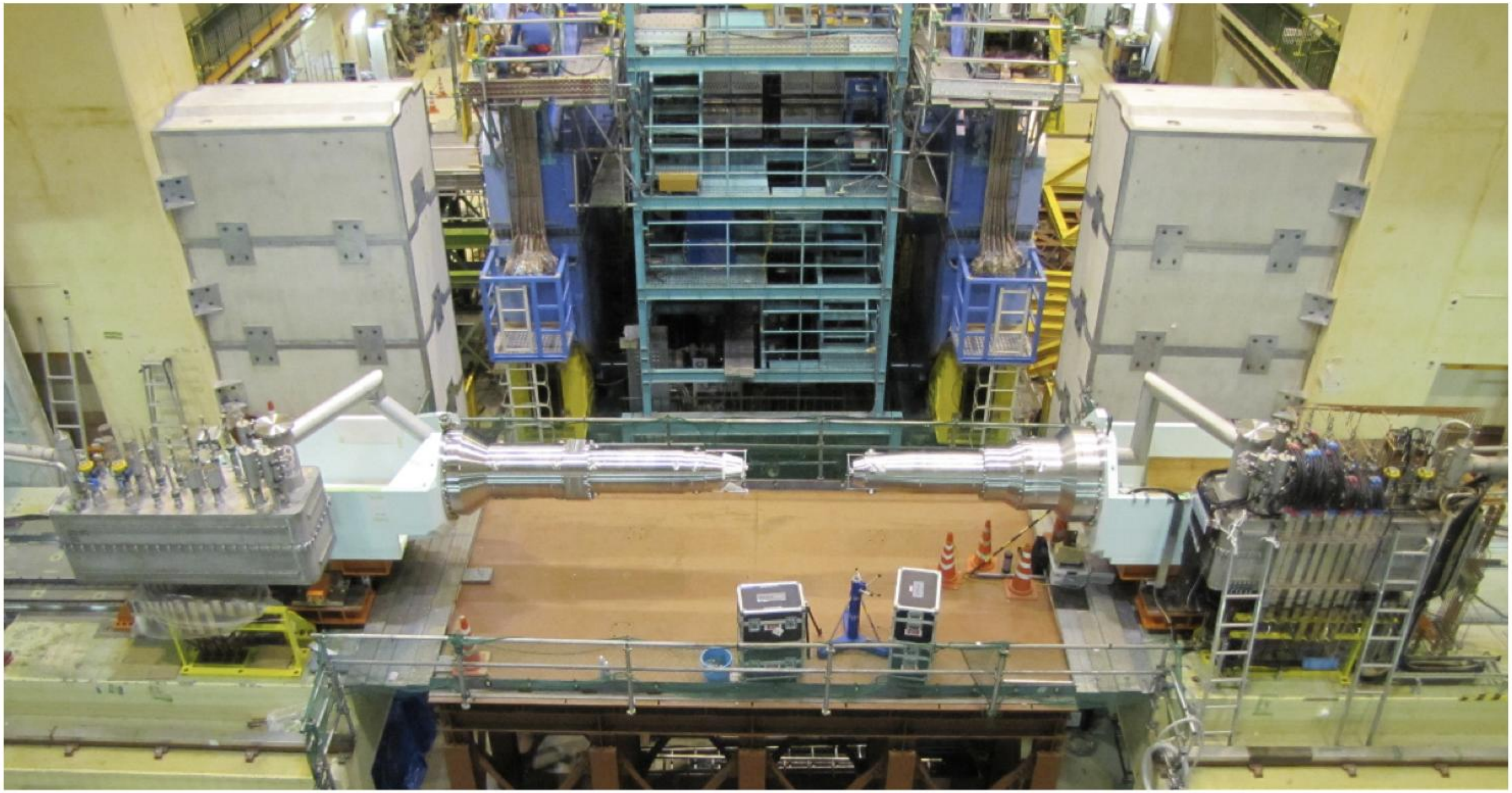

Figure 11: QCSL/R cryostats and Belle-II detector in IR.

Belle-II Center View

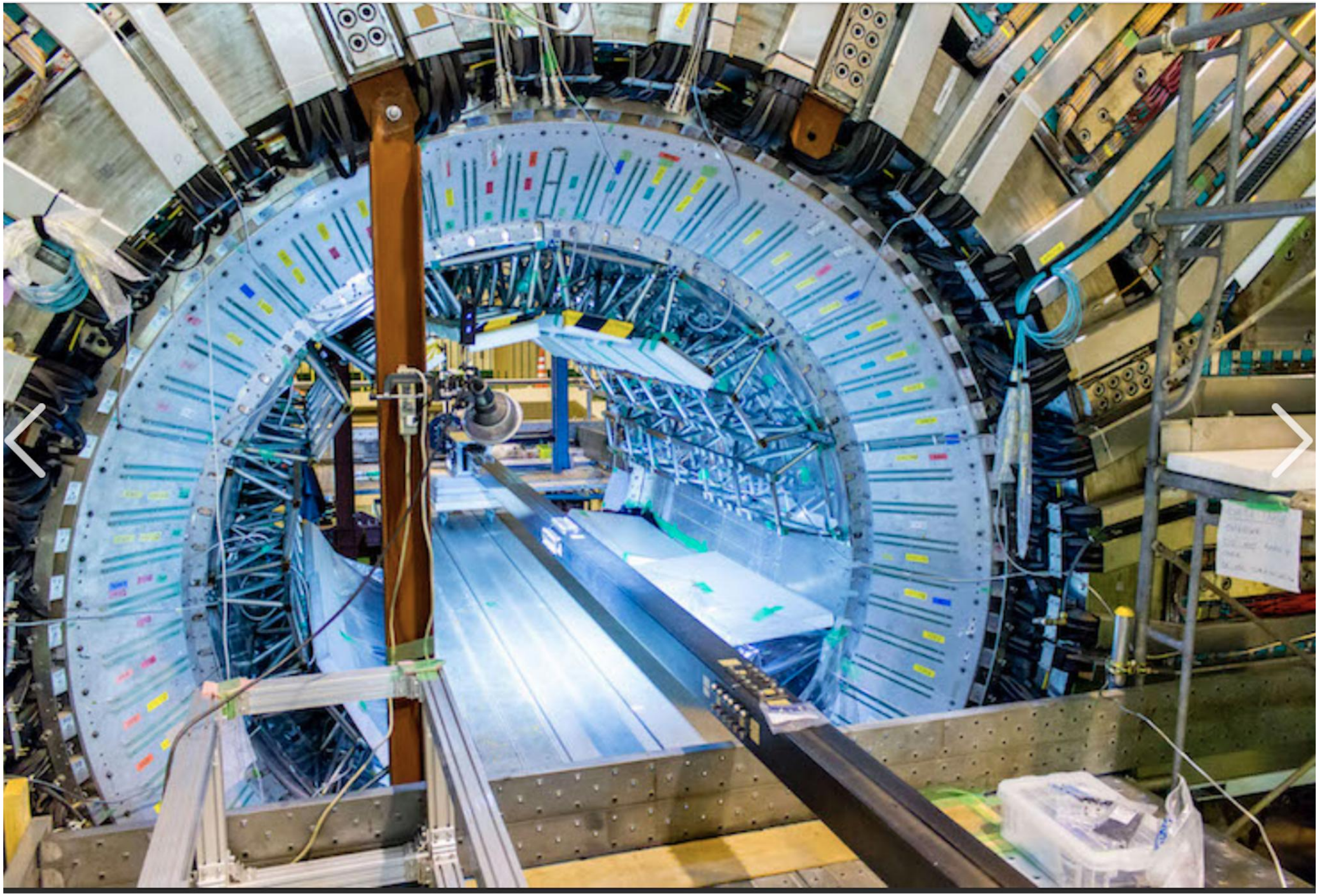

CEPC Overview (~2023)

CEPC as a Higgs Factory： ttbar, H, W, Z, followed by a SppC ~100TeV

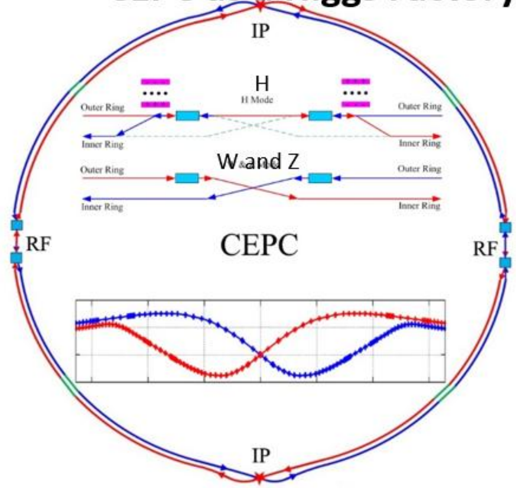

CEPC collider ring (100km)

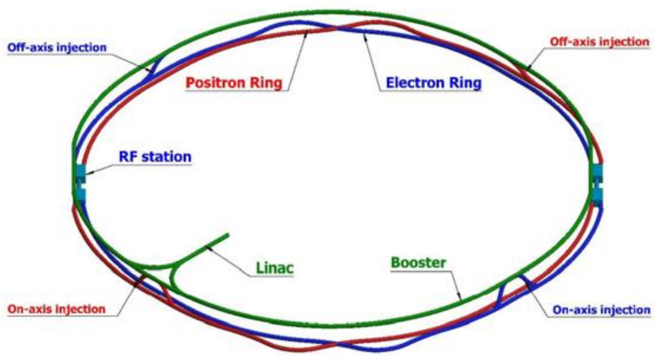

CEPC booster ring (100km)

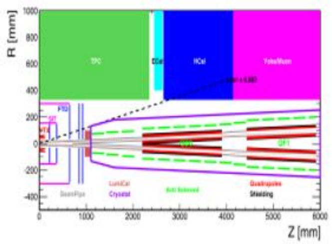

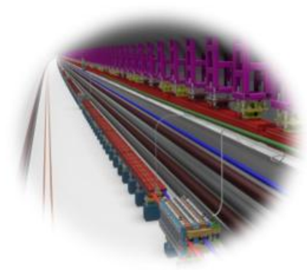

CEPC Parameters

Parameter [unit]	Higgs	Z	W	tt
Beam energy E_k [GeV]	120	45.5	80	180
L_{max}/IP ($10^{34}cm^{-2}s^{-1}$)	5	115	16	0.5
Emittance (H/V) [nm/pm]	0.64/1.3	0.27/1.4	0.87/1.7	1.4/4.7
Beam current [mA]	16.7	803.5	84.1	3.3
Bunch number	268	11934	1297	35
Bunch Population [10^{10}]	13	14	13.5	20
Momentum compaction α_p [10^{-5}]	0.71	1.43	1.43	0.71
Bunch length σ_z (natural/total) [mm]	2.3/4.1	2.5/8.7	2.5/4.9	2.2/2.9
Energy spread (natural/total) [10^{-4}]	10/17	4/13	7/14	15/20
Betatron tune ν_x/ν_y	445.10/445.22	317.10/317.22	317.10/317.22	445.10/445.22
Synchrotron tune	0.049	0.035	0.062	0.078
Radiation damping [ms]	44/44/22	816/816/408	150/150/75	14/14/7

CEPC IR magnets and cryostats (Dec 2023)

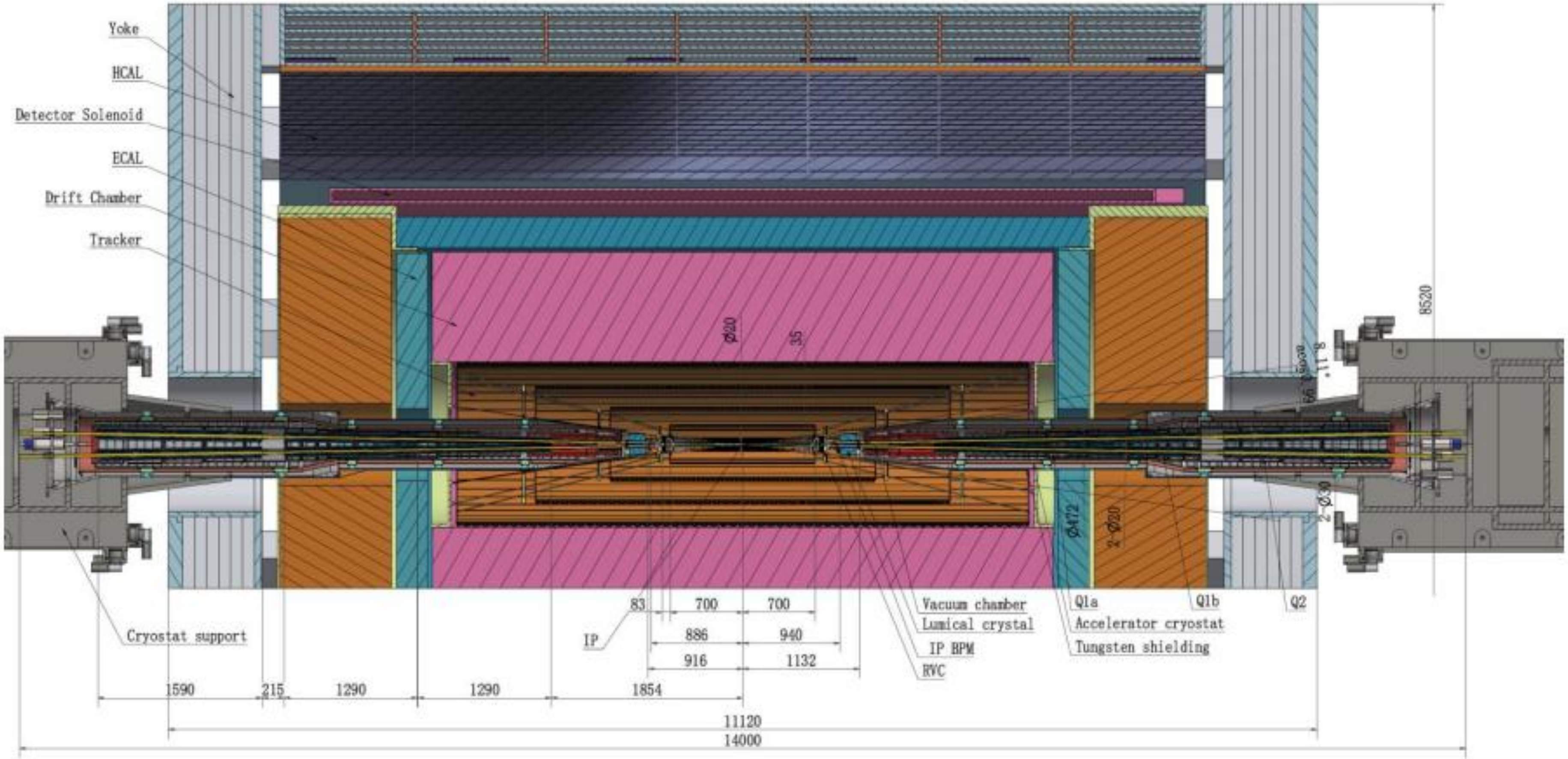

Fig 4.2.6.1: CEPC MDI layout.

ILC layout

The original plan (ILC500) for the ILC (The International Linear Collider) can be seen in the Technical Design Report (TDR) published in 2013. To reduce initial costs, a proposal has been made to lower the center of mass energy to 250 at the start of operation.

ILC250

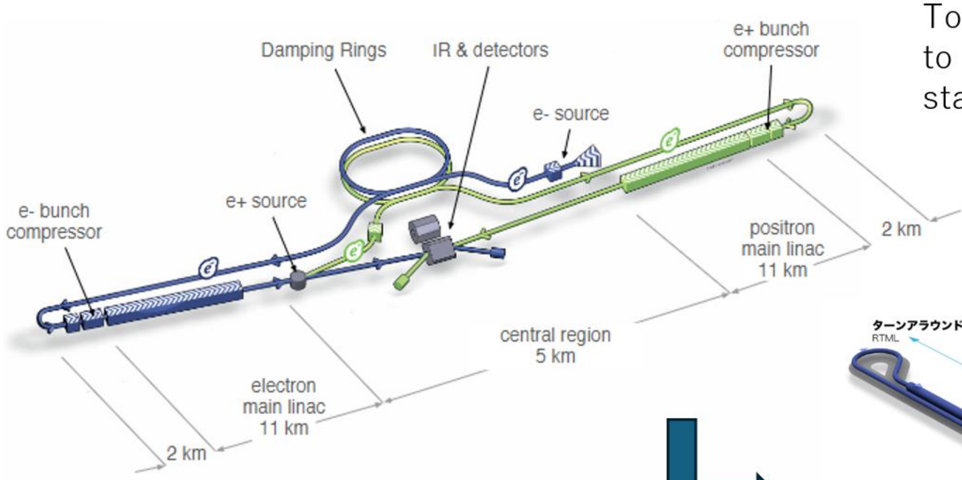

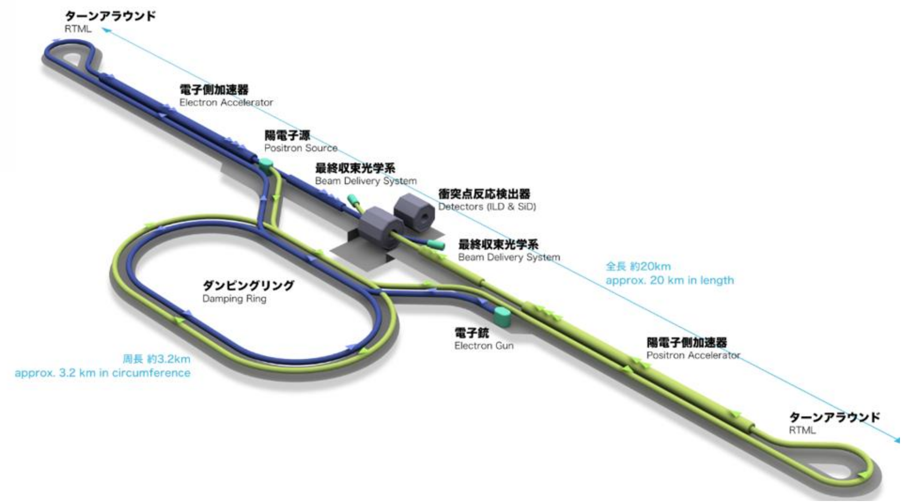

The total length of the facility was reduced from approximately 30km to 20km.

ILC Detector Concept (Accelerator IR Quads Magnets Outside)

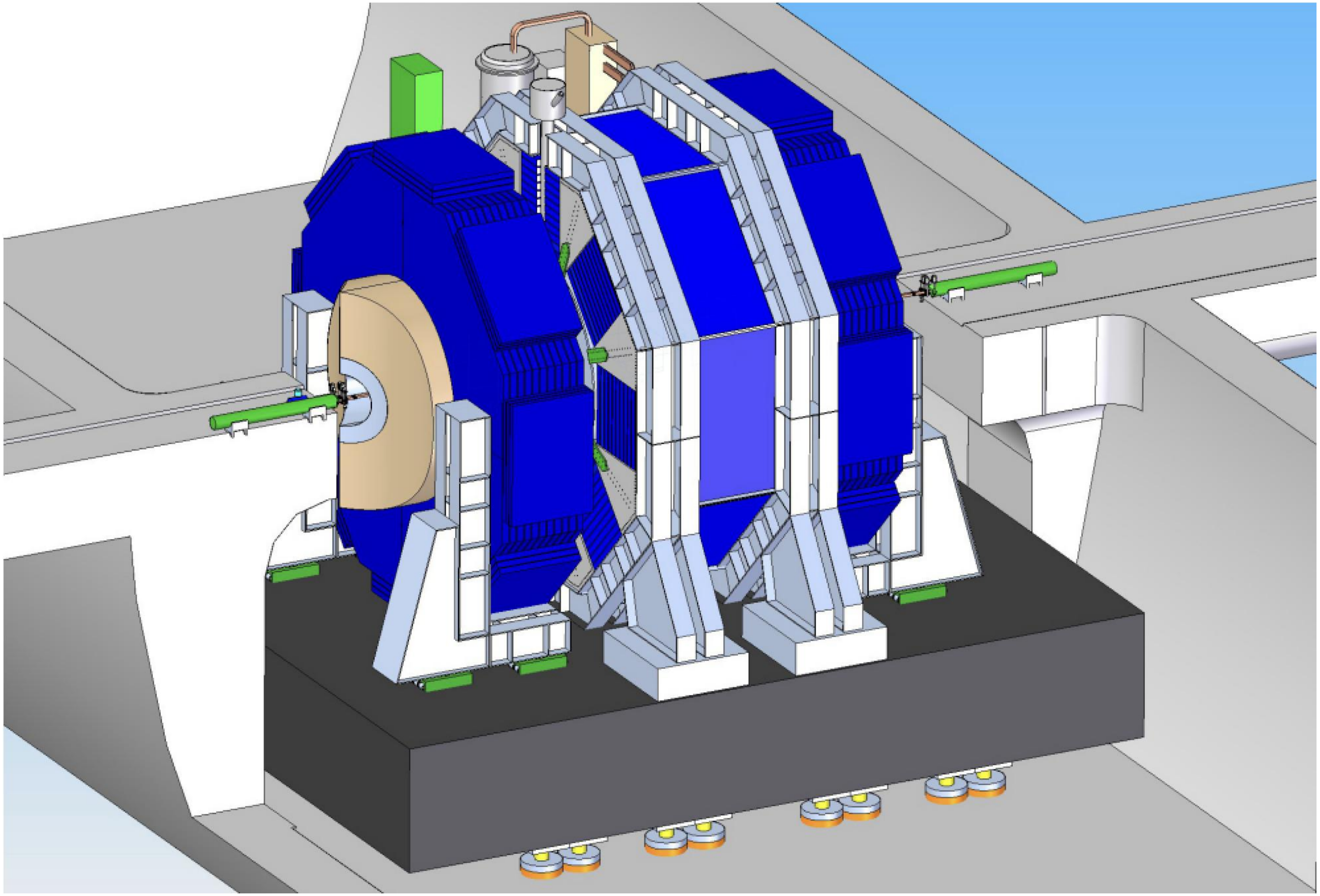

FCC tunnel cavern possibilities

(J. Szaga)

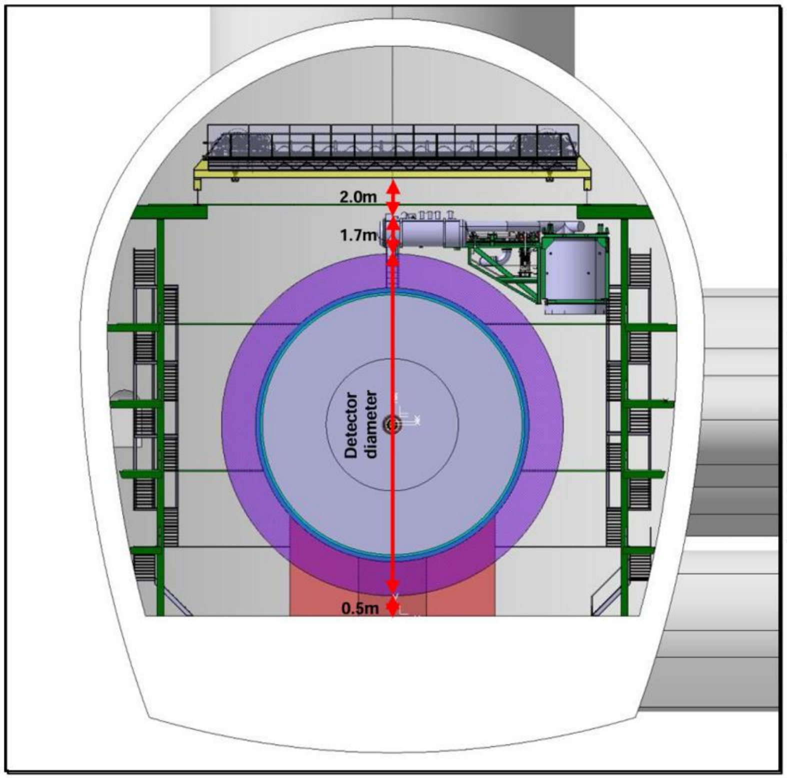

Detector	Detector global radial envelope [m]	Floor - detector distance* [m]	Detector - Cryogenics Lar (must be 13m IP-Cryo Lar)**[m]	Detector - Cryo NbTi-IP** [m]	Reserved space below the crane [m]	Distance from the floor to the IP [m] Required	Height from the floor to the crane [m] Required
CLD	7.4	0.5		1.7	2.0	**7.9**	**19.5**
ILD	8.1	0.5		1.7	2.0	**8.6**	**20.2**
IDEA	6.9	0.5		1.7	2.0	**7.4**	**19.0**
ALLEGRO	7.0	0.5	6.0		2.0	**7.5**	**23.4**
ALFA	7.5	0.5		1.7	2.0	**8.0**	**19.6**
Small FCC-hh	7.5	0.5		1.7	2.0	**8.0**	**20.0**
Large FCC-hh	10.0	0.5	3.0		2.0	**10.5**	**23.8**

* Confirmed with Transportation Team
** Confirmed with Cryogenics Team

Lowering LHC Detector Components

FCC T. Watson 29/01/2024 – 7th FCC Physics Workshop

Shafts

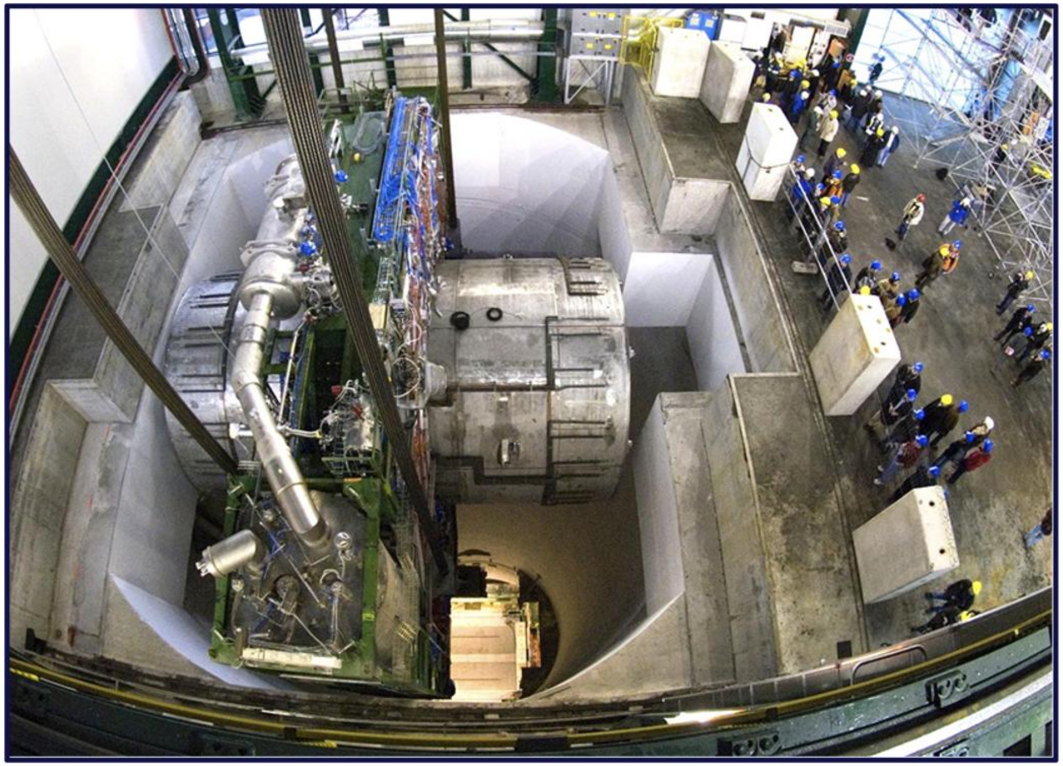

Lowering CMS Detector down 100m deep LHC shaft

IR Layout

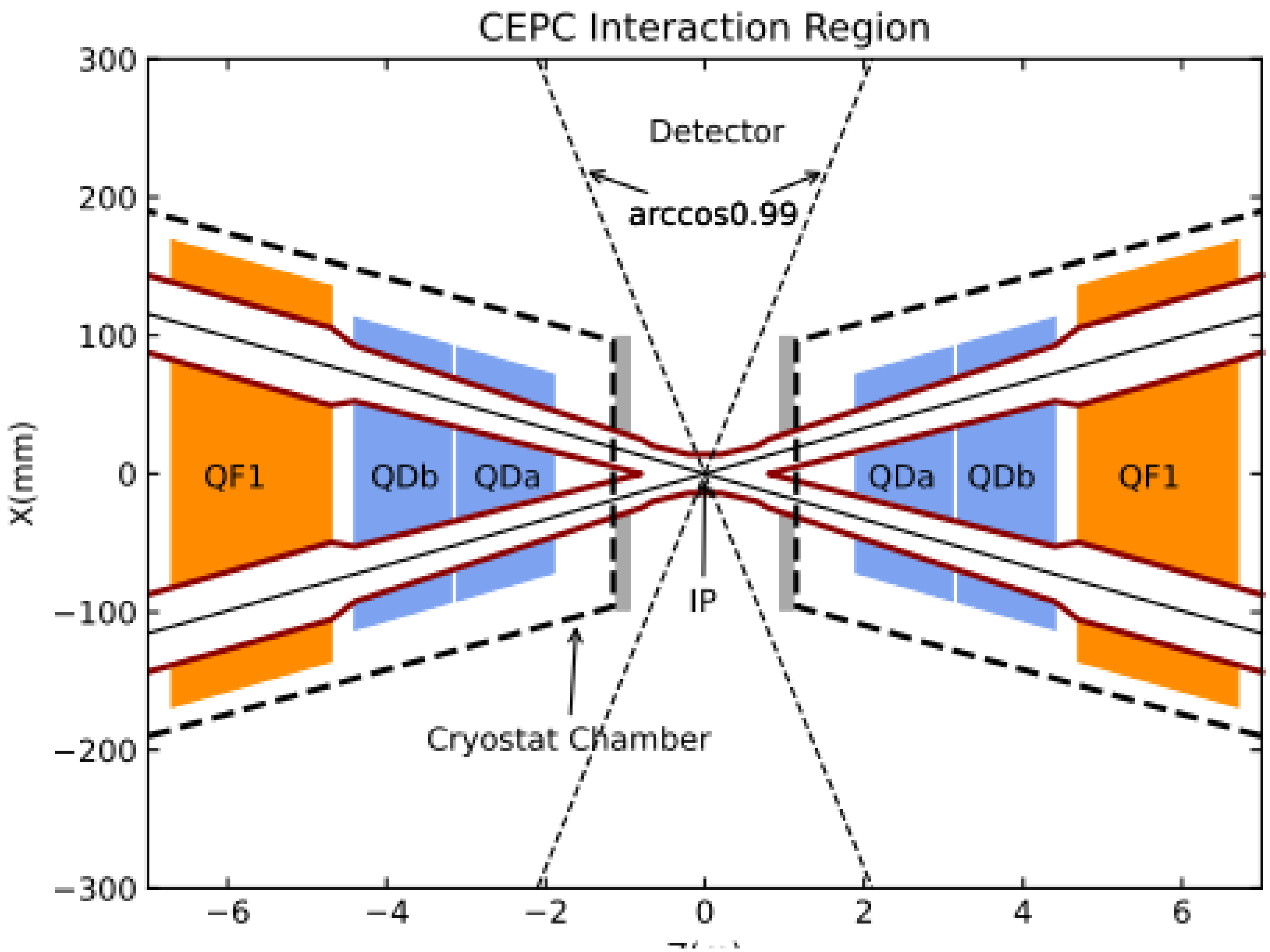
CEPC Interaction Region
Detector
arccos0.99
QF1
QDb
QDa
QDa
QDb
QF1
IP
Cryostat Chamber
X(mm)
300
200
100
0
−100
−200
−300
−6
−4
−2
0
2
4
6

Comparisons of IR (features for FCCee, CEPC, ILC, SuperKEKB)

SLAC

Machine		FCCee	CEPC	ILC	SuperKEKB
Crossing-angle	mrad	30	33	14	83
L*	m	2.2	1.9	3.5	0.935
L* x Cross-angle	mm	66	63	49	78
Vertical β_y^* at IP	mm	0.7-1.6	0.9-2.7	0.4	0.3
Detector soln field	T	2/3	3	3.5/5	1.5
Detector stay clear	mrad	100	118/141	90	350/436
He temperature	K	1.9	4.2	4.5	4.5
QC1s side-by-side		Yes	Yes	No	No

IR Final Focus Optics 1984 (SLC at SLAC)

SLAC

Final focus telescope (FFT)[1]

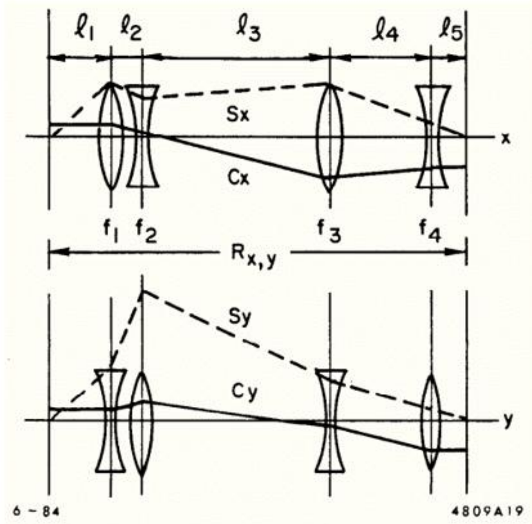

Fig. 20. A two-dimensional telescopic system.

$$R = \begin{pmatrix} -M_x & 0 & 0 & 0 \\ 0 & -1/M_x & 0 & 0 \\ 0 & 0 & -M_y & 0 \\ 0 & 0 & 0 & -1/M_y \end{pmatrix}$$

Vertical plane

Horizontal plane

- Constraints at the end of FFT：

  $\mu_x=\pi$, $\mu_y=\pi$, $\alpha_x=0$, $\alpha_y=0$

[1] K. Brown, R. Servranckx, First- and second-order charged particle optics, SLAC-PUB-3381, 1984.

Beta functions grow quadratically away from the IR

$$\frac{1}{2}\beta\beta'' - \frac{1}{4}\beta'^2 + K(s)\beta^2 = 1 \qquad (2.80)$$

The form is clearly less convenient. I may, however, use it to make the following observations.

In a field free segment of the guide field K(s) = 0, and the solution to Eq. (2.80) is

$$\beta = \beta_0\left\{1 + \frac{(s-s_0)^2}{\beta_0^2}\right\} \qquad \sim s^2/\beta^* \qquad (2.81)$$

where s_0 and β_0 are suitable constants. If β has a minimum in the field free segment then β_0 and s_0 are the values of β and s at the minimum. Generally, the

Beam size grows linearly from IP.
FF Quad size is limited by beam sizes/backgrounds.
Quad aperture limits lowest β_y^* .

(Matt Sands)

IR accelerator optics for various colliders

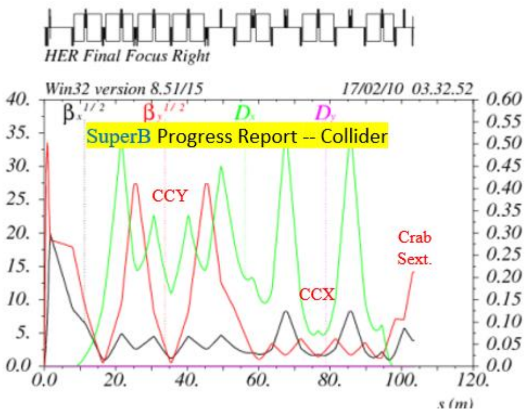

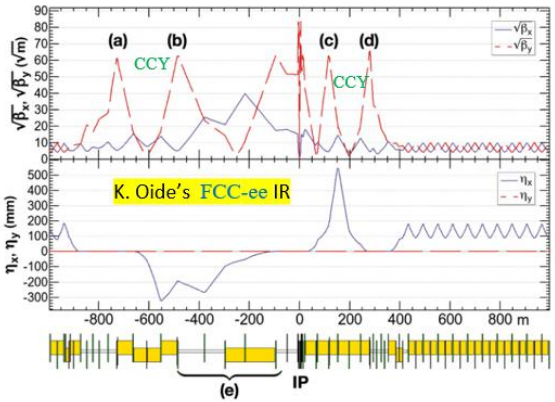

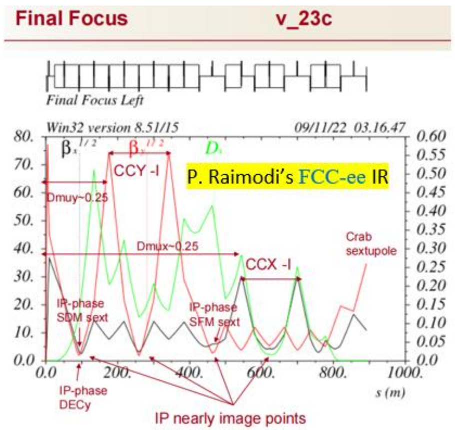

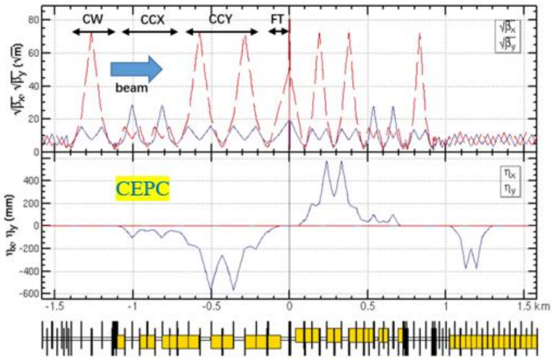

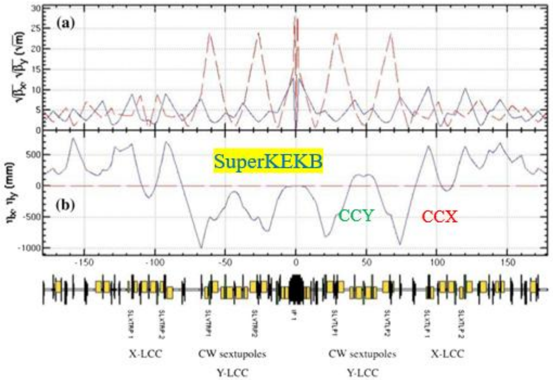

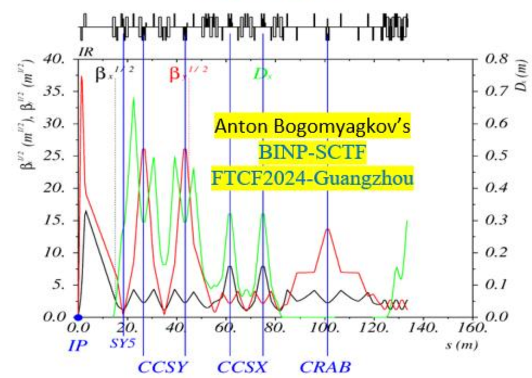

Modular IR optics layout: CCY/CCX (vertical/horizontal chromaticity correction), CS (Crab sextuples), Telescope;

Multipoles: for high-order chromaticity correction and nonlinear optimization

FCC-ee Oide's version and SuperKEKB IR integrate crab sextupole into the second one of the CCY sextupole pairs

IP off energy corrections and crab waist

Local chromaticity correction (CCY and CCX) [1]

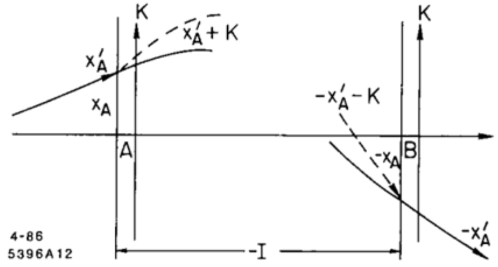

Sextupole pair with –I map

$$\begin{pmatrix} x \\ x' \\ y \\ y' \end{pmatrix}_2 = \begin{pmatrix} -1 & 0 & 0 & 0 \\ 0 & -1 & 0 & 0 \\ 0 & 0 & -1 & 0 \\ 0 & 0 & 0 & -1 \end{pmatrix} \begin{pmatrix} x \\ x' \\ y \\ y' \end{pmatrix}_1$$

- Constraints:

$$\beta_{x,1} = \beta_{x,2}, \alpha_{x,1} = \alpha_{x,2}, \mu_x = \pi;$$
$$\beta_{y,1} = \beta_{y,2}, \alpha_{y,1} = \alpha_{y,2}, \mu_y = \pi$$

Crab Sextupole (CS)

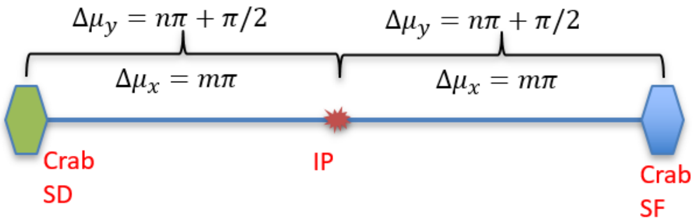

- Strict phase requirement
- To reduce crab sextupole strength

  ($K_2L = \pm \frac{1}{2\theta\beta_y^*\beta_y}\sqrt{\frac{\beta_x^*}{\beta_x}}$),

  $\rightarrow$ $\beta_y >> \beta_x$, and $\beta_x > 1$

  - This can help reduce the undesired nonlinear map coefficients[2] between crab sextupoles.

[2] A. Bogomyagkov, PRAB 19, 121005 (2016)

Accelerator Knobs for IP Tuning

$\beta^*_{x,y}$ and $w_{x,y}$ - knobs

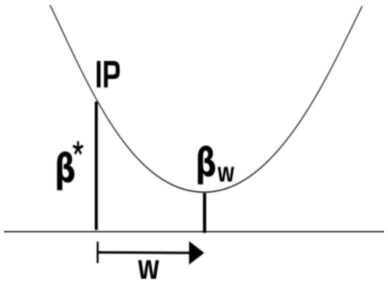

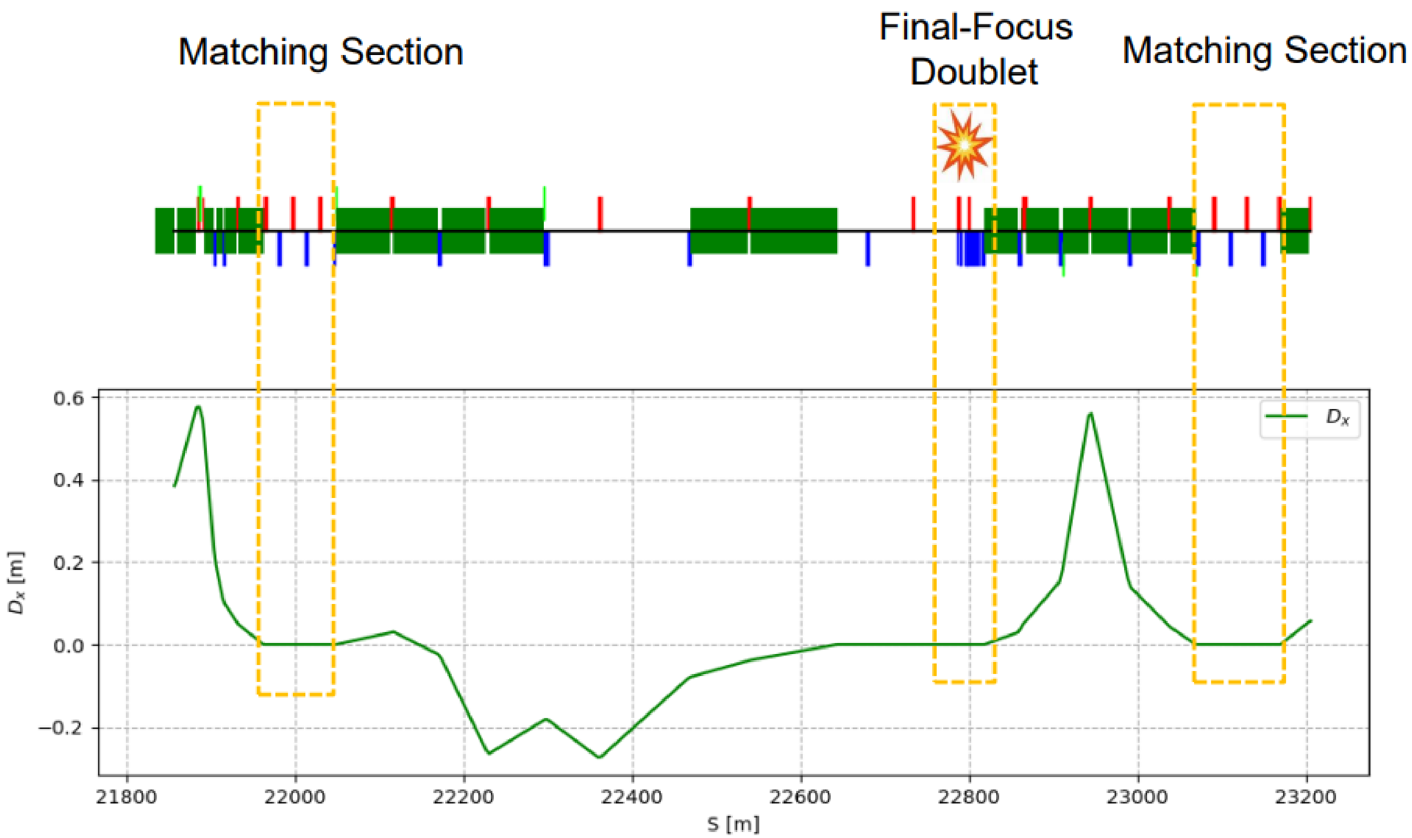

FCCee Machine Detector Interface (M. Boscolo)

FCC-ee Interaction Region rationale: crab-waist

Crab-waist scheme, based on two ingredients:

- concept of **nano-beam scheme:**
  - vertical squeeze of the beam at IP and large horizontal crossing angle
  - large ratio σ_z/σ_x reducing the instantanous overlap area, allowing for a lower β_y*
- concept of **crab-waist sextupoles:**
  - placed at a proper phase advance they suppress the hourglass effect by inducing a constant β_y along the larger coordinate of the beams overlap.

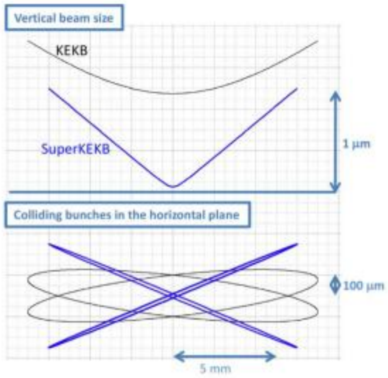

Figure 2: Schematic view of the nanobeam collision scheme.

SuperKEKB https://arxiv.org/pdf/1809.01958.pdf

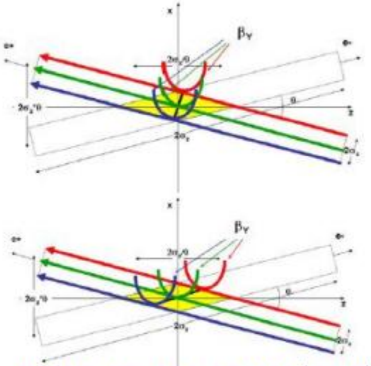

DAFNE, PRL 104, 174801 (2010)

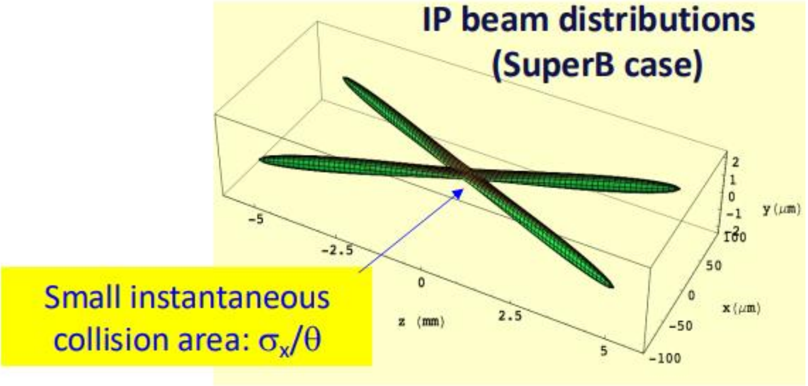

Luminosity Equations

Basic Equations

Piwinski angle: $$\phi = \frac{\sigma_z}{\sigma_x} tg\left(\frac{\theta}{2}\right)$$

Length of overlap: $$L_i = \frac{\sigma_z}{\sqrt{1+\phi^2}} \xrightarrow[\theta \ll 1,\ \phi \gg 1]{} \frac{2\sigma_x}{\theta} \approx \beta_y^*$$

Luminosity: $$L = \frac{\gamma}{2er_e} \cdot \frac{I_{tot}\xi_y}{\beta_y^*} \cdot R_{hg}$$

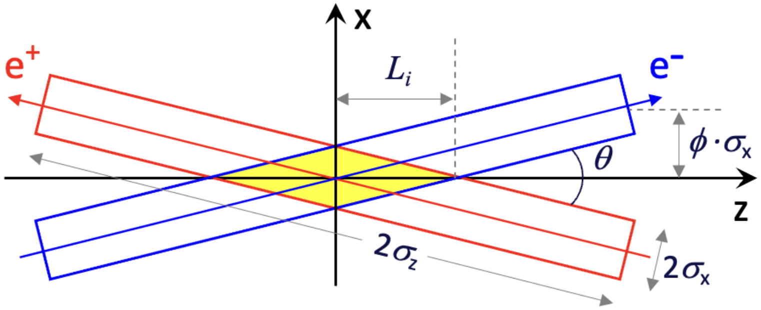

Collision scheme with large Piwinski angle

Crab Waist Collision Scheme

Collision scheme: Large Piwinski angle + Crab-waist

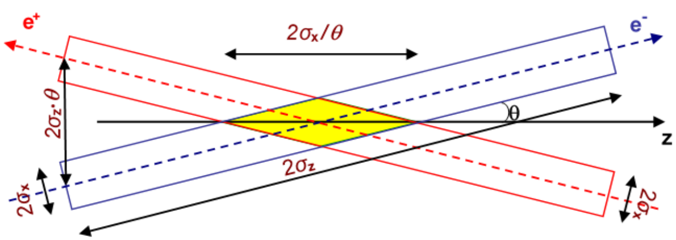

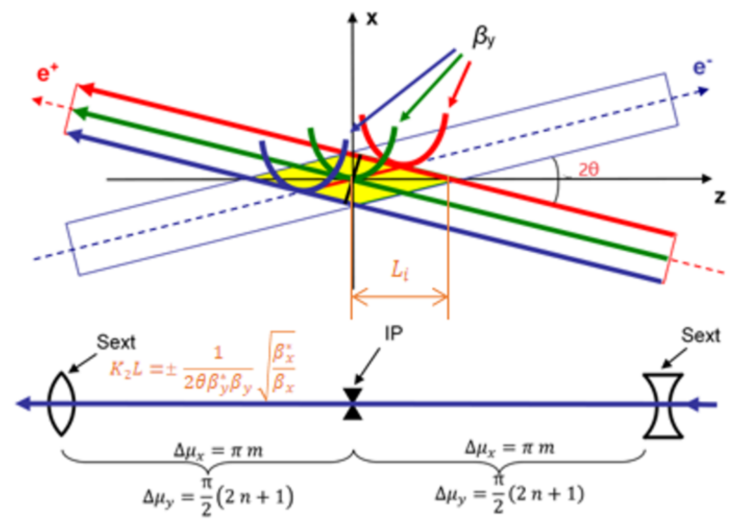

Large Piwinski angle $\phi = \frac{\sigma_z}{\sigma_x}\tan\theta \approx \frac{\sigma_z}{\sigma_x}\theta \gg 1$

--> $L_i \sim \sigma_x/\theta \approx \sigma_z/\phi$

→ $\beta_y^* \sim \sigma_x/\theta$ without hourglass effect

→ Strong betatron and synchrobetatron beam-beam resonances

- Crab sextupole (CS) pairs: suppress the adverse beam-beam resonances by shifting the vertical beam waist

$$K_2 L = \pm \frac{1}{2\theta\beta_y^*\beta_y}\sqrt{\frac{\beta_x^*}{\beta_x}}$$

[1] P. Raimondi, D. Shatilov, M. Zobov, Proceedings of 2nd SuperB Workshop, Frascati, 2006

Lattice and Beam Issues that affect the luminosity

- FCC-ee machine demands a strong focusing as well as smaller beam sizes to achieve the unprecedented luminosity
  - Luminosity for flat beam expressed as $L = \frac{\gamma}{2er_e}\frac{I_{tot}\,\xi_y}{\beta_y^*}R_g$
- Any alignment error or source of coupling leads to the spurious dispersion/coupling, as well as increase in β-functions at the IP
- This will effect the beam sizes and thus the luminosity

$$\sigma_y^* \approx \sqrt{\left\{\varepsilon_y\beta_y^* + D_y^{2*}\,\delta_p^2 + \left|\widehat{F_{xy}^*}\right|^2 - D_y^{2*}\,\delta_p^2 - \left|\widehat{F_{xy}^*}\right|^2\right\}}$$

- Therefore, there is a need to develop the tools that would help in the fine-tuning of the IP optics

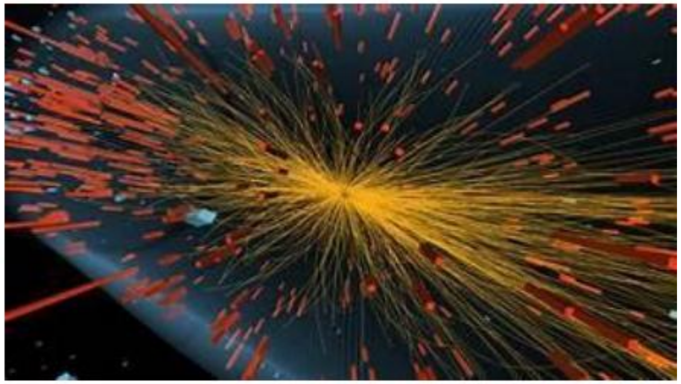

Courtesy: Internet

Tracking times for different effects

Simulation	Number of Particles	Number of Turns
Optics	~1	~few
Emittance – Matrix	~1	~few
Dynamic Aperture	~100	~few damping times (50-5000)
Emittance – Tracking	~1k	~few damping times (50-5000)
Damped Dynamic Aperture	~10k	~few damping times (50-5000)
Momentum Acceptance	~10k	~few damping times (50-5000)
Luminosity	~10k	~few damping times (50-5000)
Lifetime	~100k	~20k

Crab waist strength and luminosity (for SuperKEKB)

If crab sextupoles really work properly?

- Crab waist effects are checked by RDTs analysis (slide 17)
- Crab-waist effects are also demonstrated by beam-beam simulations with lattice

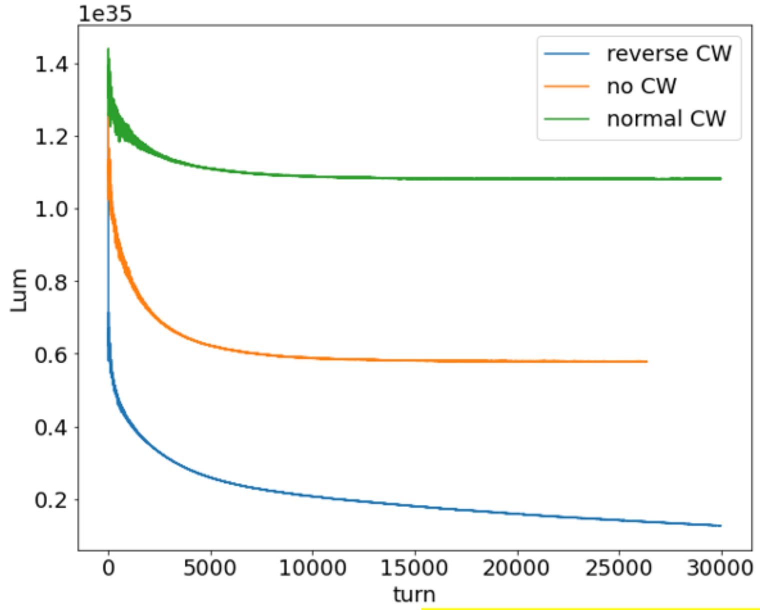

IP beam size and errors (SuperKEKB, Funakoshi)

- Luminosity

$$L \propto \frac{1}{\sqrt{\varepsilon_y \beta_y^*}} \qquad \xi_y \propto \sqrt{\frac{\beta_y^*}{\varepsilon_y}}$$

Smaller β_y^* and ε_y
→ Larger Luminosity with Constant Beam-Beam Parameter

- Beta Function at IP
  - β_x^* = 60 mm, β_y^* = 1 mm (0.8 mm for Short Term)
- Vertical Emittance

Achievement	Spring 2022	Spring 2024	Autum 2024
HER	20 - 40 pm	10 - 30 pm	50 - 80 pm
LER	20 - 40 pm	10 - 30 pm	30 - 40 pm

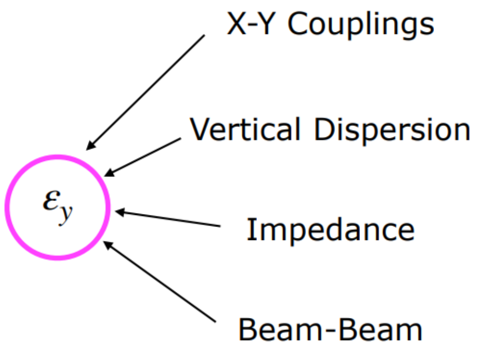

- Machine Error at IP

$$\sigma_y^{*2} = \mu^2 \varepsilon_y \beta_y^* + (\eta_y^* \sigma_\delta)^2 + \frac{\varepsilon_x}{\beta_x^*} r_2^{*2} + \varepsilon_x \beta_x^* r_1^{*2} \quad \text{for } \Delta s = 0$$

← IP Coupling and Vertical Dispersion

Luminosity Tuning

SLAC

Luminosity: Dispersion and Coupling

- At FCCee-Z and FCCee-$t\bar{t}$

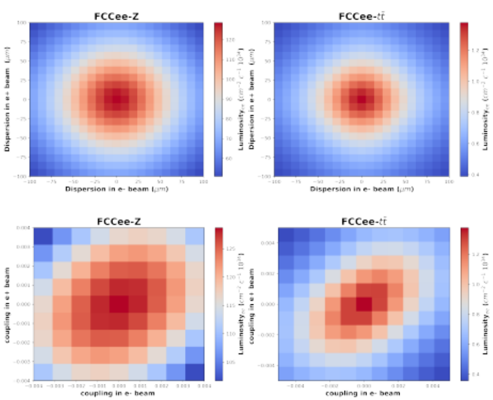

Vertical Dispersion

- Symmetric reduction in luminosity for -/+ values of dispersion
- Dispersion to be ideally contained within 50 μm

Skew Coupling

- Luminosity drops drastically for coupling ($a \sim 0.004$)
- Largely impacts FCCee-$t\bar{t}$

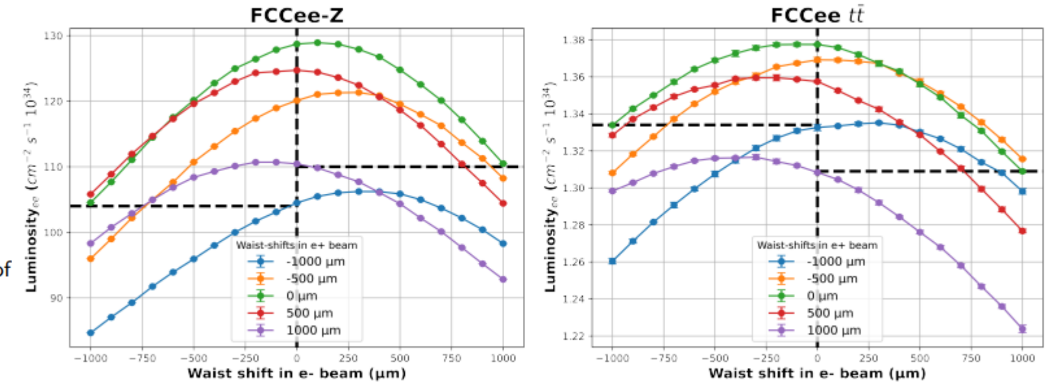

- Travelling waist effects focus the beam 'ahead of the collision point'
- Optimum waist follows the direction of the waist shift of the other beam
- The effect in FCCee-$t\bar{t}$ could be due to strong focusing caused by short bunch length and high bunch density

Study effects of L* on Luminosity In FCCee

Enlarging L*

$t\bar{t}$ Optics

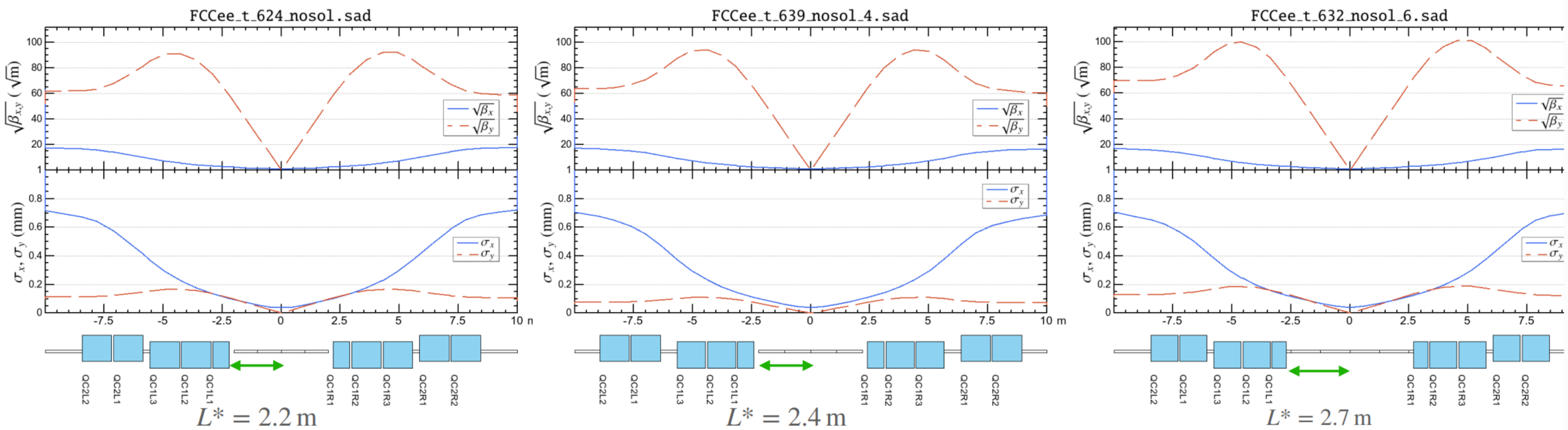

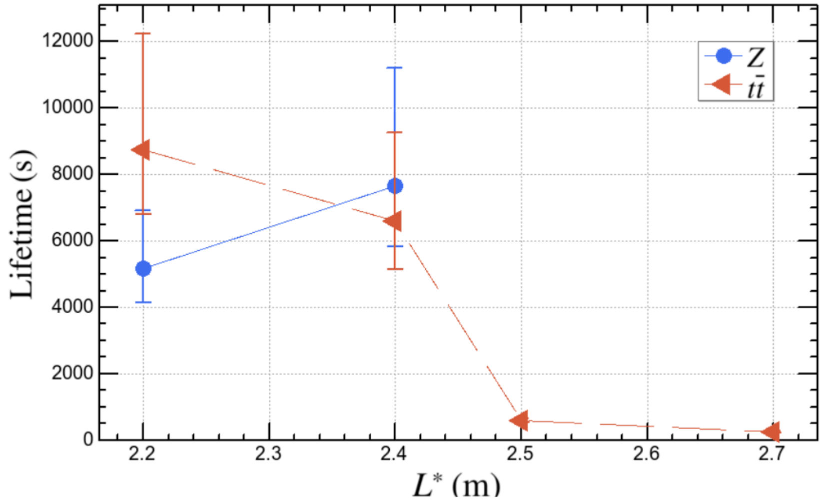

Beam–beam resonances in FCCee with different symmetries

FCC 14 Sep 2022 / eeFACT2022 D. Shatilov

Footprint Size
(machine resonances w/o beam-beam)

Ideal lattice (4-fold symmetry)	Seed 2, 1/4 of the ring	Seed 2, 1/2 of the ring	Seed 2, full ring
Only the quarter ring footprint matters. For the whole ring, the footprint will be 4 times larger, but most of the resonances it crosses will be forbidden.	A quarter of the ring is artificially repeated 4 times. New resonances appeared due to errors, but many remained forbidden due to symmetry.	The half ring is artificially repeated 2 times. Two different quarters form a super period, which corresponds to a doubled footprint. And new resonances appeared.	A realistic situation where there is no symmetry between quarters, and accordingl all resonances are allowed.

Betatron tunes (footprint)

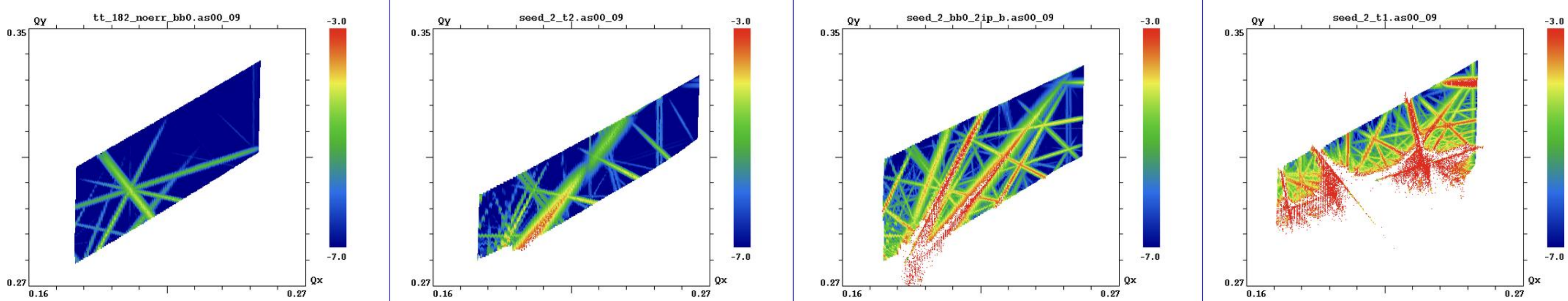

Normalized betatron amplitudes

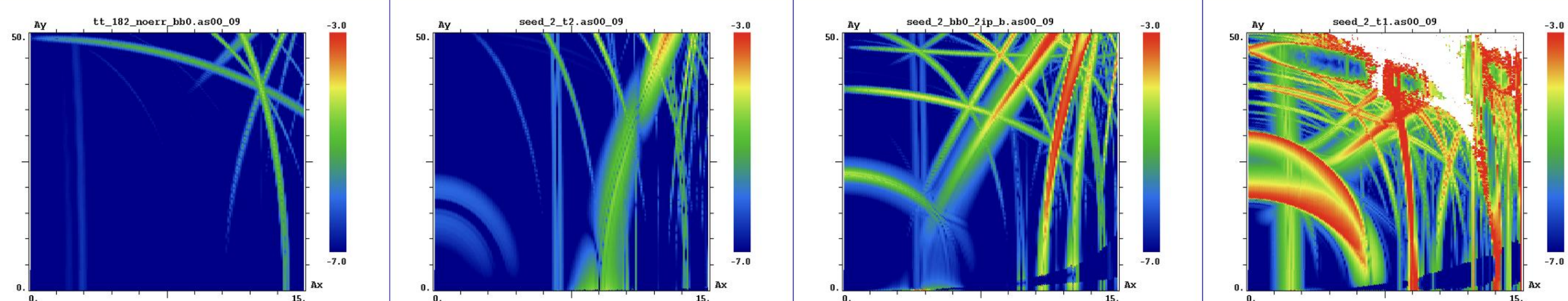

SuperKEKB Vertical tune and Vertical Emittance

Bunch core particles are at a different tune than the bunch tail particles.

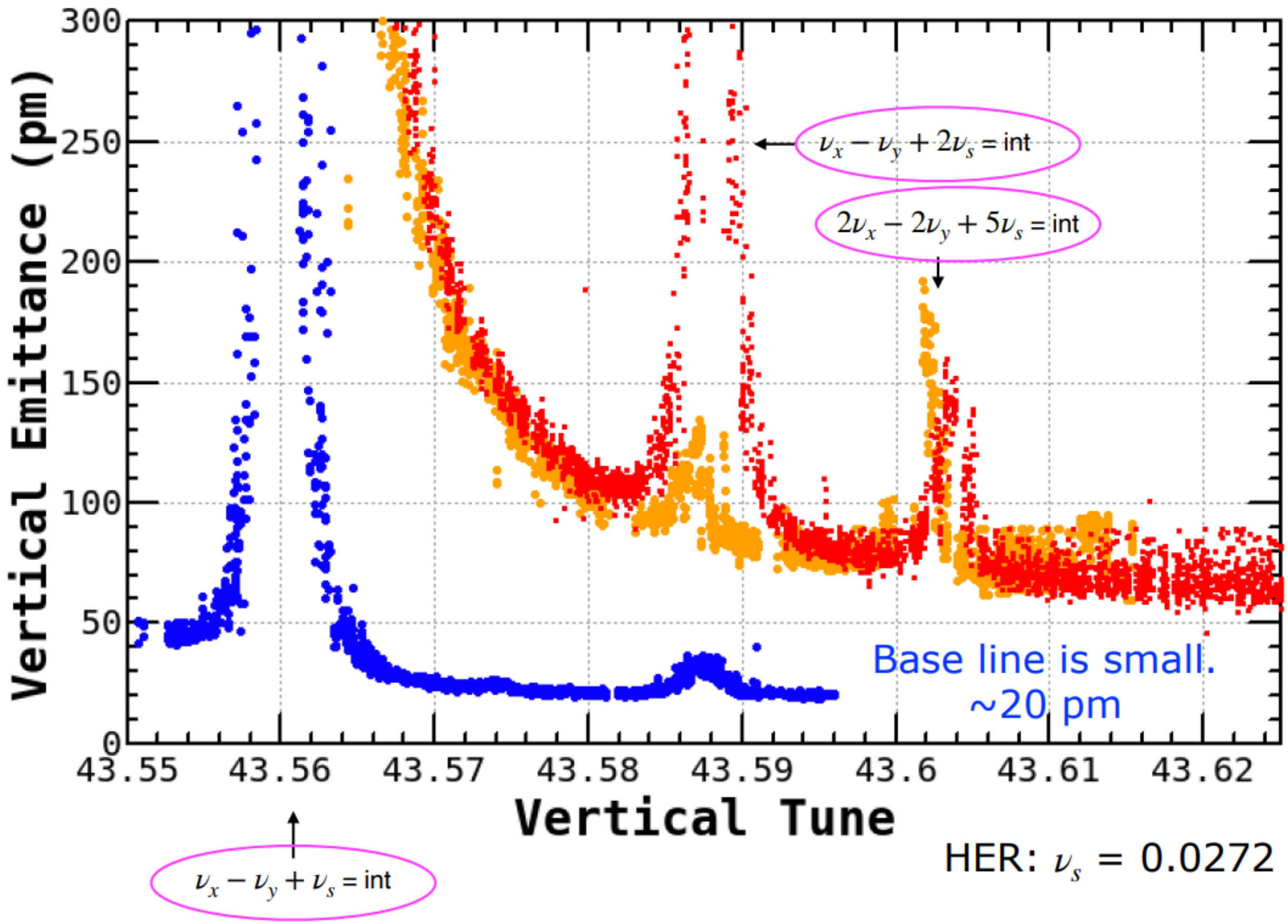

Tracking and errors tolerances for Luminosity

SLAC

Sextupole Errors – Emittance and Luminosity

21

an Riesen-Haupt

P. Kicsiny

- Track and observe particles in lattice with beam-beam and sextupole errors
  - **Same error seeds** and setup as previous studies
  - Initially matched to unperturbed conditions
  - Tracked until **new equilibrium** is reached
  - With and without **beam-beam** element (and beamstrahlung)
- Observe **luminosity** at interaction point
  - Only computed in case with beambeam element
- New **equilibrium emittance** computed after blow-up

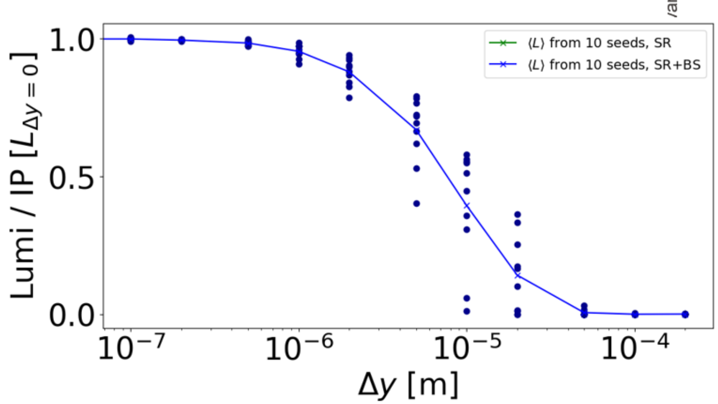

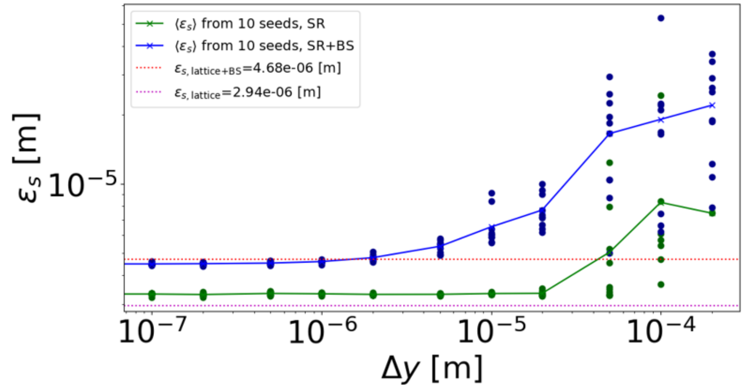

SuperKEKB Beam-Beam Measurements (Funakoshi)

Beam-Beam Study (June 27)

2024b

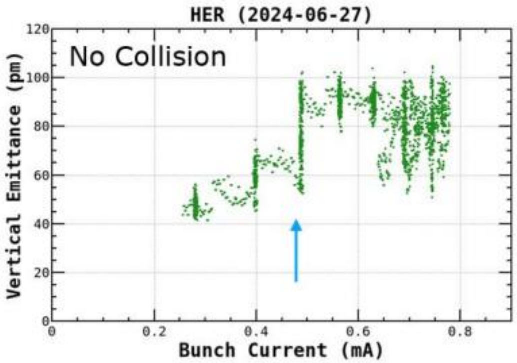

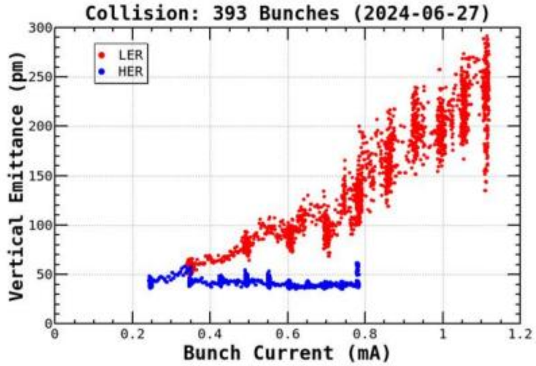

Single Beam Blowup
> 0.5 mA/Bunch

Blowup in LER due to
Beam-Beam

LER injection can be possible
at high current
by changing horizontal tune
($\Delta\nu_x$ = -0.001 Step)

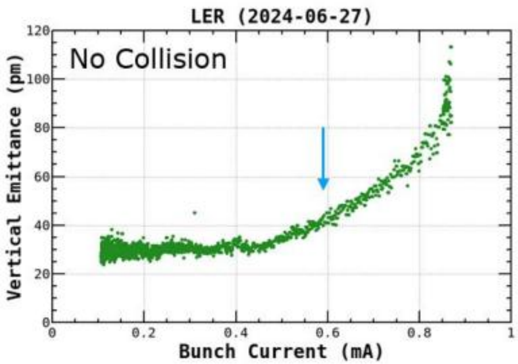

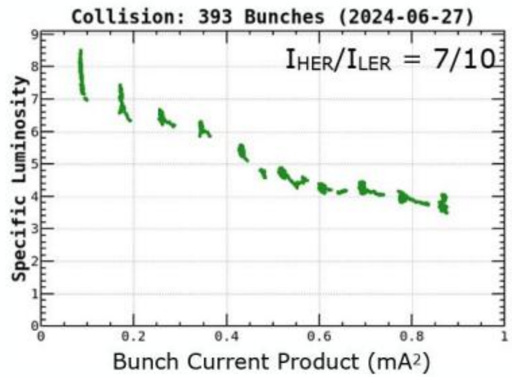

L_p = 1.38 x 10^{34} $cm^{-2}s^{-1}$
with 393 Bunches

L_p = 8.24 x 10^{34} $cm^{-2}s^{-1}$
with 2346 Bunches

SuperKEKB Specific Luminosity

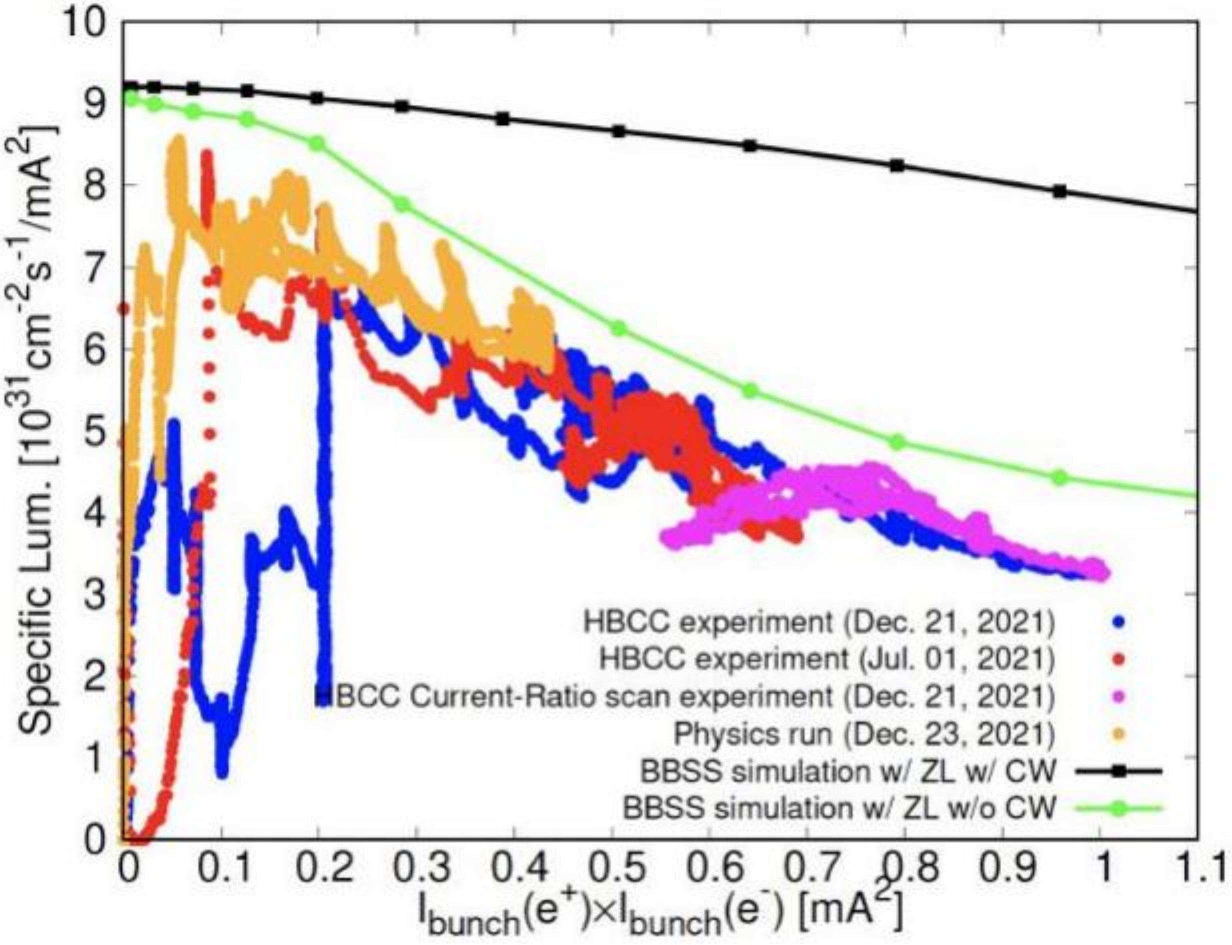

Future: AI and Machine Learning for Luminosity Tuning

Putting it together in ML framework

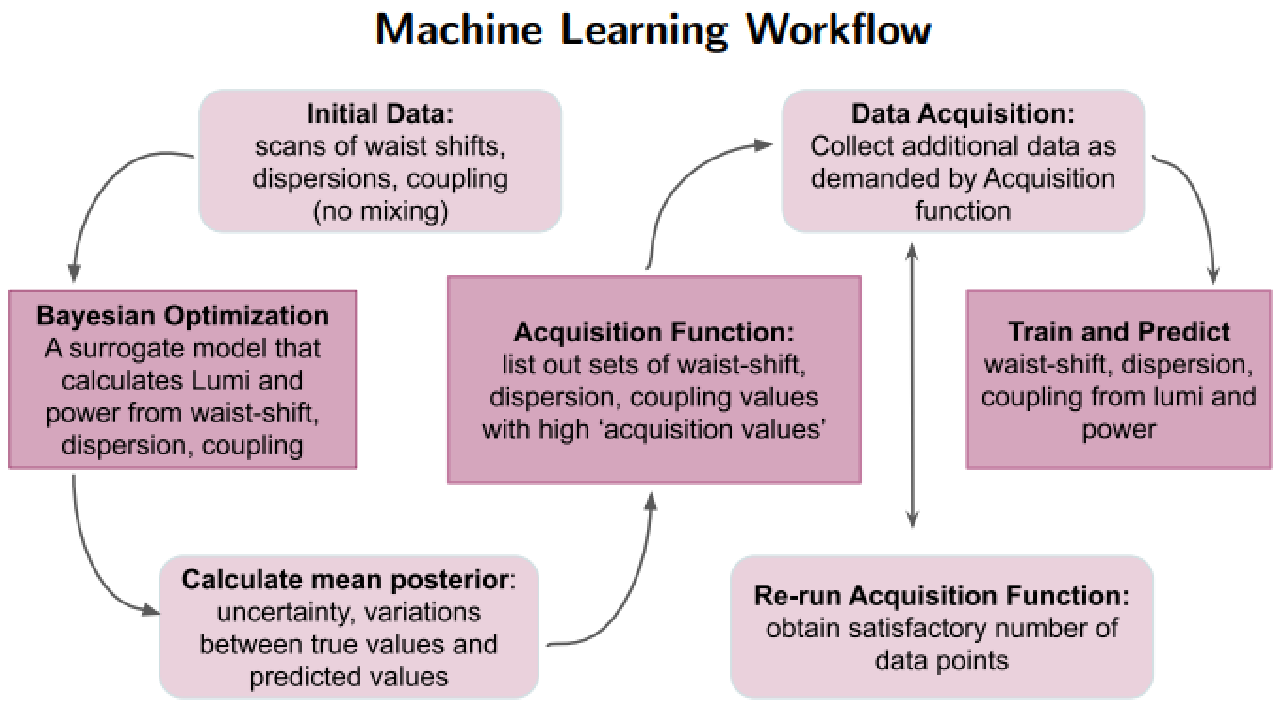

Near Detector IDEA with L* of 2.4 m to front of QC1A.

SLAC

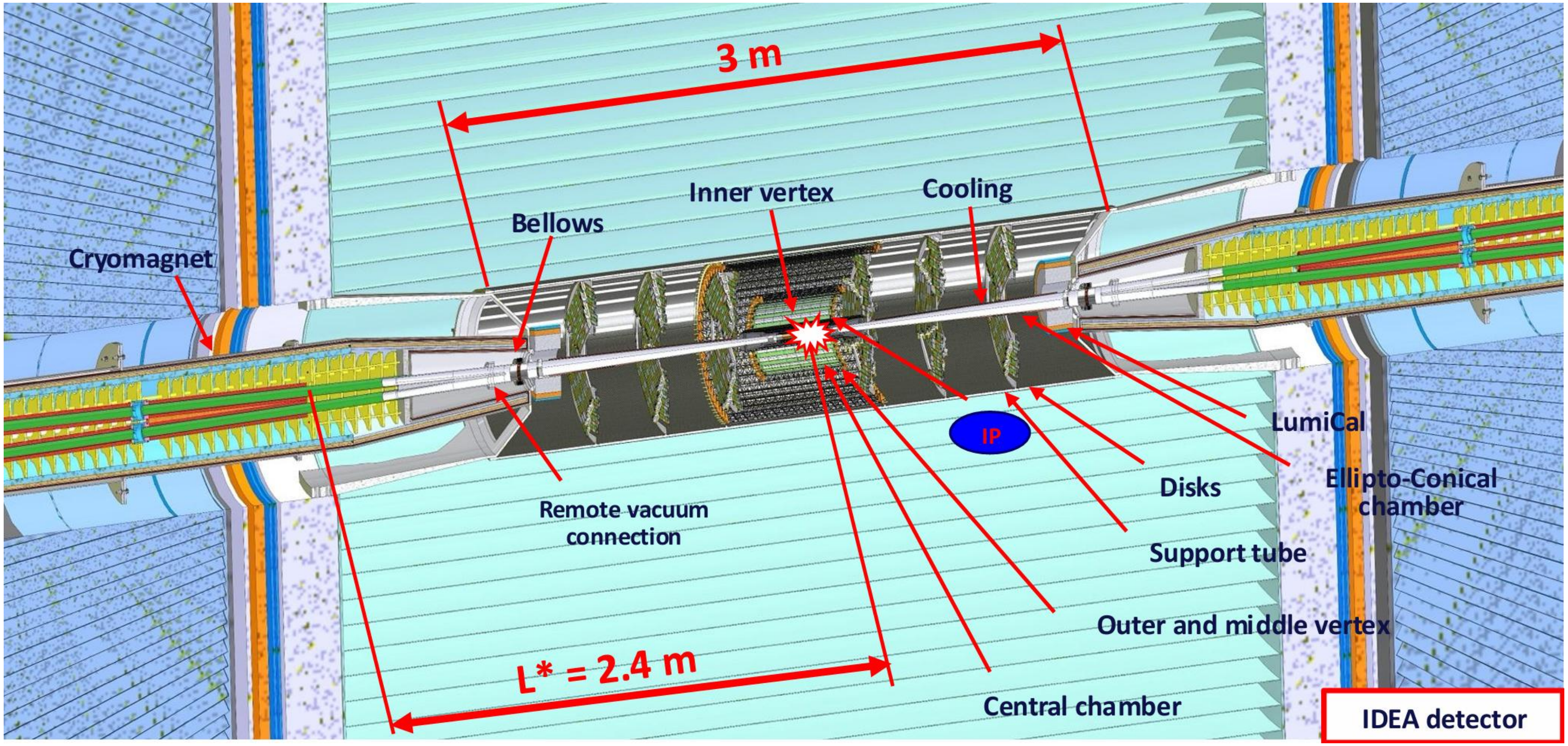

FCCee ALFA Detector near the FCCee IP

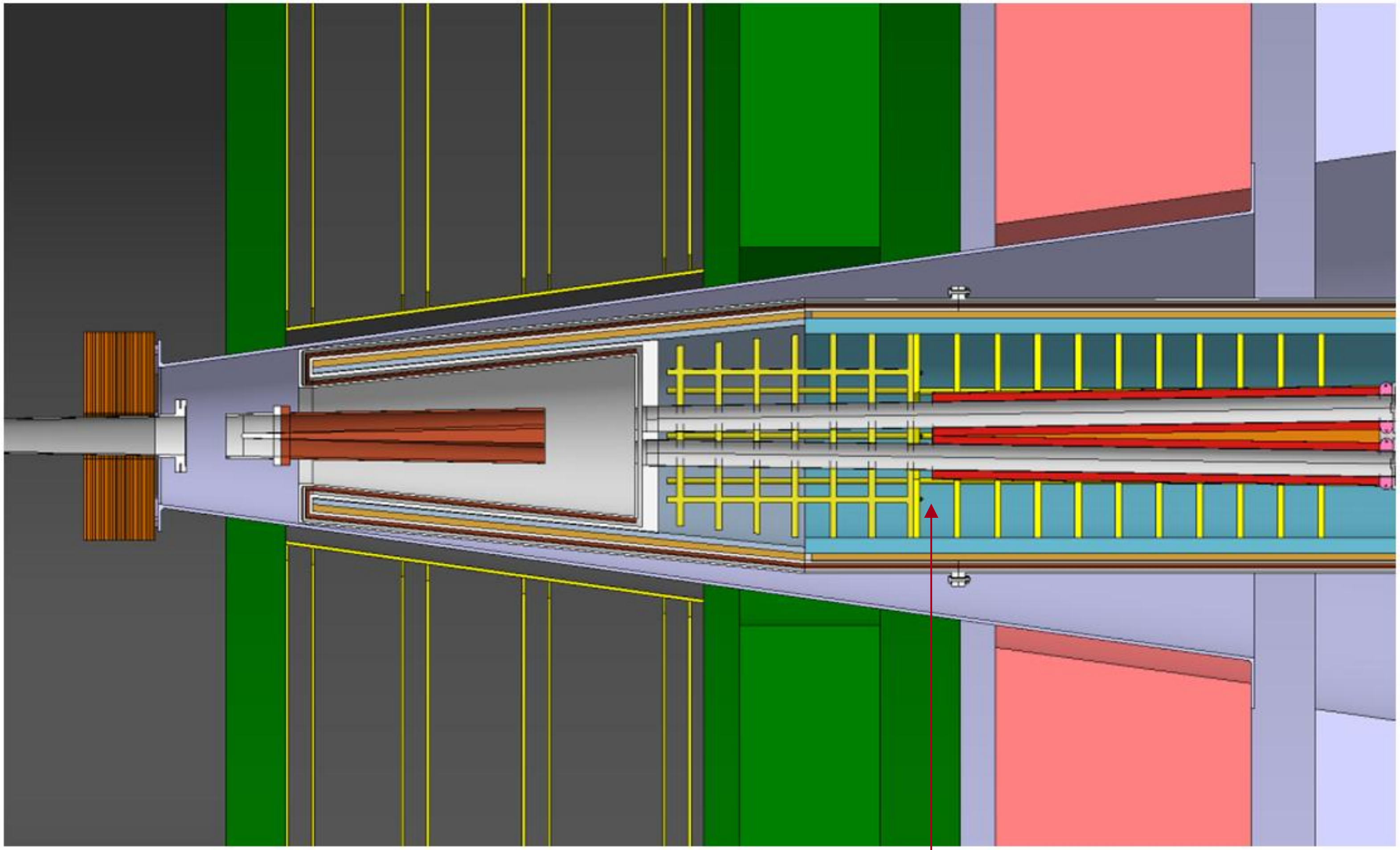

IP ← L* = 2.4 m → Face of QC1A

Remote Flange disconnect (IDEA detector + Accelerator Cryostat

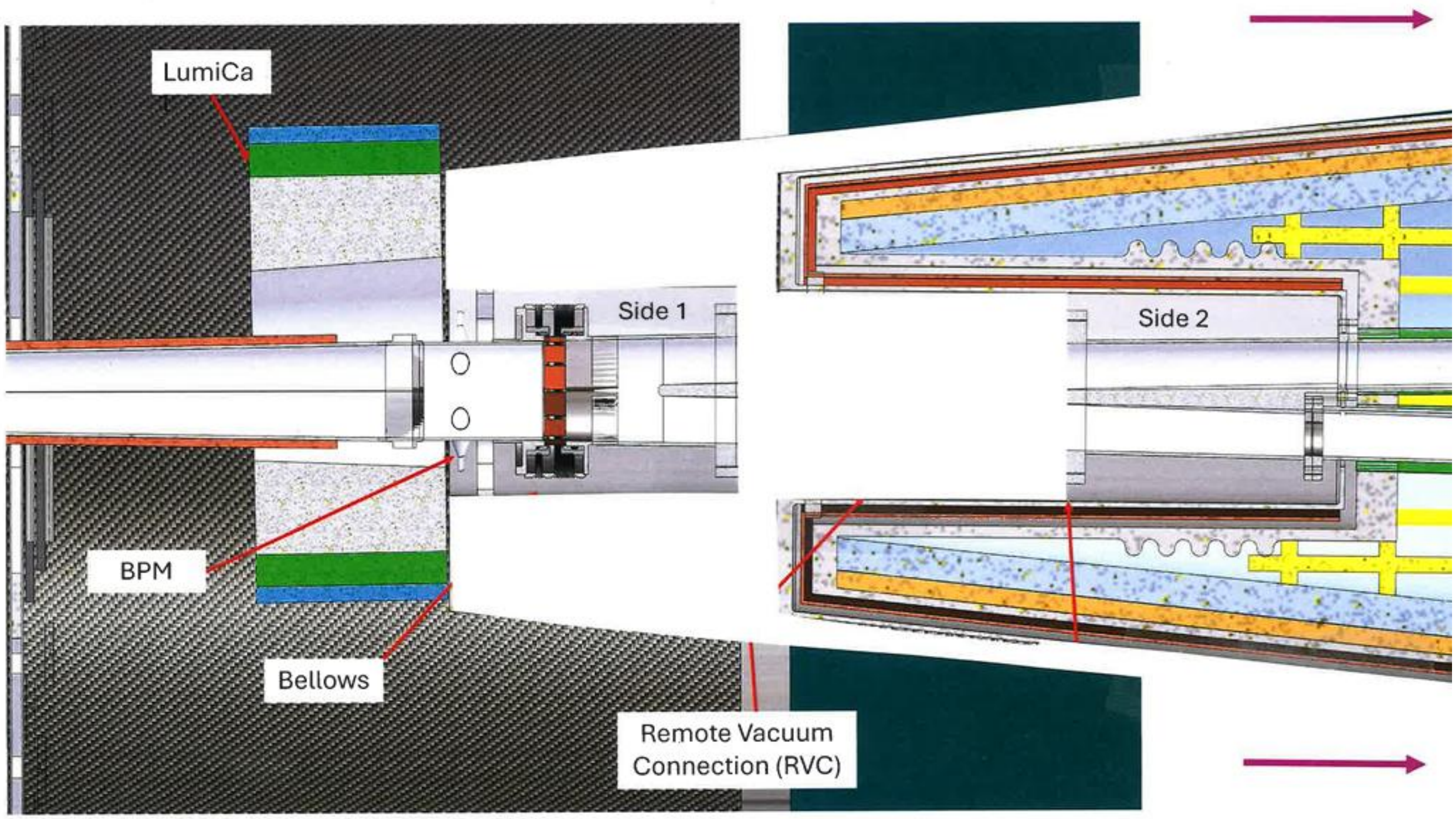

IR accelerator Components Inside the Detector

Interaction region layout

- **Beam pipes in AlBeMet (62% Be, 38% Al)**
- **Central beam pipe 1 cm internal radius**
  - Internally 5 µm gold coated to reduce impedance and shield of sync. rad. photons.
- **Actively cooled**
  - Liquid paraffin for the central one (~60 W) and water for the lateral ones (~130 W).
- **Minimised material budget**
  - Central beam pipe double wall AlBeMet, paraffin and Au (0.68% X_0)
  - Lateral beam pipes minimised within LumiCal acceptance: (mostly 7% X_0, few regions up to 50% of X_0). Shaped to minimise showers off manifolds

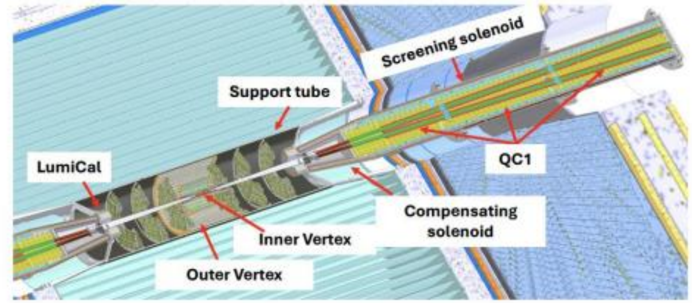

Fig. 47: Interaction Region overall layout. The support tube allows to integrate the luminosity calorimeter (LumiCal) and the vertex detector. Also shown the three segments of the final focus quadrupoles (QC1) together with the screening and compensating solenoids.

Fig. 48: Central chamber in AlBeMet162 including cooling inlets and outlets (left); cross-section view and zoom of the structure of the cooling channel for the paraffin flow.

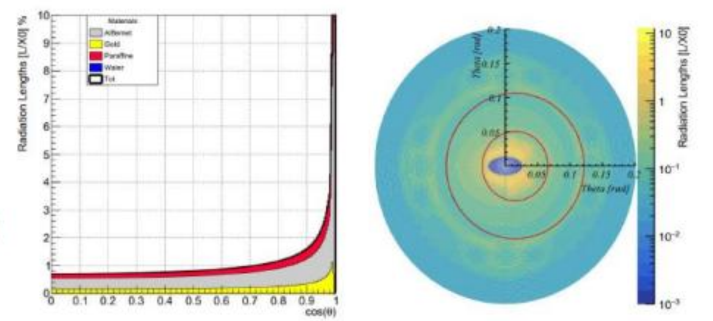

Fig. 50: Material budget of the beam pipe as a function of the polar angle (left) and in front of the LumiCal (right) in the region $\theta \in [0, 0.2]$ rad. The red lines represent the LumiCal acceptance, i.e. the 50 mrad and 105 mrad cones.

Central Beam Pipe, Vertex and Lumi-Cal Integration

Support tube provides integration of beam pipes, vertex and LumiCal

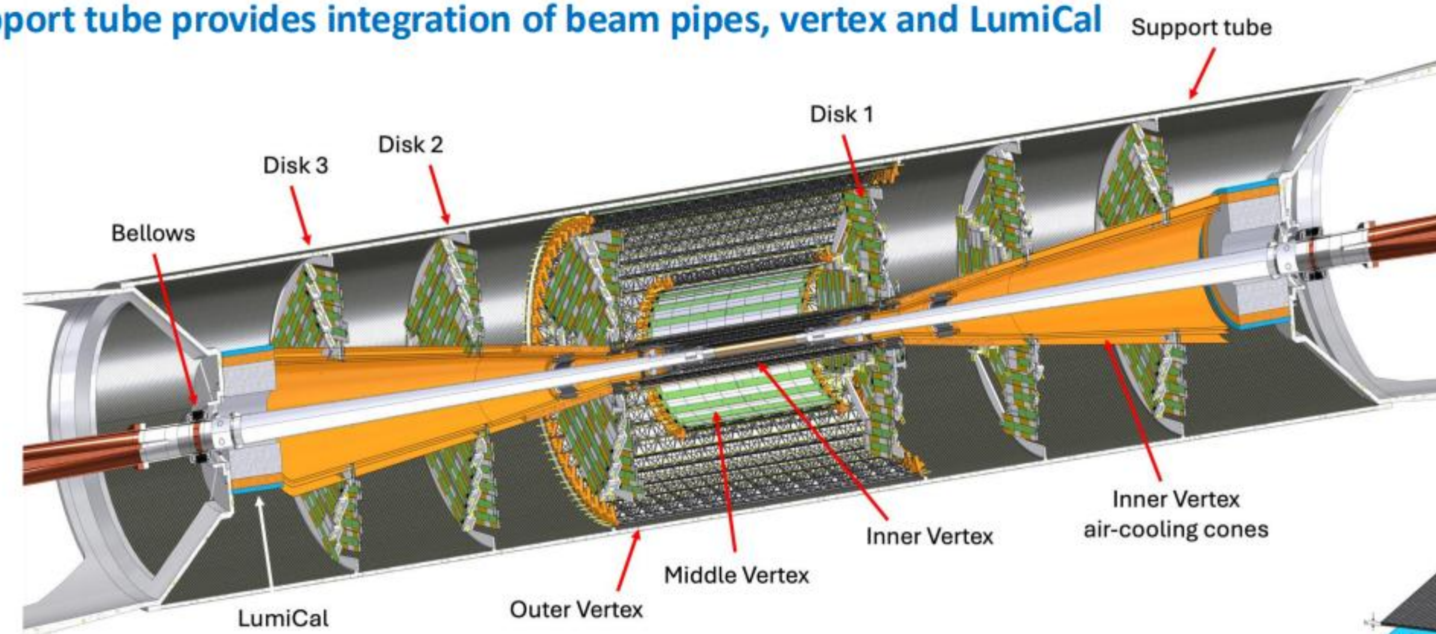

- 1mm CF + 4mm HC + 1mm CF

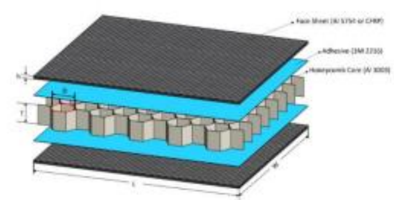

Ref: M. Boscolo, F. Palla, et al., *Mechanical model for the FCC-ee MDI,* EPJ+ Techn. and Instr., https://doi.org/10.1140/epjti/s40485-023-00103-7

Luminosity Monitors

Each of the four experimental IPs will be equipped with a pair of Beamstrahlung extraction lines and associated dump.

Each of these extraction lines will be equipped with the same instrumentation systems (8 lines total).

Monitoring of the Beamstrahlung signal and the Bhabha scattering events will allow precise IP tuning for increased luminosity.

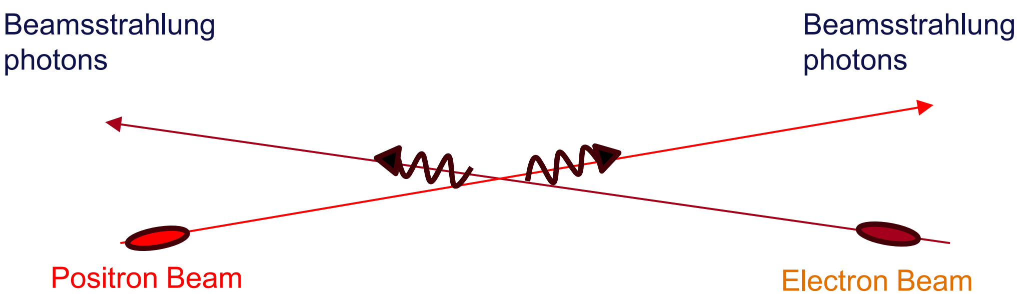

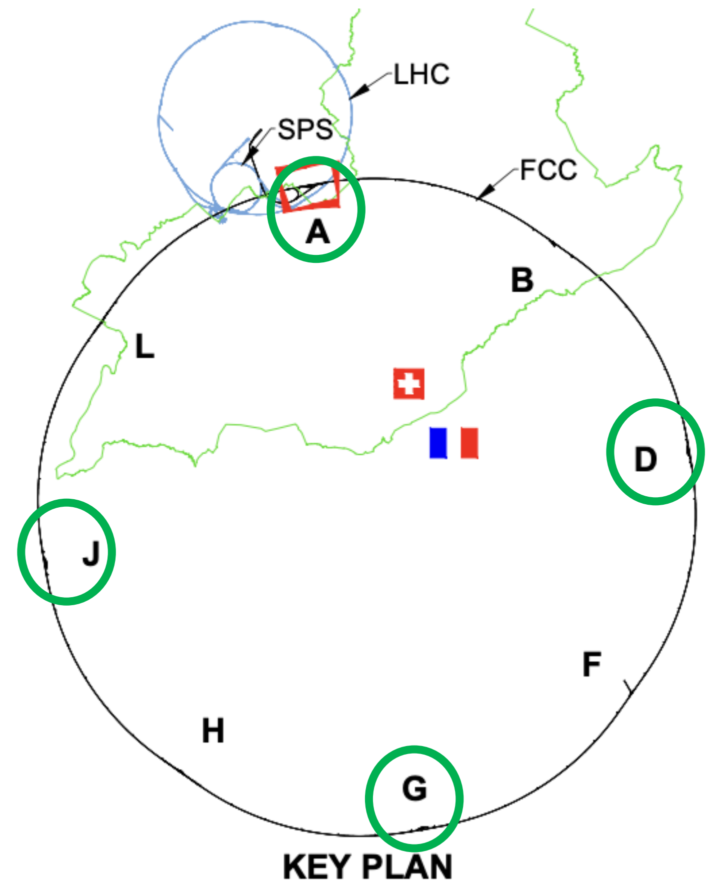

FCCee Accelerator IR Vacuum Chamber (Mock-up)

- Engineered design
- Thermal simulation
- Structural simulation
- Under fabrication

Heat load
54 W central
130 W each side

- **Paraffin flow (central chamber)**
  - Flow rate: 0,015 kg/s
  - Section:68,17 mm^2
  - Velocity: 0,3 m/s
  - Inlet temperature: 18°C
  - Convective coefficient: 900 W/m^{2}K

- **Water flow (Ellipto-Conical chamber)**
  - Flow rate: 0,01 kg/s (4 channels per side)
  - Total flow rate per side: 0,04 kg/s
  - Section: 12,25 mm^2
  - Velocity: 1 m/s
  - Inlet temperature: 16°C
  - Convective coefficient: 1200 W/m^{2}K

M. Boscolo et al)

IR Mechanical Design

Mechanical Design of the detector beam pipe

Q. Ji, L. He

Outer Be Layer: 0.15mm
Gap: 0.35mm, Coolant
Inner Be Layer: 0.2mm
Thickness: ~0.2%X_0

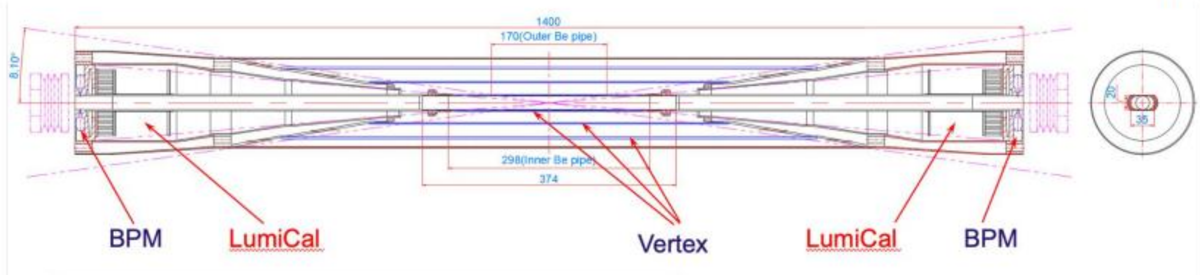

Q. Ji, H. Wang

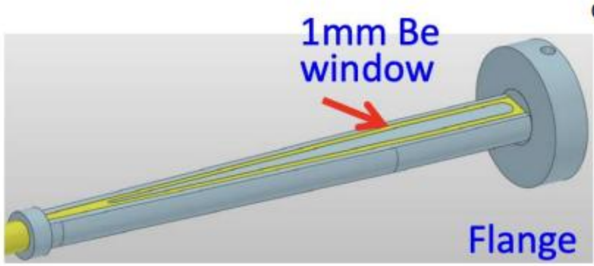

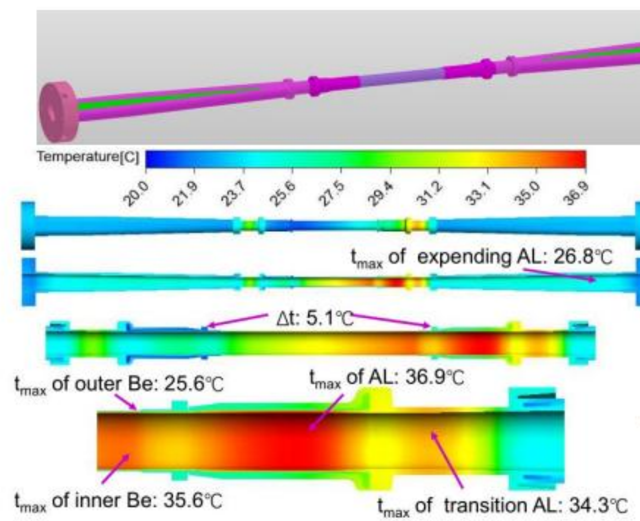

~110w in total

- Water or Paraffin could be used as the coolant
- Preliminary analysis shows that the dynamic temperature/pressure could meet the requirements.

FCCee Interaction Pont Mock-up at INFN-Frascati

- Experimental validation of the IR beam pipes manufacturing and cooling system, vertex and LumiCal integration, vertex cooling, services and routings, and assembly.

- Central beam pipe prototype in aluminium delivered to Frascati.
- First measurements started.

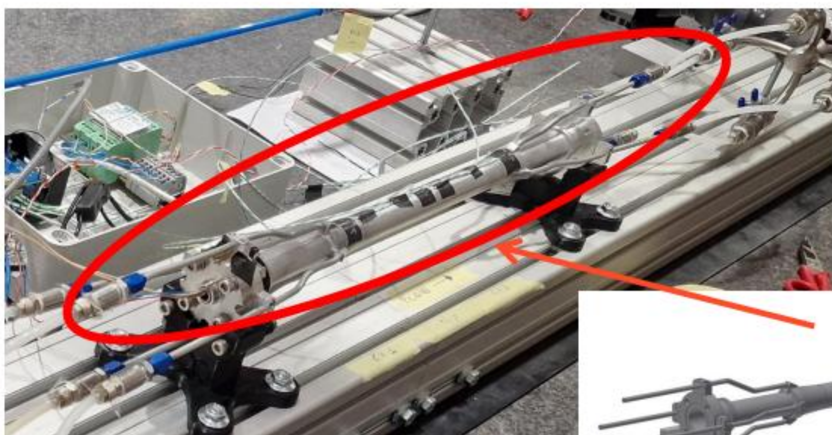

Central chamber connected to the hydraulic circuit

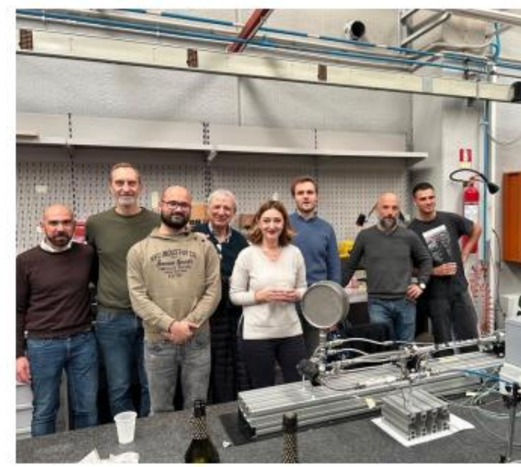

Manuela Boscolo et al + …

KEKB IR Layout and Cryo-plant Overview

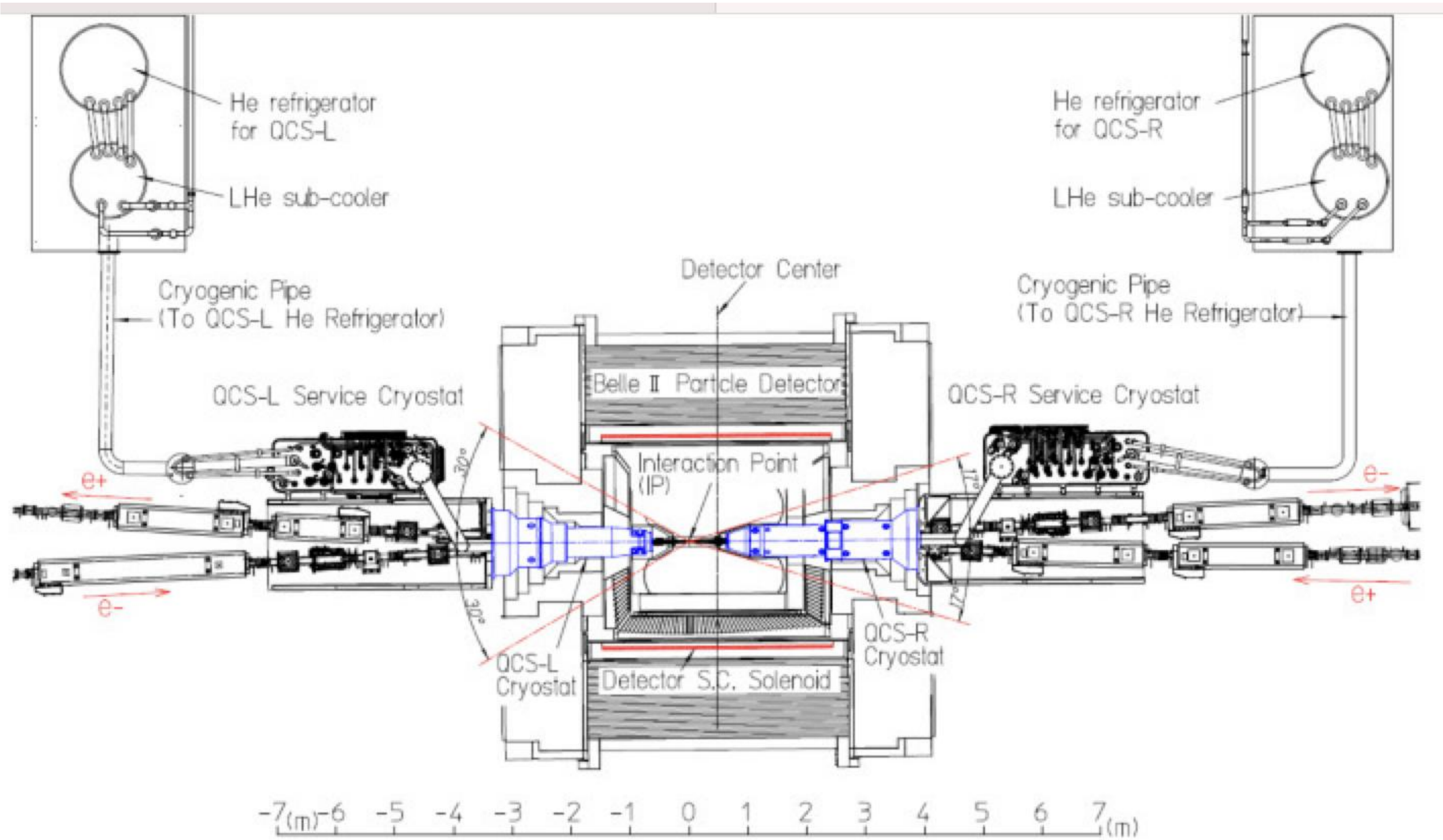

SuperKEKB SC magnet cryostat and feedlines

How the cryogens and power leads enter and leave the cryostat, needed instrumentation and cables

QCS-L cryostat

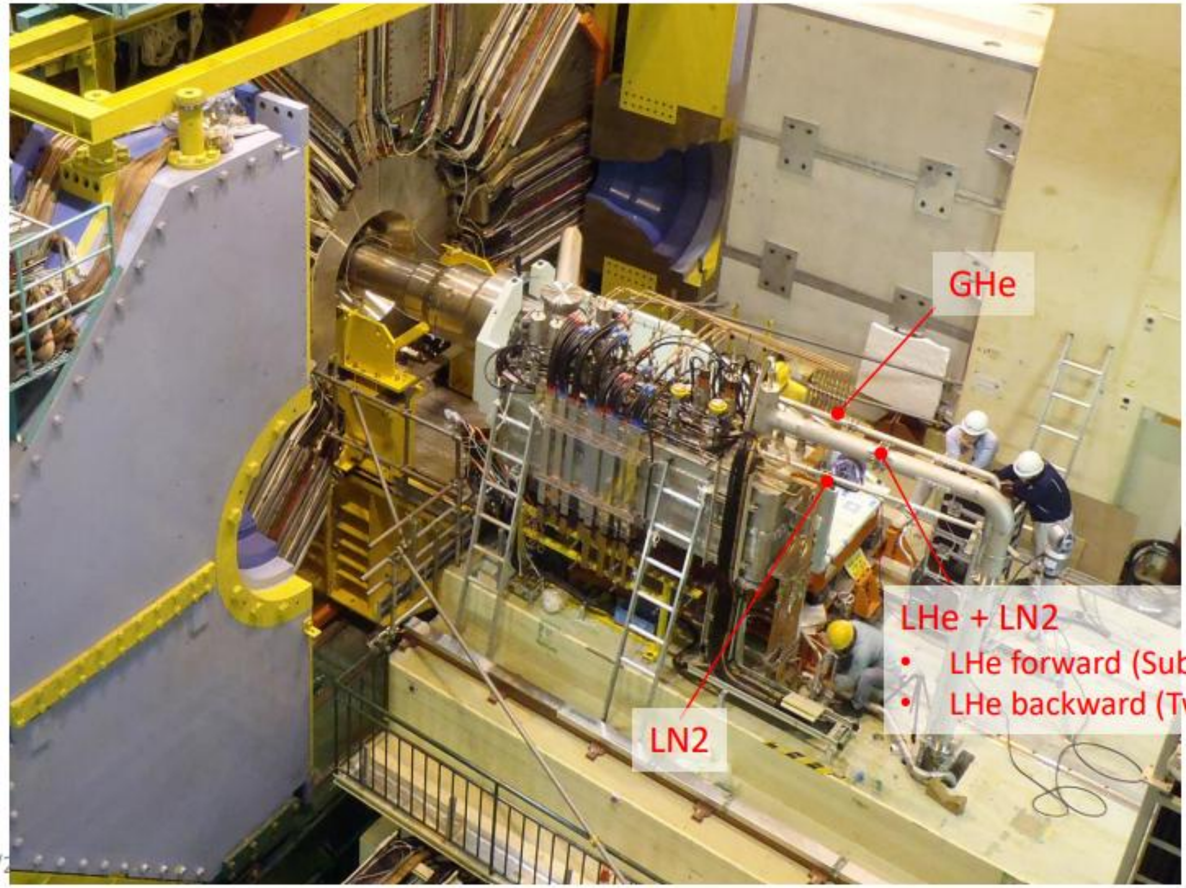

2023/09/2 10

For comparison: SuperKEKB IR SC Magnet System

Norihito Ohuchi (2013): “IR SC magnet system is the most important and complicated hardware in SuperKEKB.”

SuperKEKB IR SC magnets:

8 quadrupoles, 4 solenoids, 43 correctors

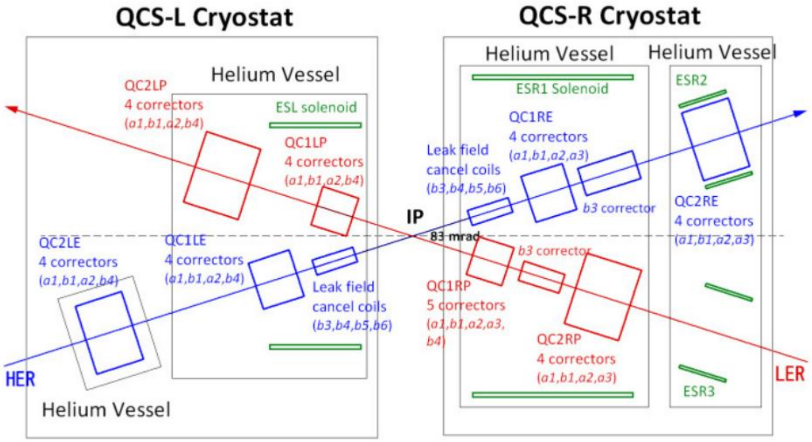

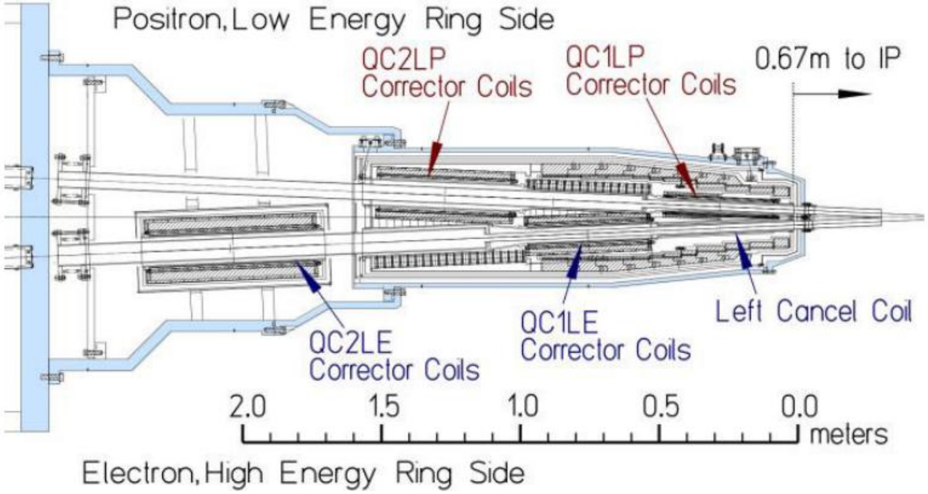

SuperKEKB SC magnet cryostat and slice box

QCS-R cryostat

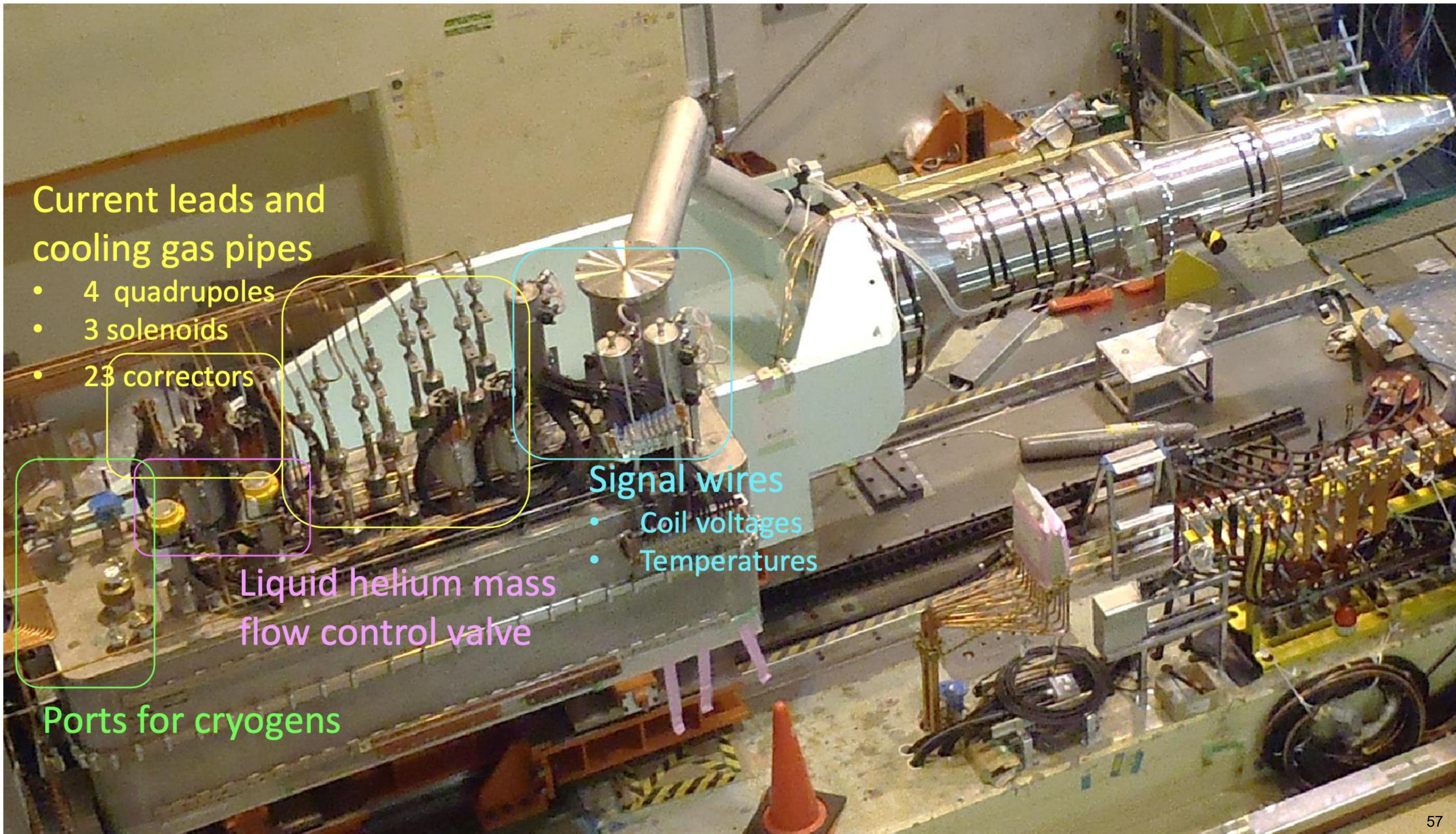

(possible) PFD for He II cooling

Adapted from HL-LHC D2 magnet

Shown:

- Cryogenic distribution line (top)
- Jumper connection (middle)
- IR magnets (bottom)

Considered inner triplets cooled via He II pressurised/He II saturated HEX

Considered solenoids and quadrupoles in the same bath

Thermal shields can use a 40 K – 60 K circuit as in HL-LHC or could potentially be cooled by conduction only from the jumper into the magnet cryostat (shown)

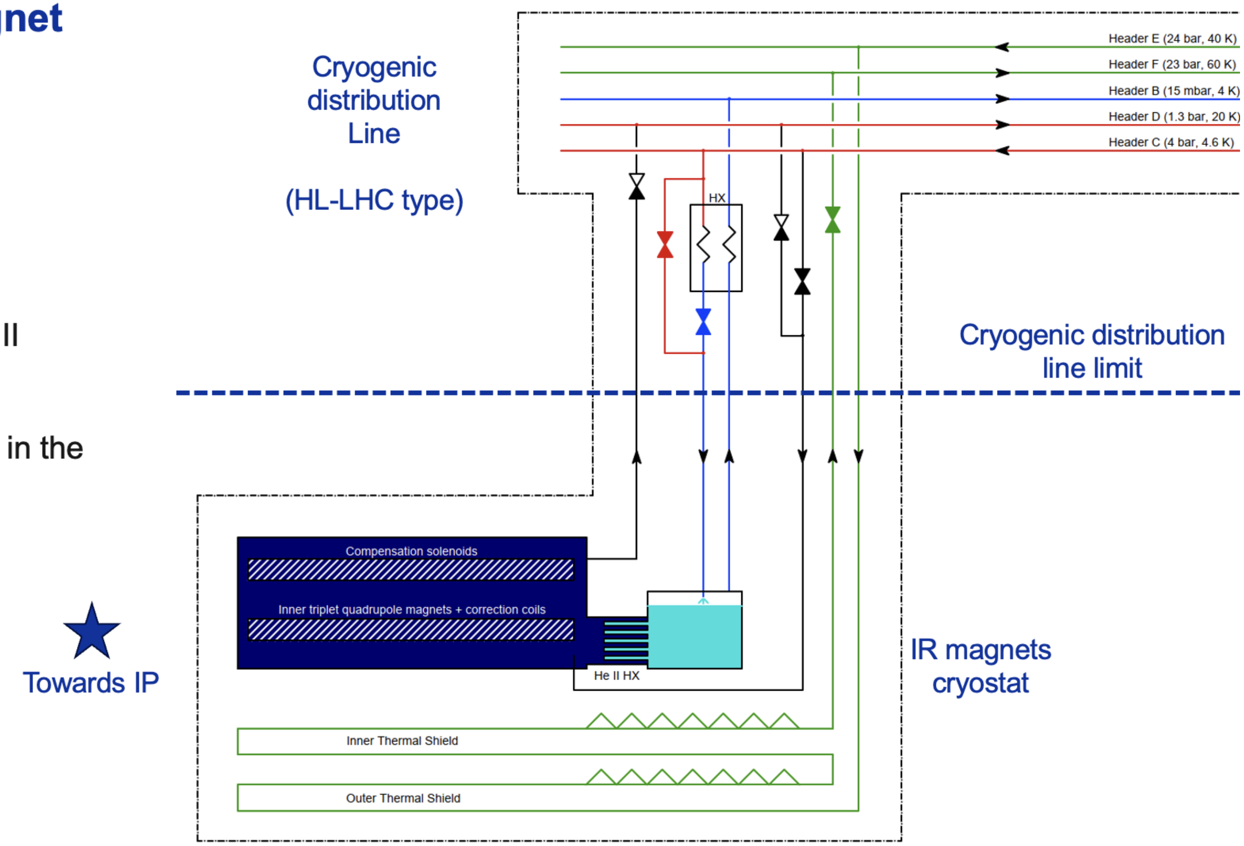

Remote Vacuum Connection Details (KEK and DESY)

SLAC

Super KEKB

How the in-board BPM, bellows and magic flange are positioned and supported, overall alignment, vibration control, etc.

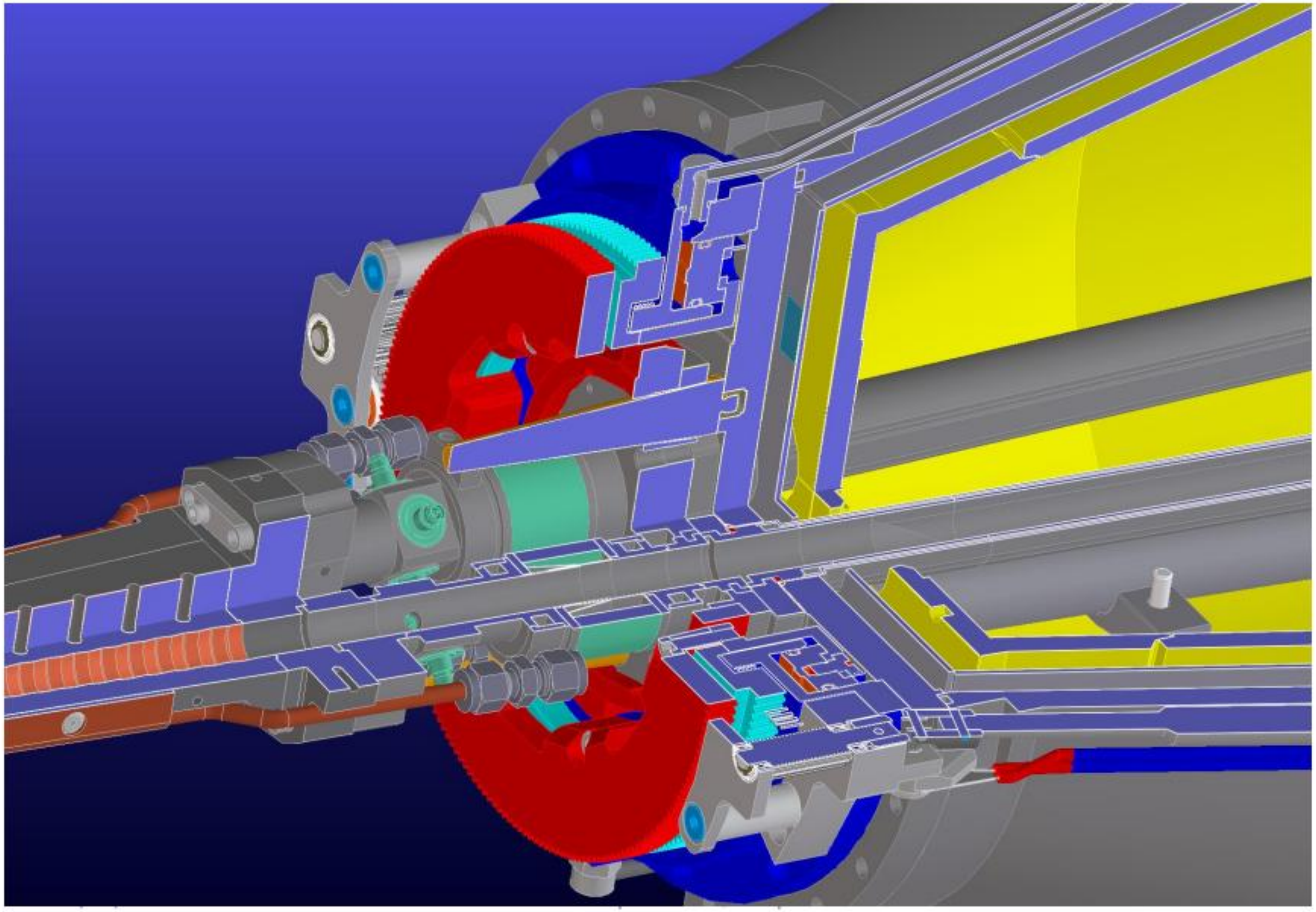

Remote Vacuum Flange (SuperKEKB, Ohuchi)

Super KEKB

How the in-board BPM, bellows and magic flange are positioned and supported, overall alignment, vibration control, etc.

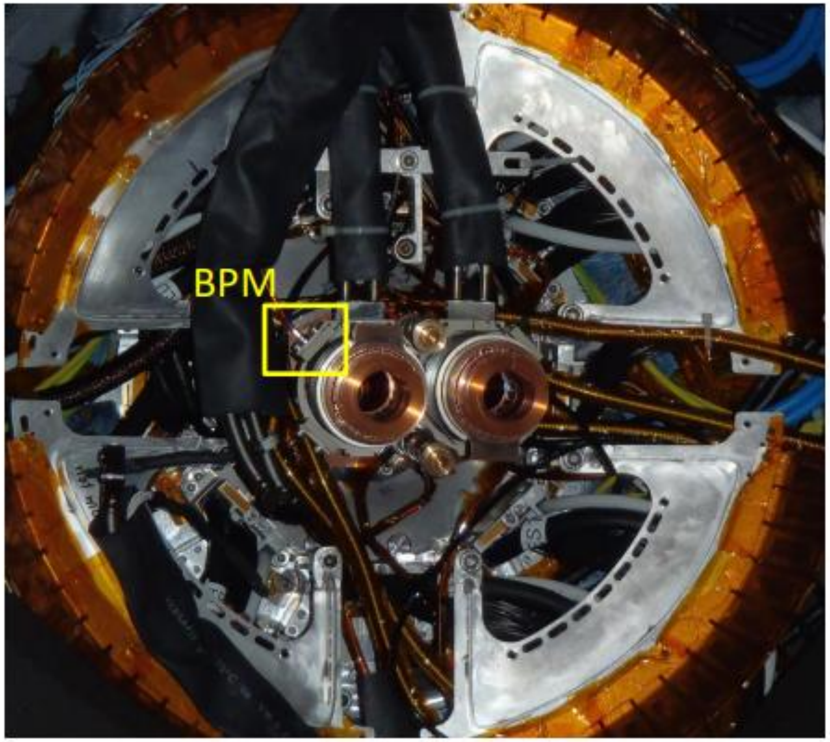

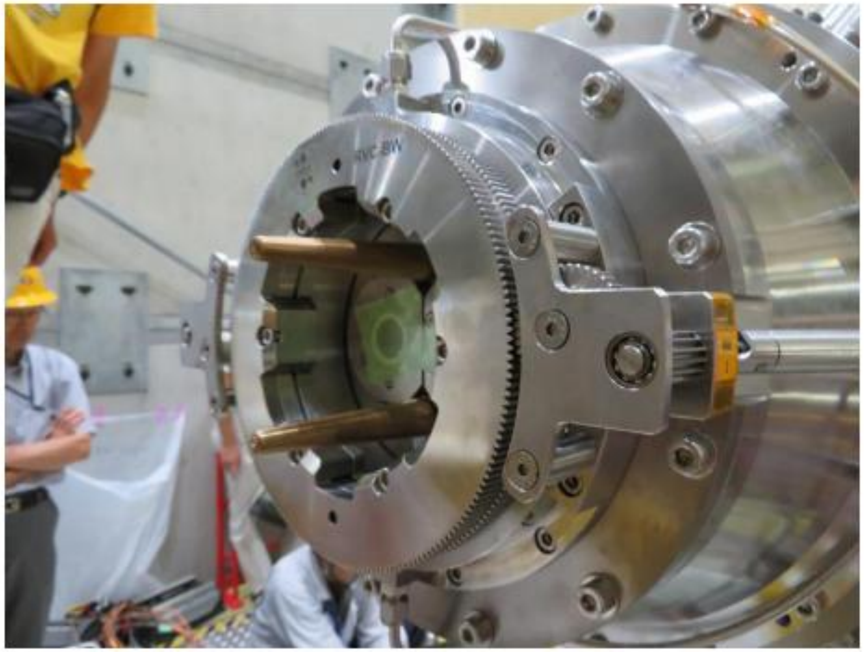

New concept: Remote connection option : SMA

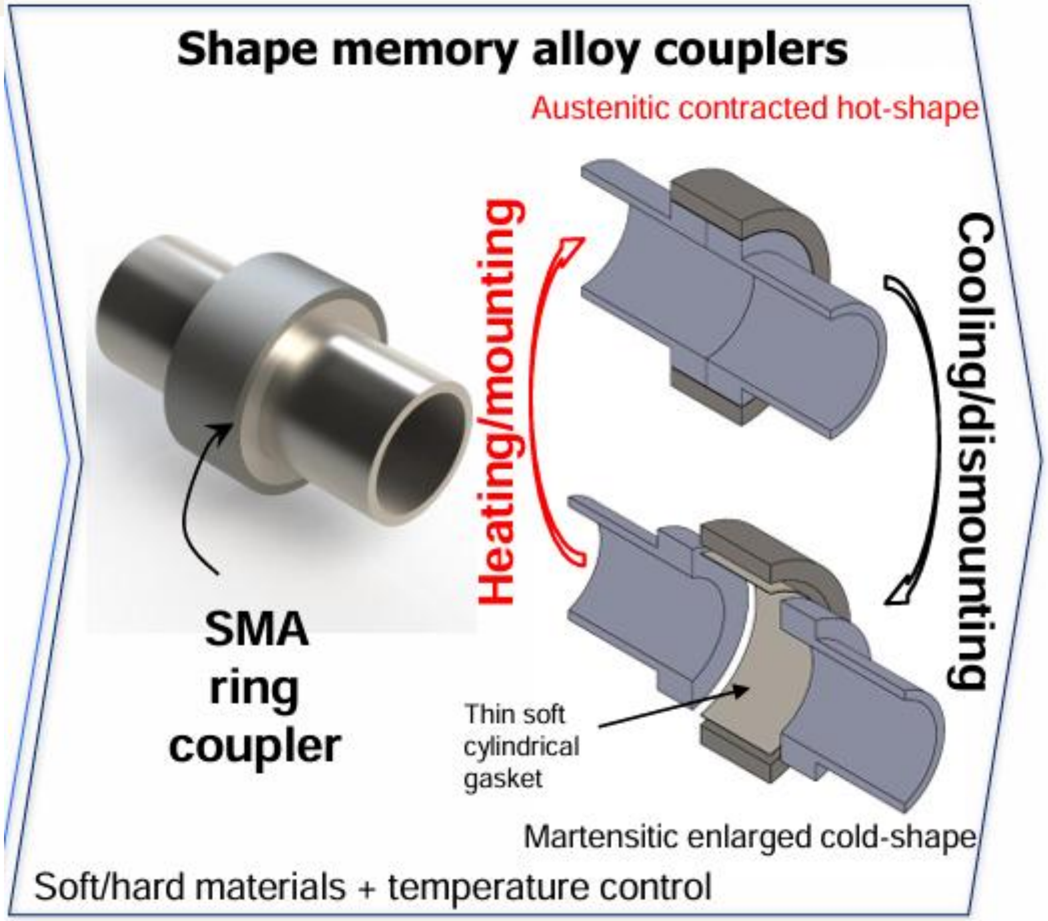

F. Niccoli,
F. Fransesini
…

FCCee Detector End-caps Open Longitudinally

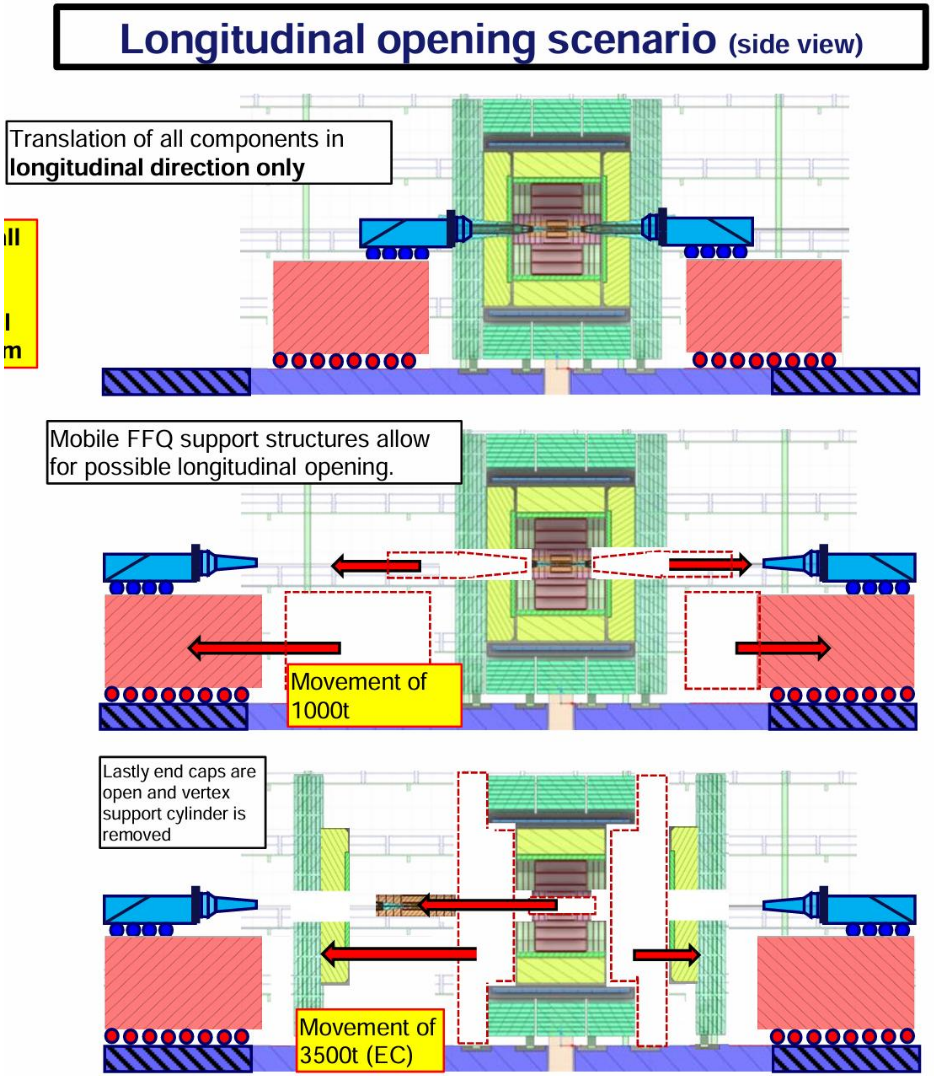

J. Szaga,
O. Beltramello …

Magnets: Beam trajectories in FCCee IR

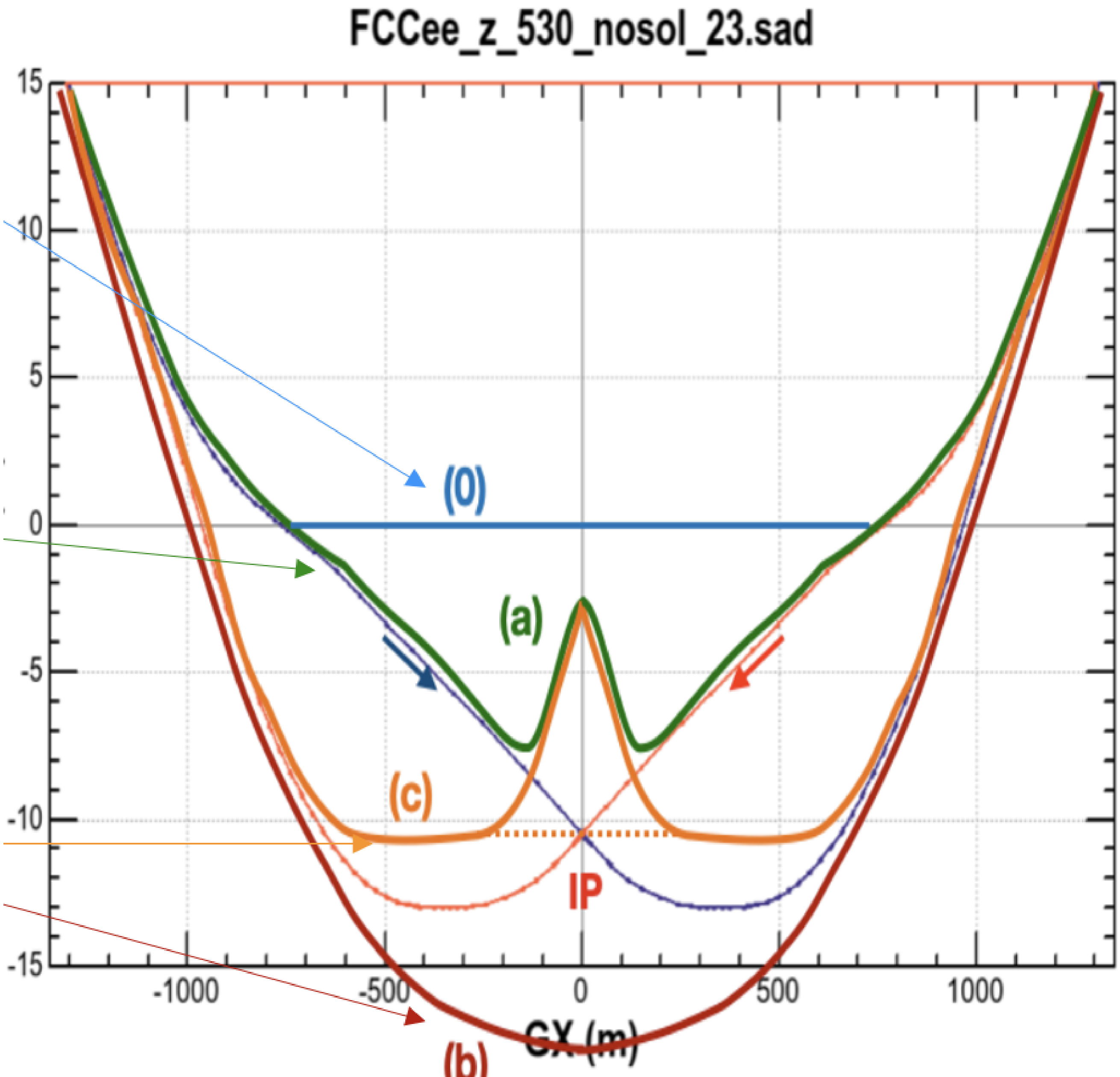

IR MAGNETS: longitudinal locations, lengths, and strengths (K. Oide)

quads	L (m)	s (near)	s (far)	B’ @Z(T/m)	B’ @tt(T/m)
QC2L2	1.25	-7.190225	-8.440225	14.714061	62.103023
QC2L1	1.25	-5.860225	-7.110225	16.568025	41.767626
QC1L3	1.25	-4.310225	-5.560225	-18.109897	-99.714408
QC1L2	1.25	-2.980225	-4.230225	-24.629491	-88.924038
QC1L1	0.7	-2.200225	-2.900225	-43.72333	-96.796669
QC1R1	0.7	2.200225	2.900225	-43.72333	-96.796669
QC1R2	1.25	2.980225	4.230225	-30.963853	-97.183137
QC1R3	1.25	4.310225	5.560225	-15.401024	-82.712171
QC2R1	1.25	5.860225	7.110225	41.716447	17.331058
QC2R2	1.25	7.190225	8.440225	2.96821	62.122116

Z: FCCee_z_575_nosol_5_bb.sad
tt: FCCee_t_572_nosol.sad

K. Oide
27 Sep 2023

K. Oide is available to discussion any needed changes. P. Raimondi’s lattice has more space from QC1 to QC2.

FCCee some cryo-stat dimensions

Cross section views

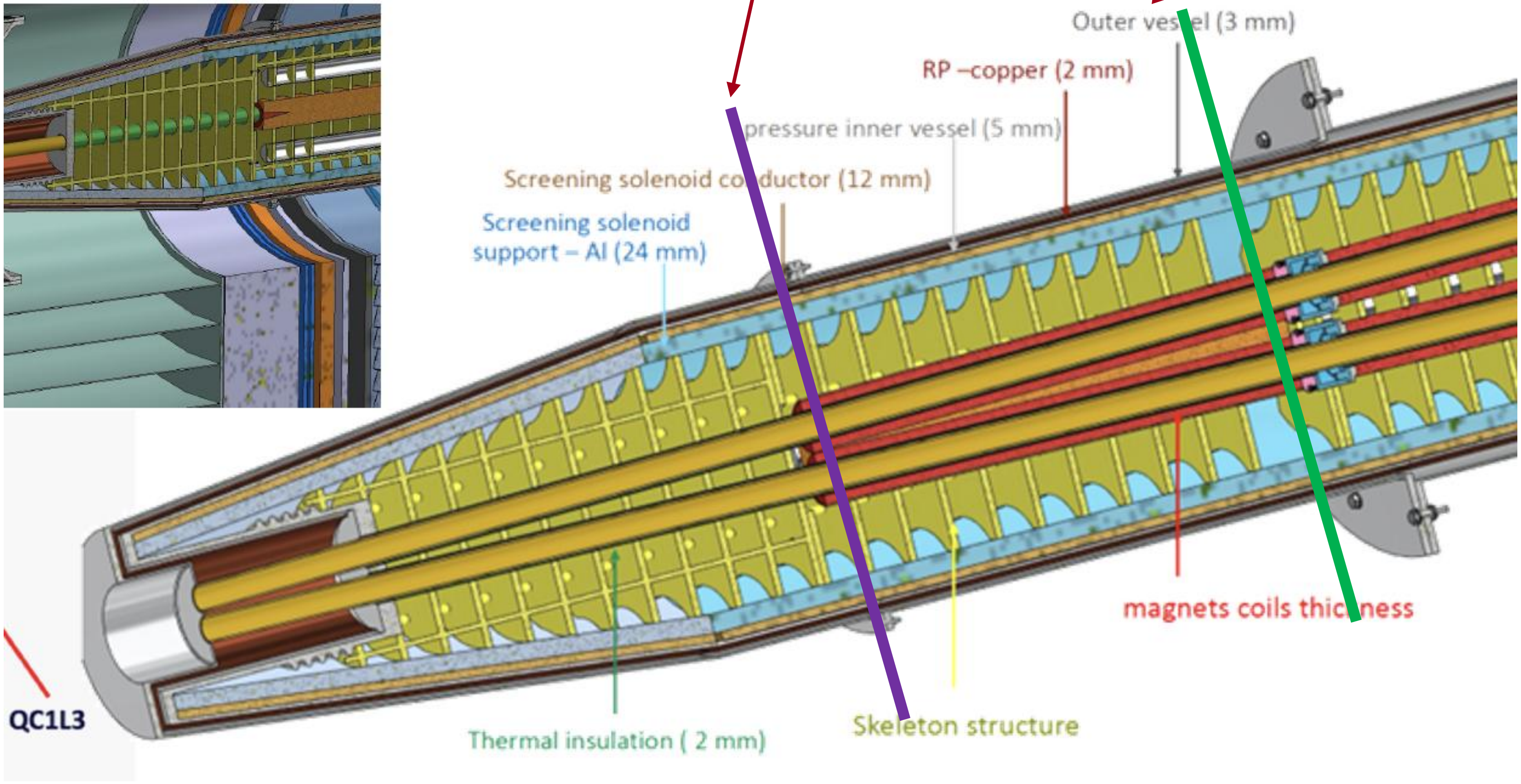

M. Koratzinos, M. Boscolo

IR Magnet Cross Section View (front and end of each magnet)

Showing separated heat shield and vacuum vessel.

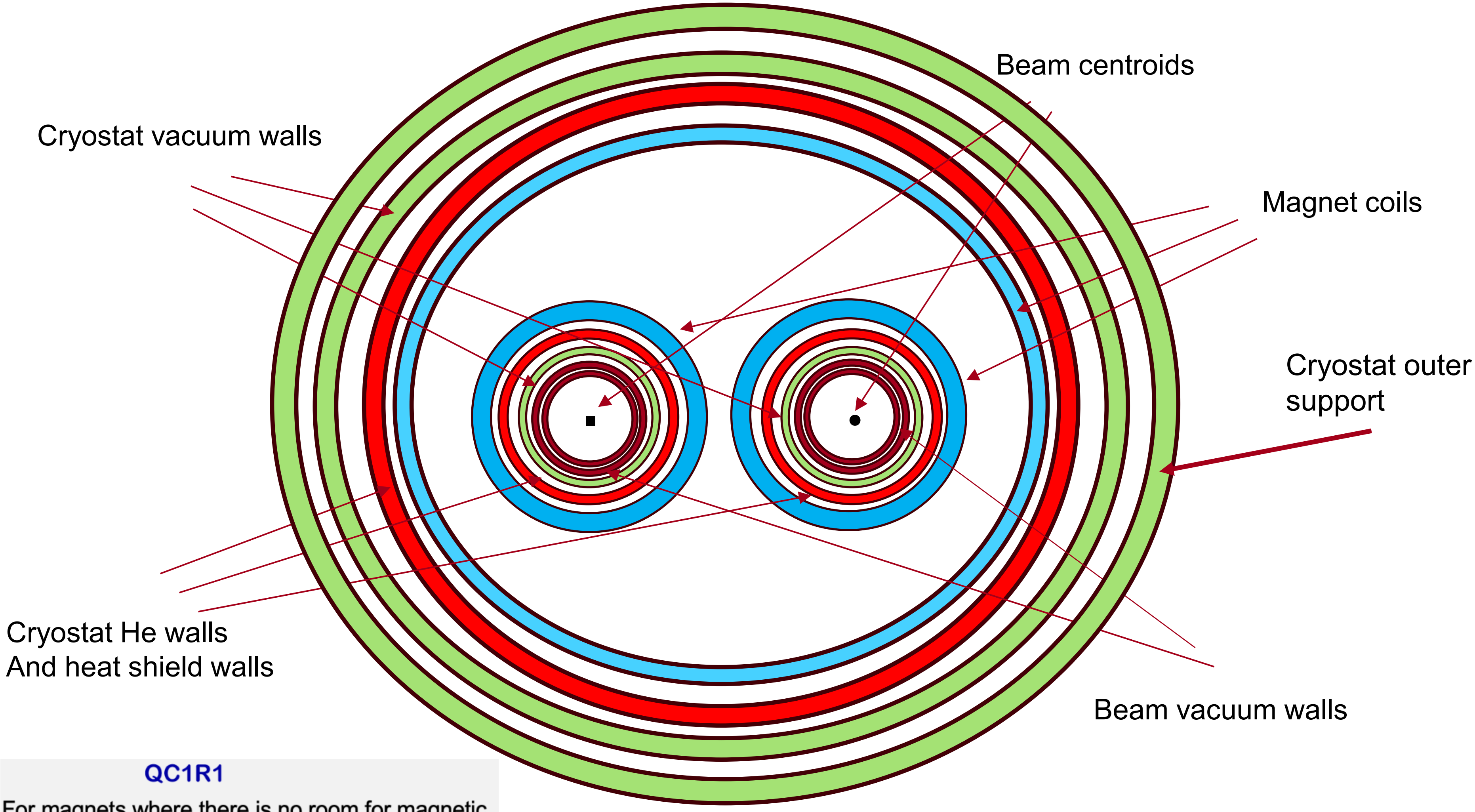

QC1R1

For magnets where there is no room for magnetic yoke material between the coils, the only practical solution is to use flexibility of CCT (double helical) to make local compensation of the magnetic cross talk between side-by-side quadrupole apertures.

J. Seeman November 2023

IR cryostat component dimensions

10	**Solenoid axis line**
11	
12	Support shim thickness
13	Trim coil thickness
14	Magnet coil thickness
15	Support shim thickness
16	He vessel thickness
17	Insulating vacuum thickness
18	Heat shield (~50K)
19	Insulating vacuum thickness
20	Vacuum vessel thickness
21	Air gap
22	Outer beam pipe thickness
23	Water cooling layer for pipe
24	Inner beam pipe thickness
25	Inner vacuum wall to beam
26	Beam center
27	**Sum: solenoid axis to beam**
28	
29	**Beam location (15 mrad)**

29	**Beam location (15 mrad)**
30	
31	Beam center
32	Outer vacuum beam to wall
33	Inner beam pipe thickness
34	Water cooling layer for pipe
35	Outer beam pipe thickness
36	Air gap
37	Vacuum vessel thickness
38	Insulating vacuum thickness
39	Heat shield (~50K)
40	Insulating vacuum thickness
41	He vessel thickness
42	Support shim thickness
43	Magnet coil thickness
44	Trim coil thickness
45	Support shim thickness
46	Anti-solenoid support
47	Anti-solenoid coil thickness
48	Large spacer
49	Shim thickness
50	He vessel thickness
51	Insulating vacuum thickness
52	Vacuum vessel thickness
53	Copper shielding thickness
54	Support rod gap
55	External support thickness
56	**Sum: beam center to outside**
57	
58	**Overall sum**
59	
60	**Dectector stay clear (100 mrad)**

FCCee IR Cryostat (preferred option):

IR QC1 and QC2 in different cryostats but one integrated raft (not to scale)

Need to make space for cryogens, leads, and cantilever supports.

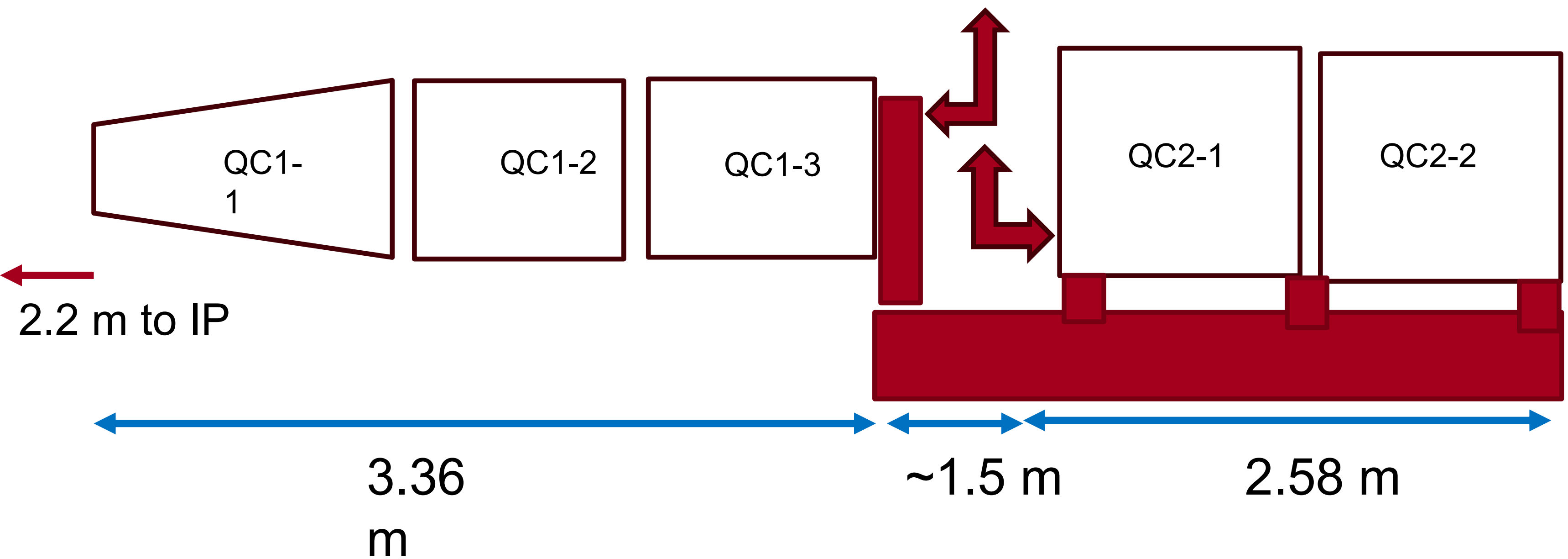

Needed functions for the space between QC1 and QC2

1) Beam pipes (cold vs warm)
2) e+ and e- BPMs (radial space)
3) Cantilevered supports (many forces)
4) Detector shielding near beam pipe (backgrounds and magnet quenches)
5) Vibration mitigation and control (orbit control)
6) Two cryostat end caps, cryogenic ports, disconnects (cryogen flow, heat load)
7) Magnet leads (warm to cold)
8) Alignment (internal positioning, remote)
9) Instrumentation (what to measure and how)
10) Remote operation flange controls and access (design, safe operation)
11) Vacuum disconnects (locations)
12) Assembly strategy (order of installation)
13) Cool down radial differential movements ($\Delta r/r$ ~3x10^-3, 0.5 mm movements)
14) Cables (routes, numbers)

CEPC IR 6.8 m cryostat (Dec 2023)

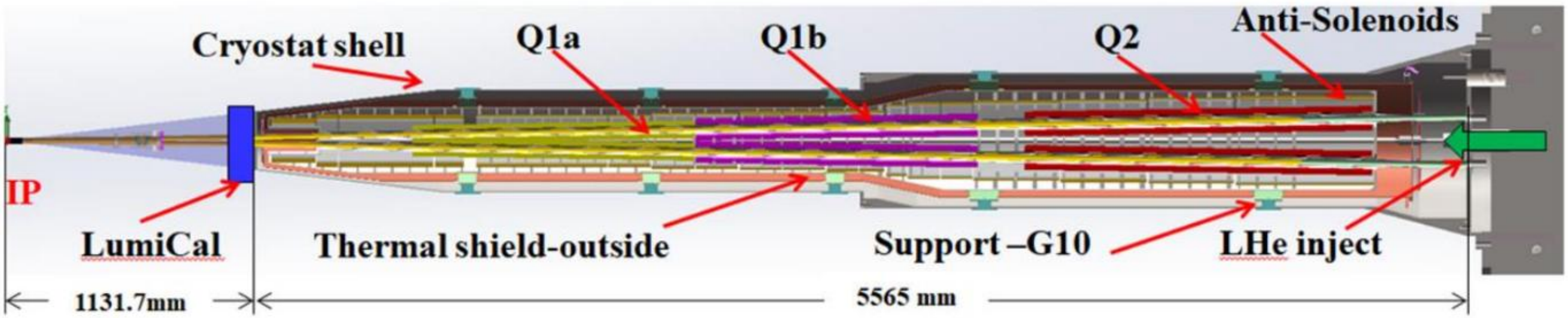

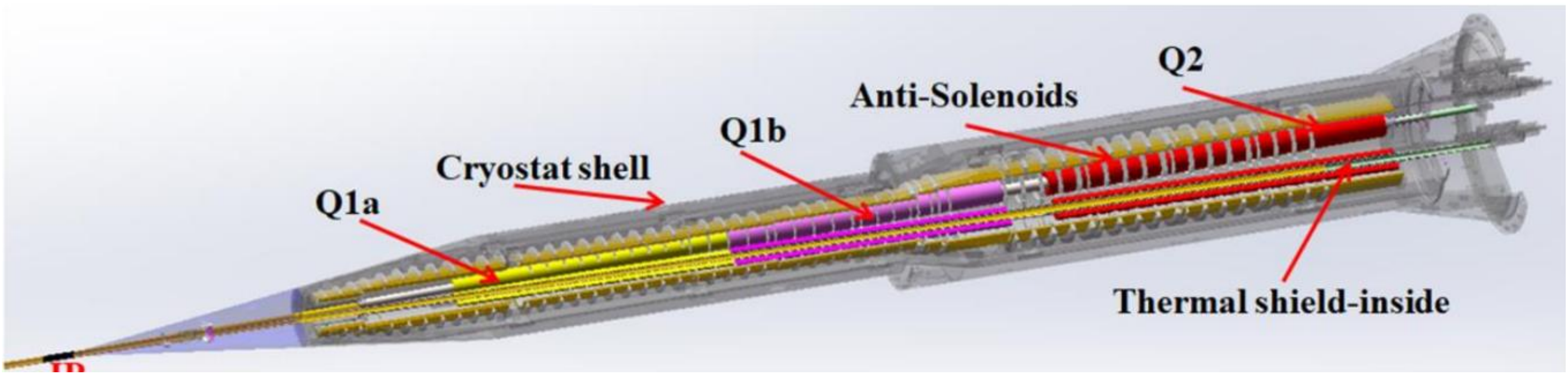

ILC IR magnet locations (2013)

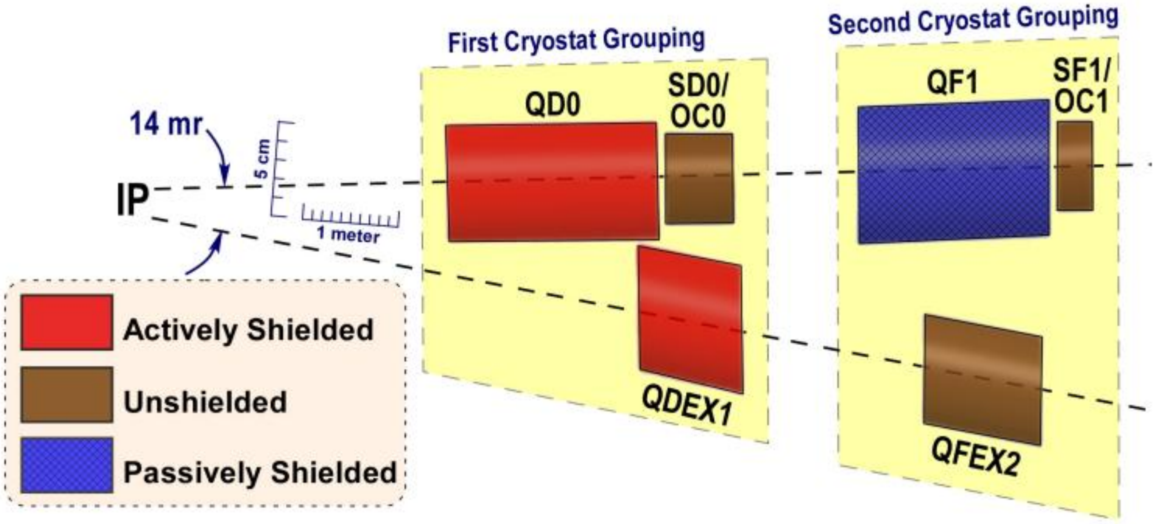

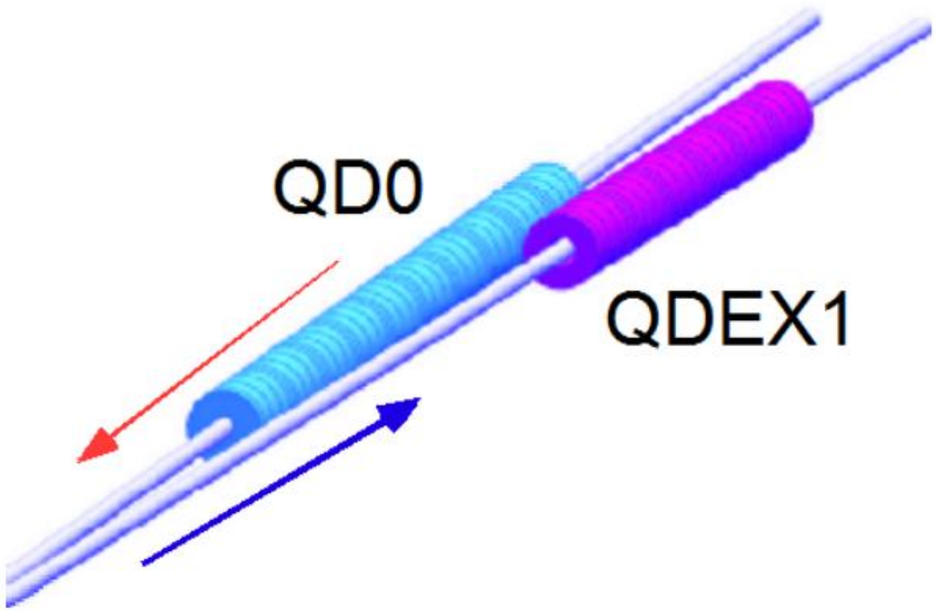

ILC IR magnets (2013)

Figure 8.8
Engineering model of the detector-mounted final-focus magnets [173]. The QD0 magnet is split into two coils to allow for energy flexibility.

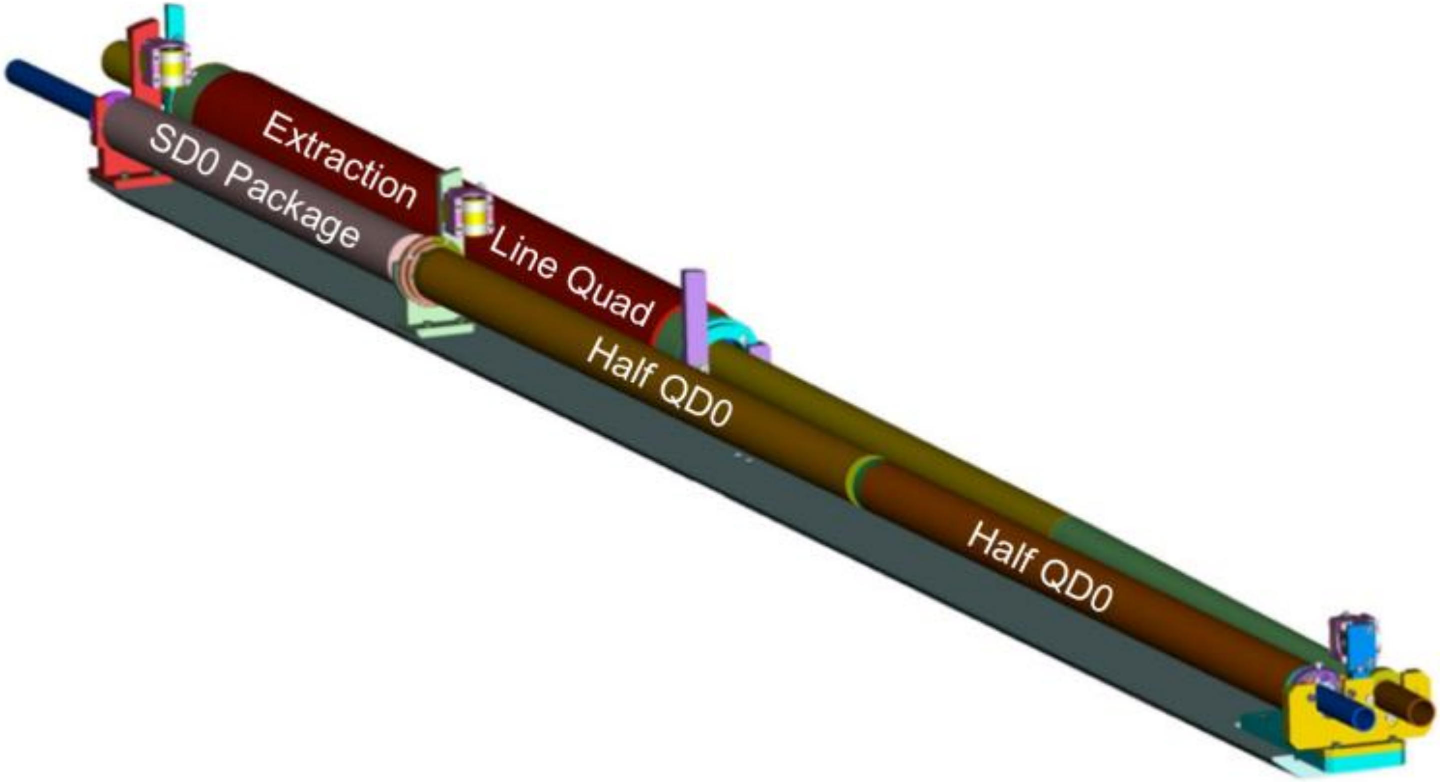

Canted Cosine Theta quadrupoles and direct wind (BNL)

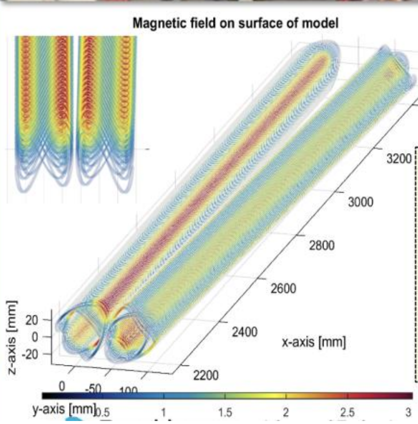

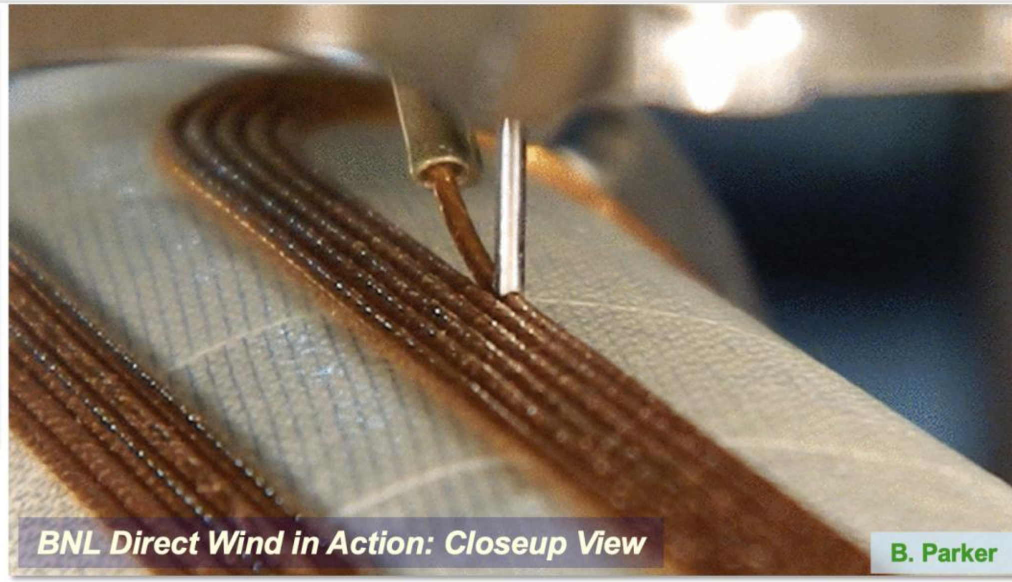

In addition to main quad coils, we need a slew of correctors (b_1, a_1, a_2...).

BNL Direct Wind process is natural for making the necessary correctors.

All coil designs must take into account the mutual external field cross talk.

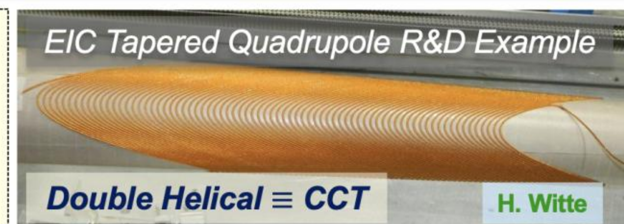

Direct Wind Tapered Double Helical Coil

Field quality - cold

- Work under way, but already <1unit for all multipoles
- We did not do the same trick during cold measurements
- The 'warm' measurements below come from the unrotated data

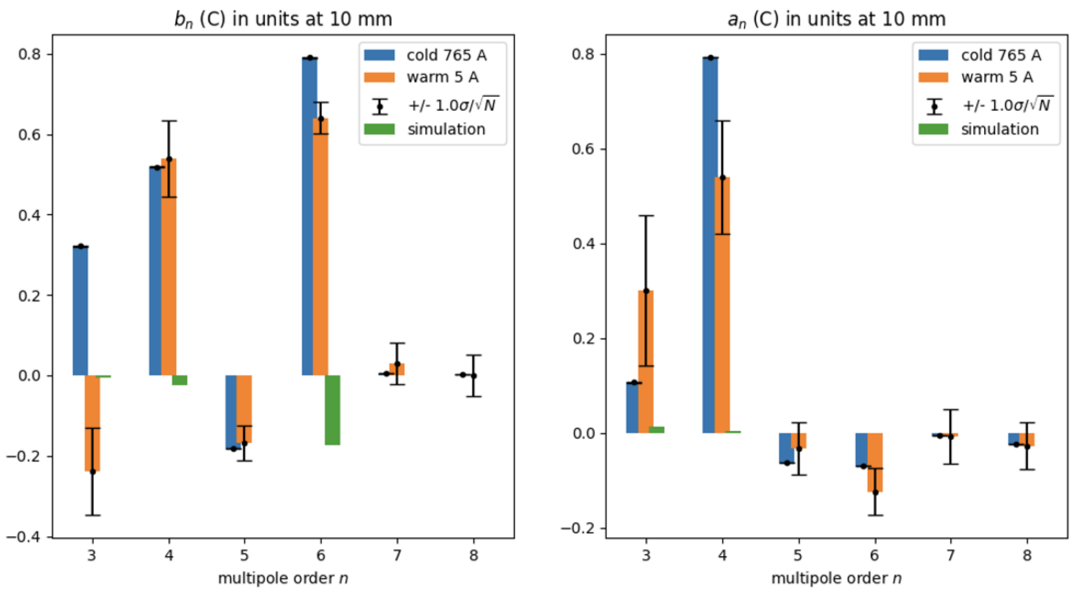

Detector and accelerator solenoid magnetic fields

SLAC

FCC eeFACT 2025 - Tsukuba 05/03/2025 Andrea Ciarma INFN LNF 6

Magnetic Fields in the IR

In addition to the 2T solenoidal field of the experiment, allow for correct tracking of charged background particles, in particular those generated in the separated beam pipe region of the MDI area.

- Field coming from the **anti-solenoids** (screening-S, compensating-S) imported via **field map** to account for fringe effects

- Implementation of **FF quadrupole fields** in the Key4hep geometry

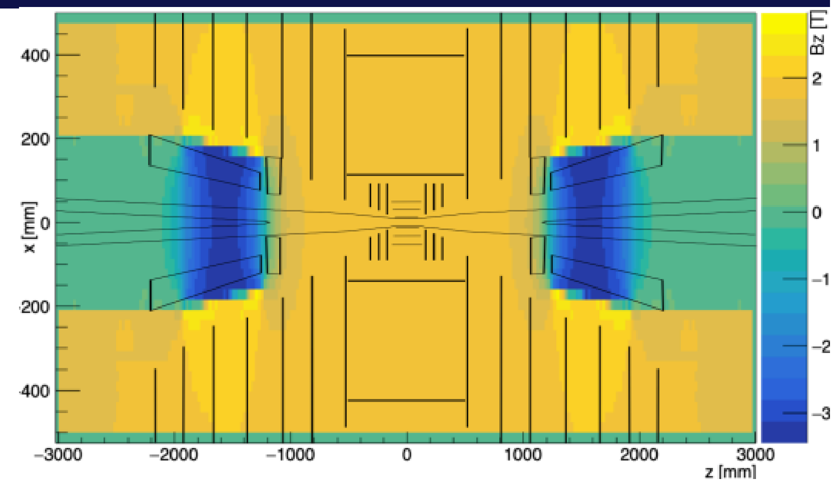

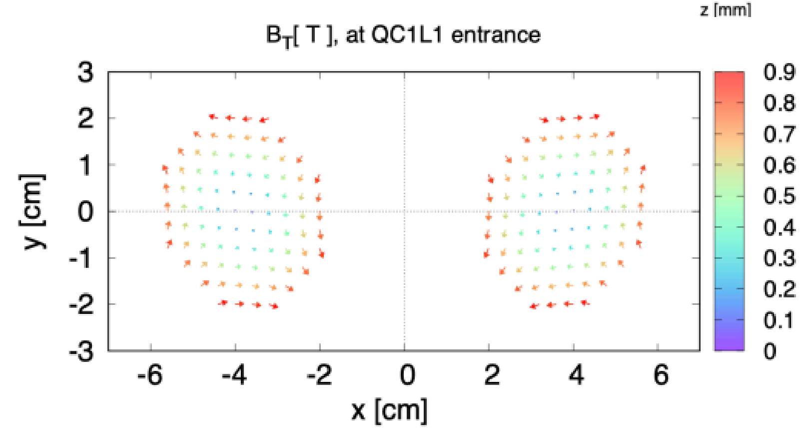

IR Accelerator Optics – Solenoid Compensation

Two schemes to compensate the coupling induced by the detector field.

Screening solenoid around portion of QC1 inside the detector

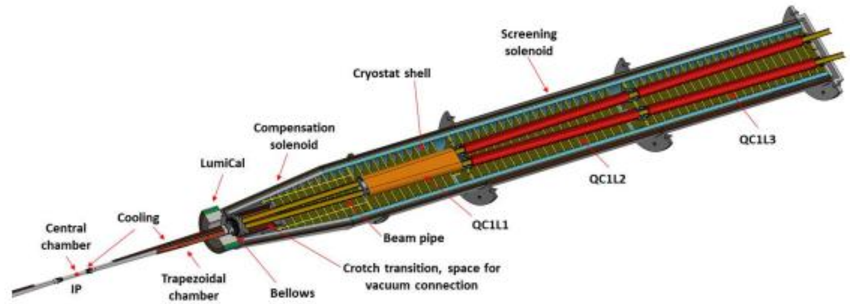

Local **solenoid compensation scheme (Baseline design)**

- Strong anti-solenoid (-5 T) in front of QC1

Non-Local **solenoid compensation scheme**

- Anti-solenoid outside (~ 10 m from the IP)
- Weak corrector dipoles
- Skew quads windings around FFQs

A. Ciarma et al: https://doi.org/10.18429/JACoW-IPAC2024-TUPC68

- This solution is optics independent (in terms of final focus quads)
- The tuning knobs -correctors and skews- are needed for orbit and coupling correction for all optics.

BNL Direct Wind

"3D Printing" Superconductor

Alternative IR Solenoid Compensation Scheme

SLAC

A. Ciarma†, M. Boscolo, INFN-LNF, Frascati, Italy
H. Burkhardt, CERN, Geneva Switzerland and Univ. Freiburg, Germany
P. Raimondi, Fermilab, Chicago, USA

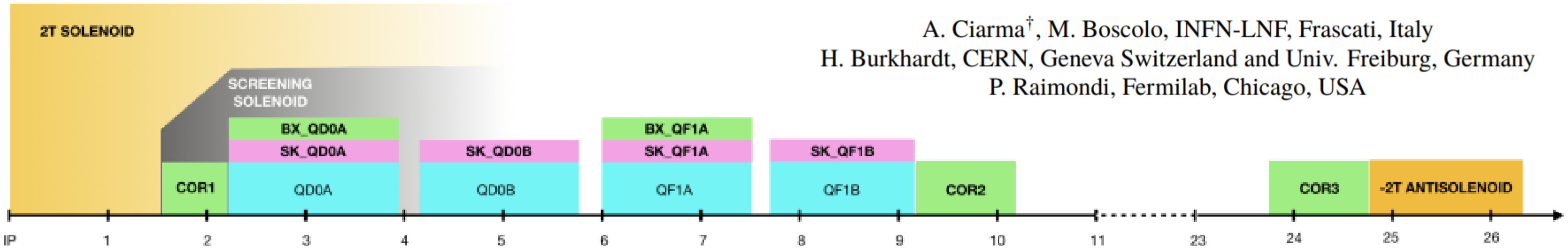

Figure 2: Layout of the standard solenoid compensation scheme for LCCO lattice v92.

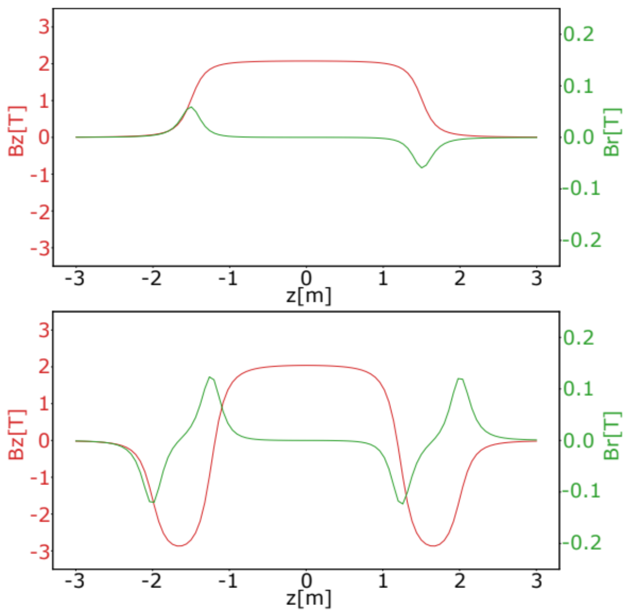

Figure 1: Longitudinal (red) and radial (green) magnetic fields along the 15 mrad axis in the two compensation schemes (standard proposed here on the top, baseline on the bottom).

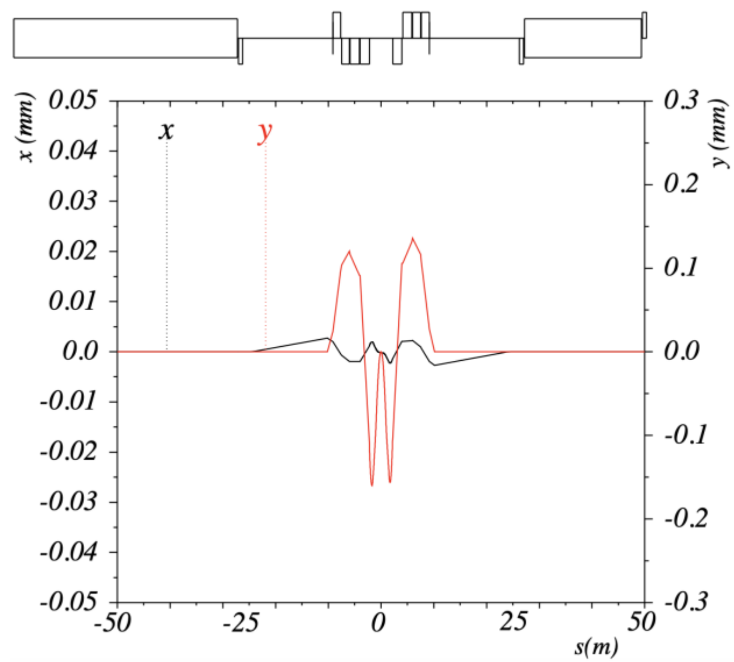

Figure 3: Horizontal and vertical orbit bumps.

Solenoid Compensation Scheme (B. Parker, V. Teotia, BNL)

Field Profile for IDEA Detector & Screening Solenoid

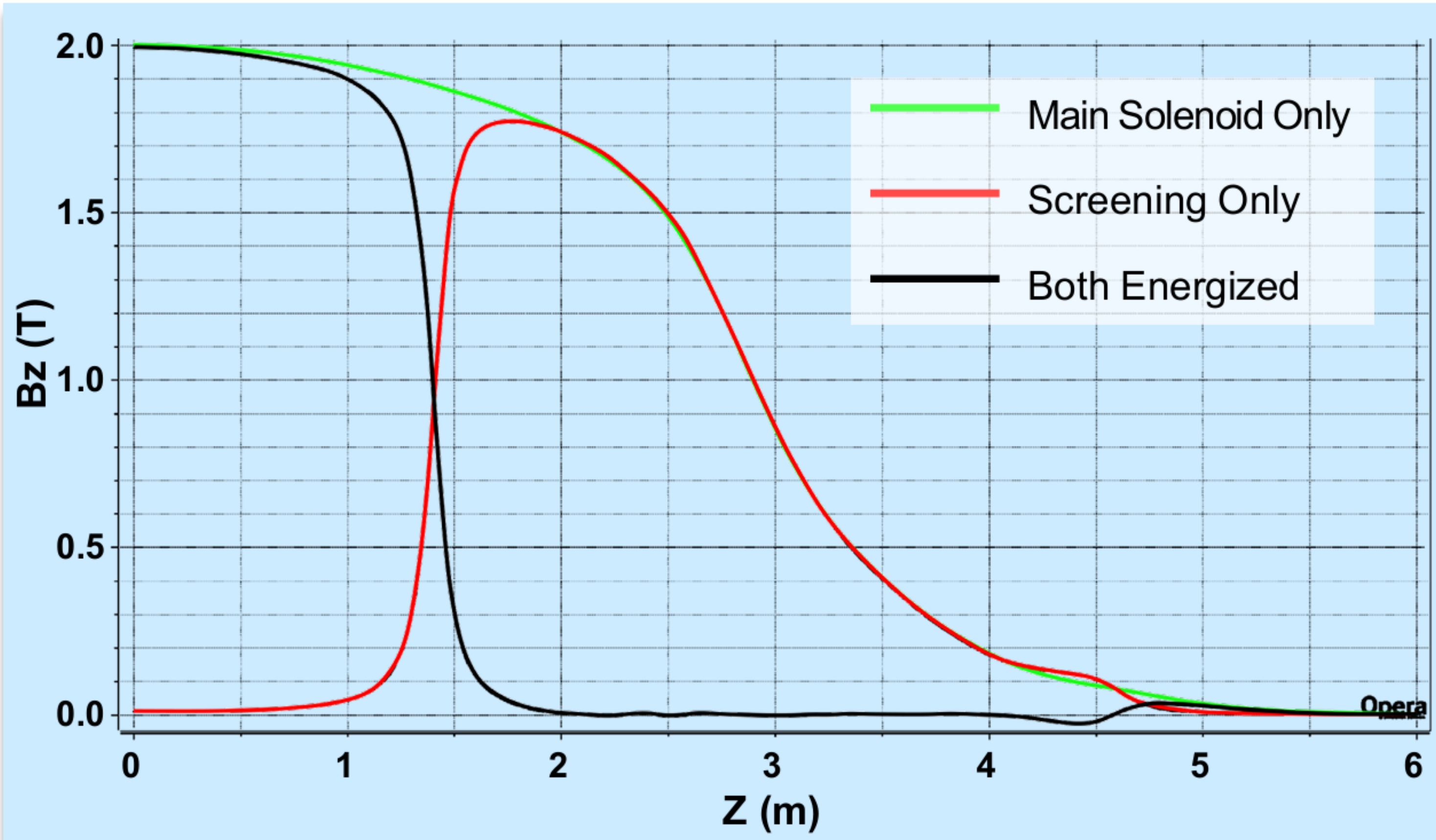

PEP-II IR BaBar detector field measurements

Permanent magnets were used inside of BaBar.
Outside quadrupoles were steel magnets.
We calculated the solenoid field escaping outside the central hole using OPERA-2d to see if the near steel magnets would saturate. OK in end.
Measured fields in the hole were measured.

OPERA-2d field calculations.

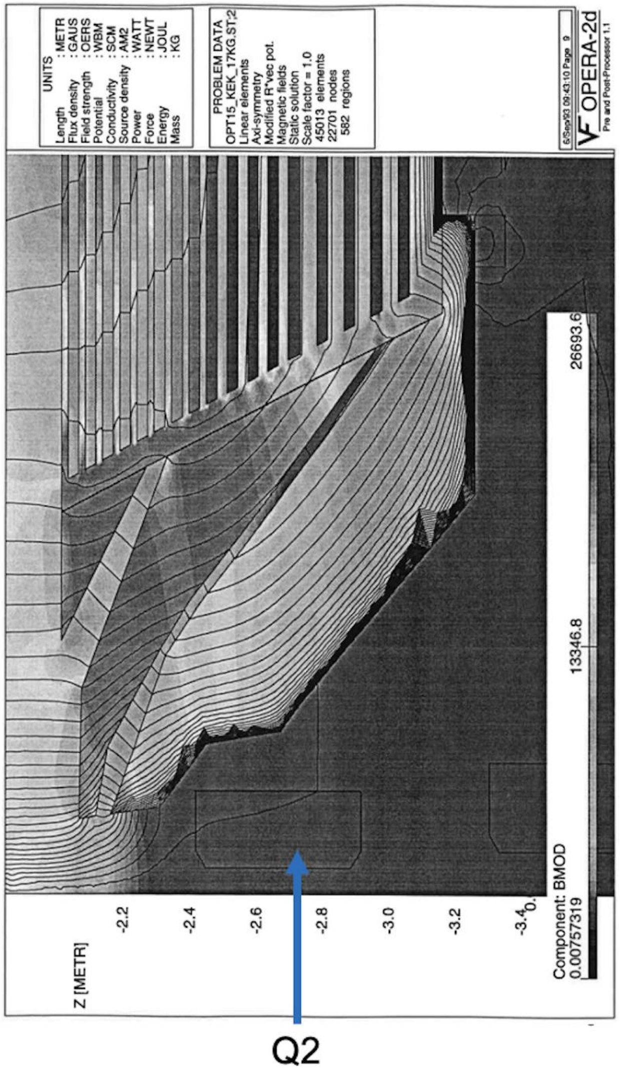

PEP-II IR rafts near BaBar detector

Q2, Q4, Q5 rafts were assembled in the shop and then installed by the overhead crane in the IR hall. These cantilevered supports were vibration sensitive and much work was invested in damping them.

Raft 15: Lifting Back Raft In HFB 04/21/99

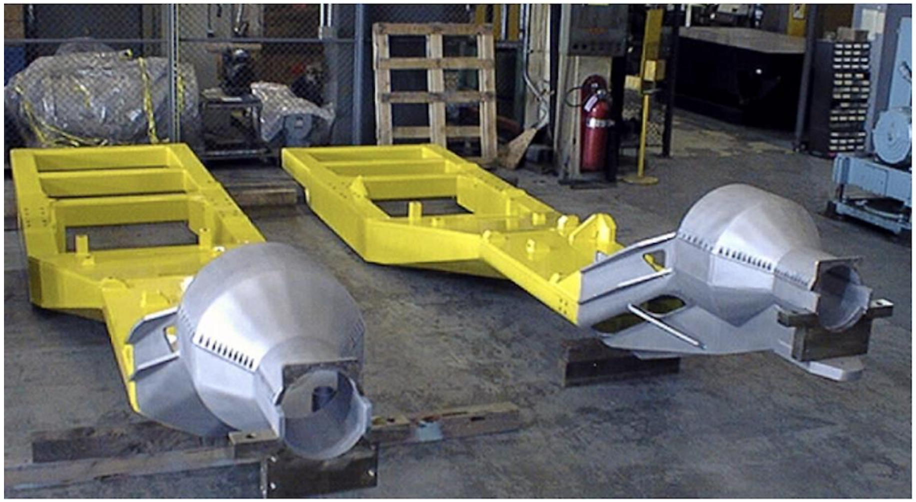

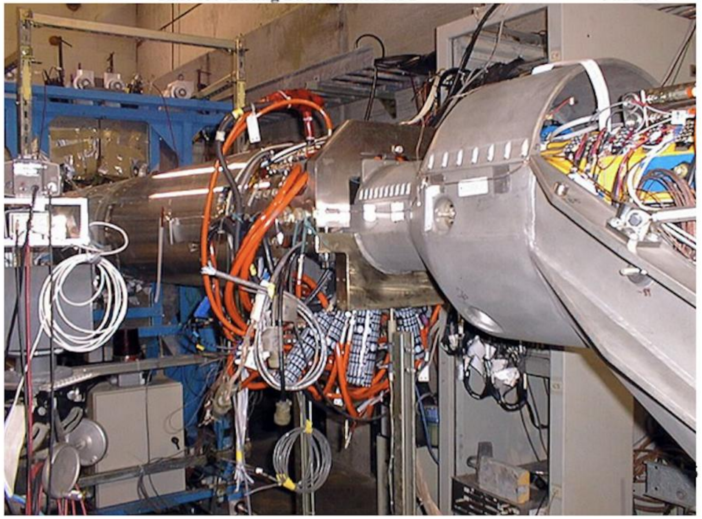

Cables: Example BaBar Vertex Chamber

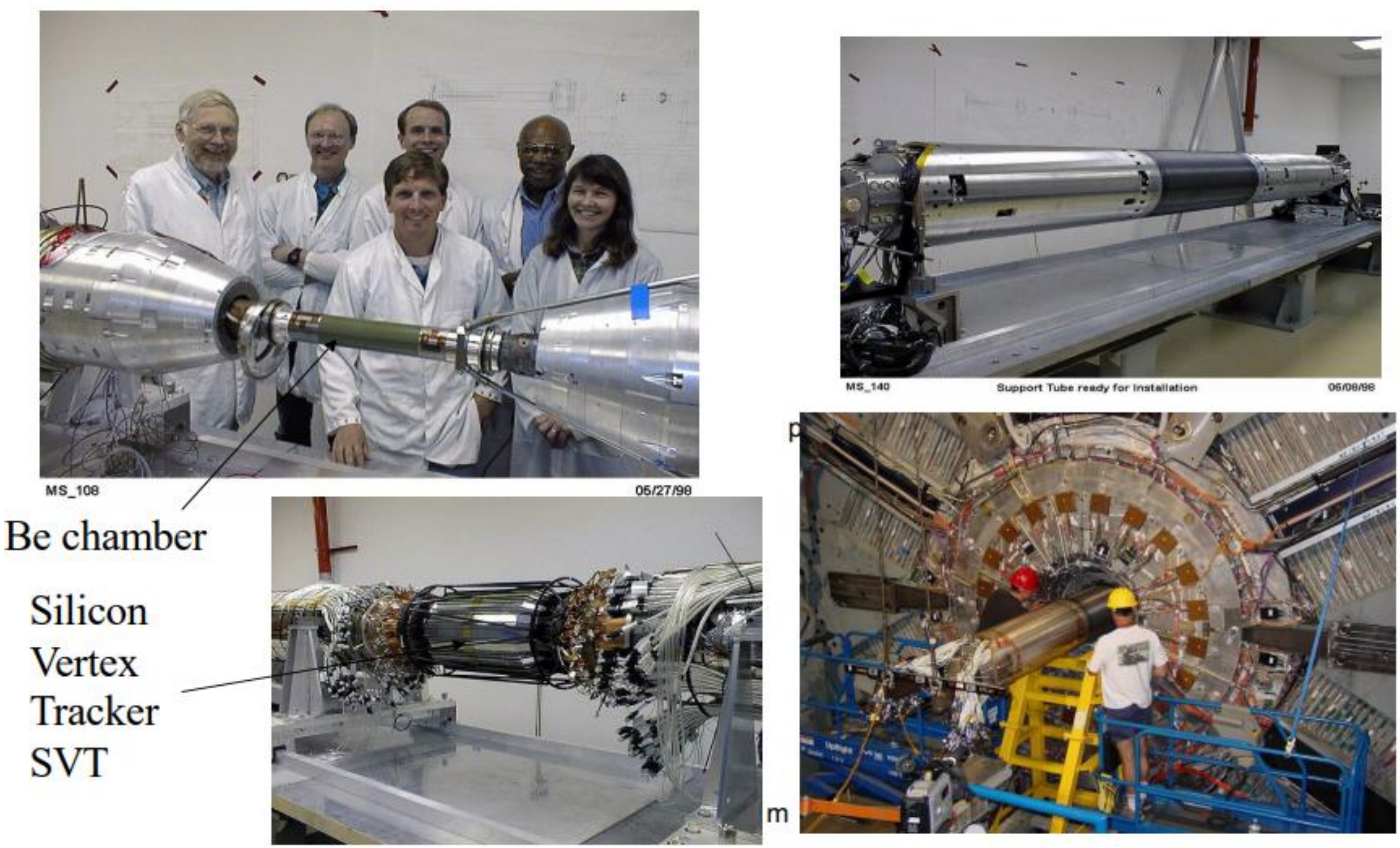

Assembly instructions has >100 pages!

PEP-II IR Vacuum Chamber with 3D structures

IR chambers made of GlidCop for strength. Special NEG and radial ion pumping. 3-D surfaces for synchrotron power absorption and to reduce HOM generation.

HER downstream high power dump was ~4 m long tapered copper, absorbing 90 kW at 1.8 A.

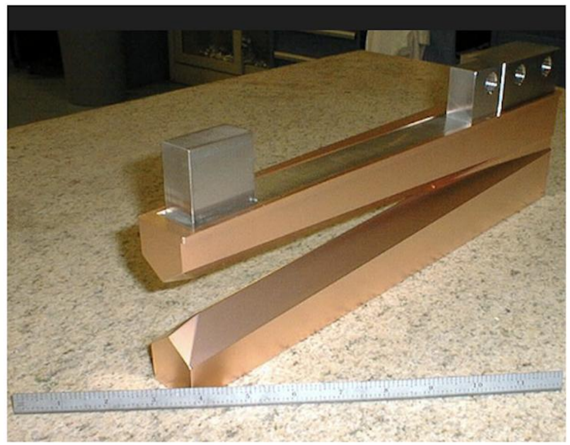

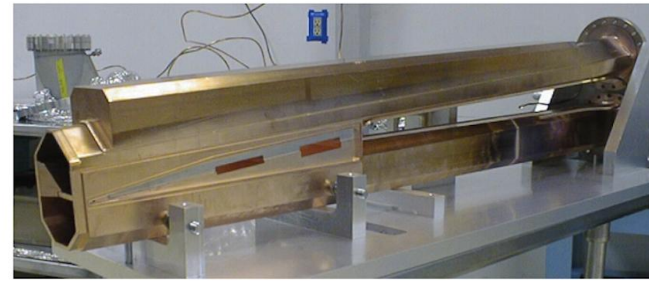

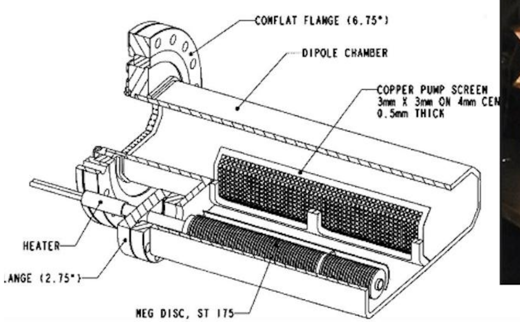

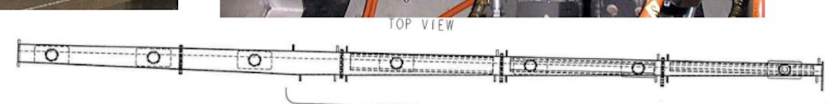

FCCee Center Accelerator Vacuum Chamber (Fransesini)

Chamber design – central chamber

The central has the following characteristics:

- AlBeMet 162 as main material
- Three layers from 0-90 mm from IP
  - 0.35 mm of AlBeMet162 (62% Be, 38% Al)
  - 1 mm gap for Paraffin
  - 0.35 mm of AlBeMet162
- Paraffin as coolant
- Geometry studied to integrate the central chamber with the vertex detector

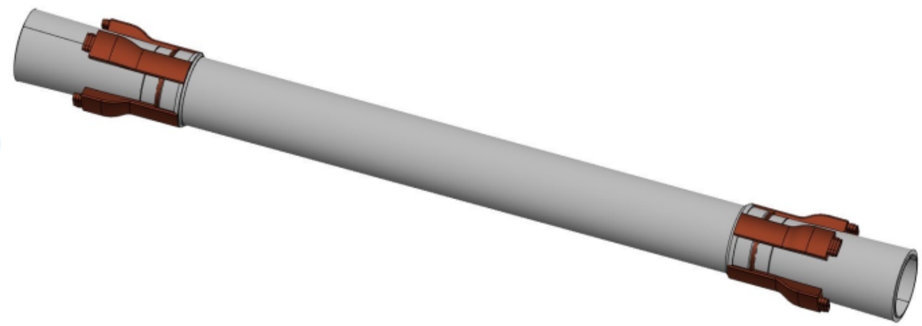

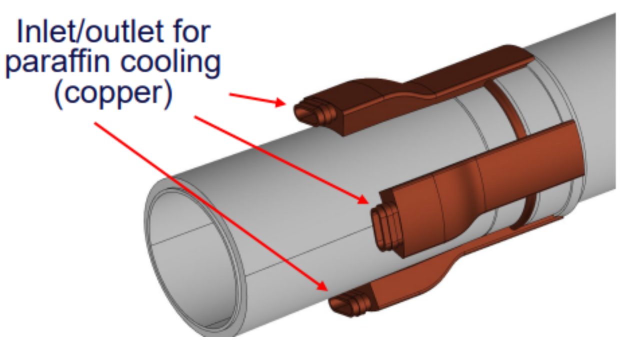

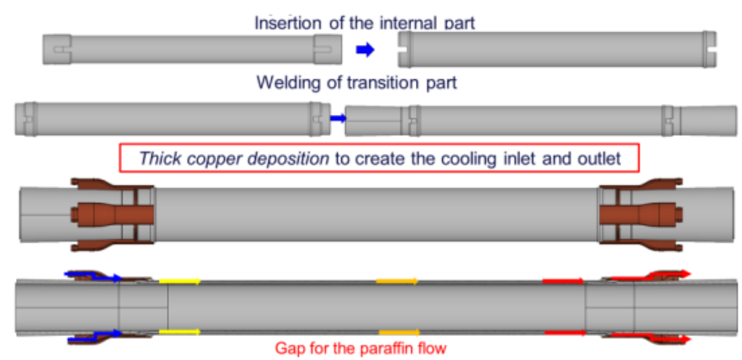

IP Vacuum Chamber Design (Fransesini)

SLAC

Crotch chamber

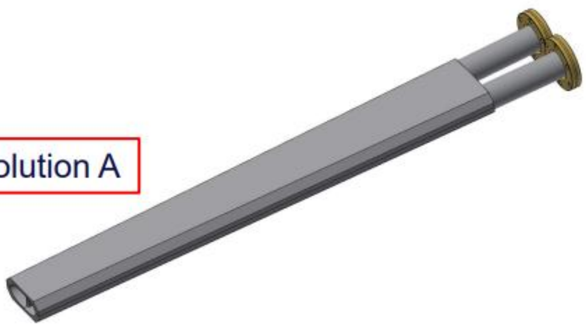

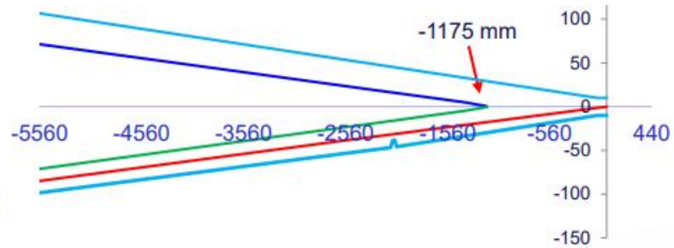

Work in progress

Solution A

Solution B

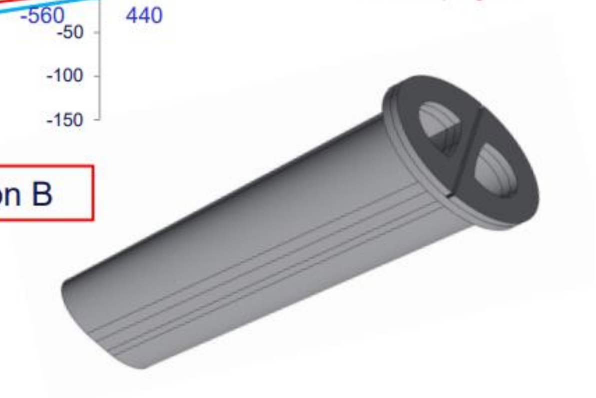

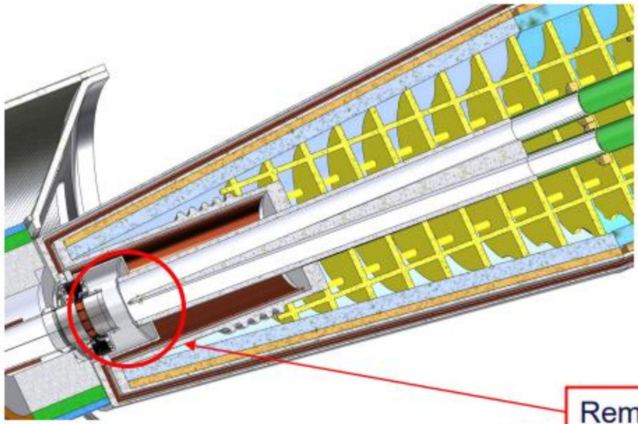

Solution A:
- Standard flanges
- More space available for the crotch
- Flanges in Helium

Solution B:
- Flanges not in contact with Helium
- Shorter chamber than solution A
- No standard flanges

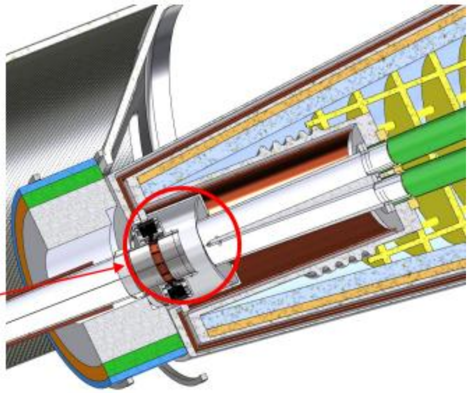

Remote vacuum connection

Example at SLAC of thin-walled water chamber:

Water pump pulled ~1 Bar pressure on water tank at SLAC causing it to crush.

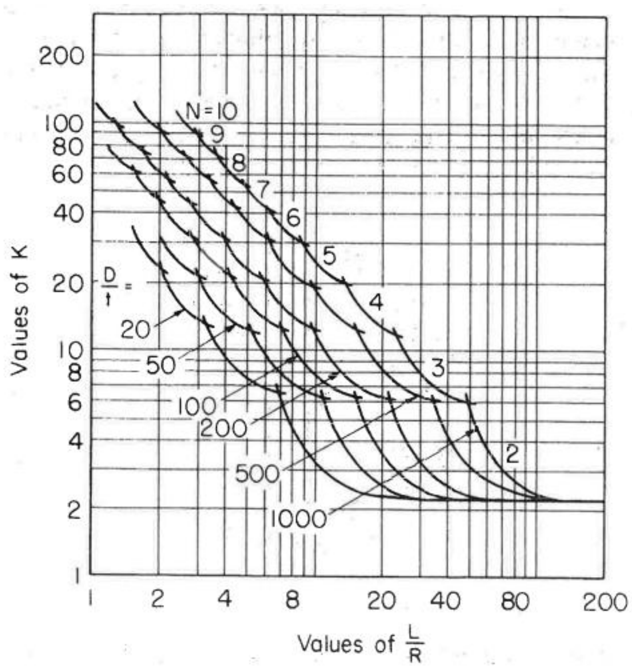

Radial external pressure with fixed edges.

Accelerator and Detector Survey and Alignment

Alignment

- **Aligment system based on three levels**
  - A deformation monitoring system of the shape of the screening solenoid with laser and fibres interferometric system (IMD-FSI)
  - A short-distance monitoring system, targeting QC1, LumiCal, etc, similar to FSI and HL-LHC MDI
  - A long-range FSI system joining the two sided of the detector

External alignment system

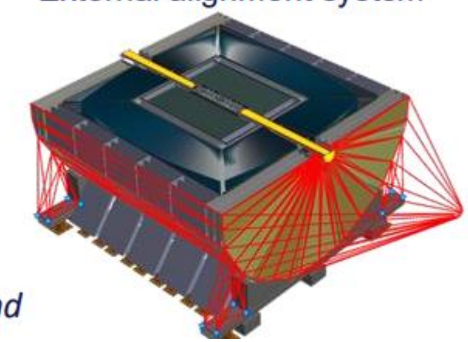

see talk by H. Mainaud-Durand

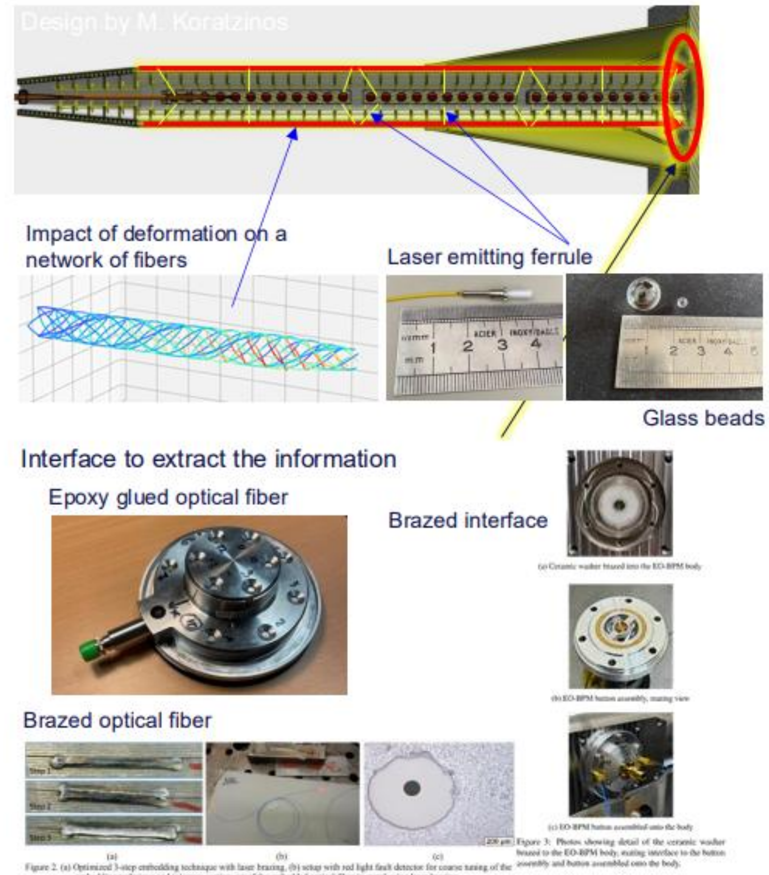

Grandal, Tania, et al. "Laser brazing metallic embedding technique for fiber optic sensors." 2017 25th Optical Fiber Sensors Conference (OFS). IEEE, 2017.

HOM calculations of IP vacuum Chambers (A. Novokhatski)

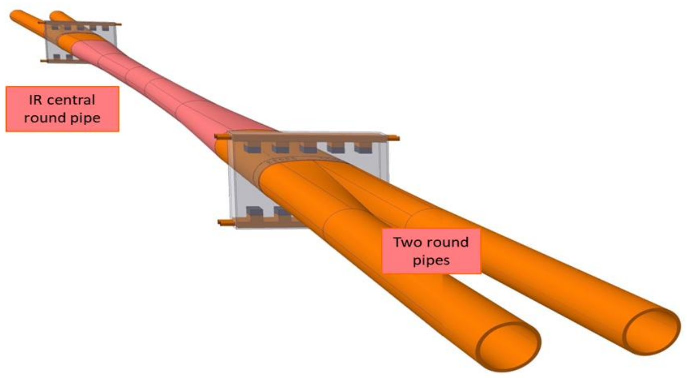

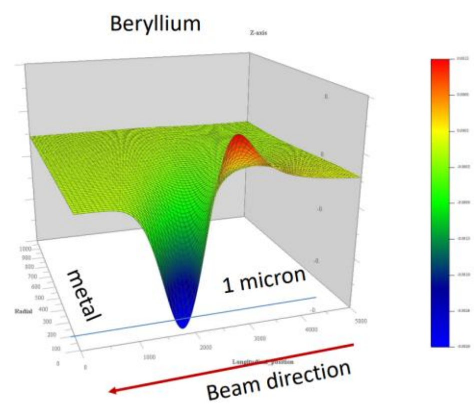

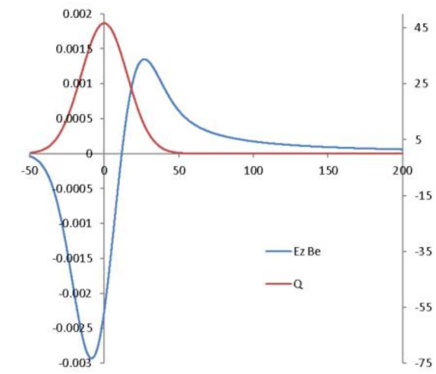

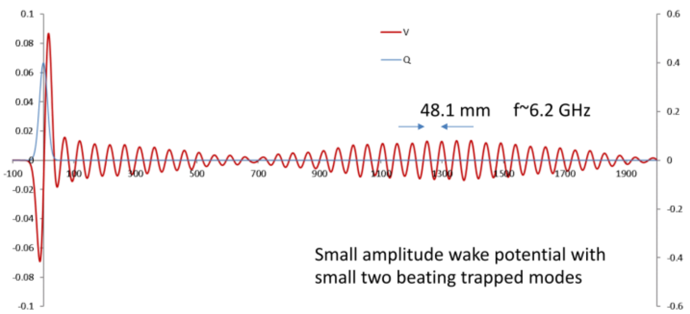

Parameter	Old (2022)	New (2024)	Change
Beam Current	1.39 A	1.27 A	-20 % (I*2)
Bunch spacing	19.5 ns	27 ns	+38 %
Heat power change			**+18 %**
Loss factor depends on bunch length	12 mm	15.4 mm	-28%

IR Trapped HOM Mode at Y chamber (Novokhatski)

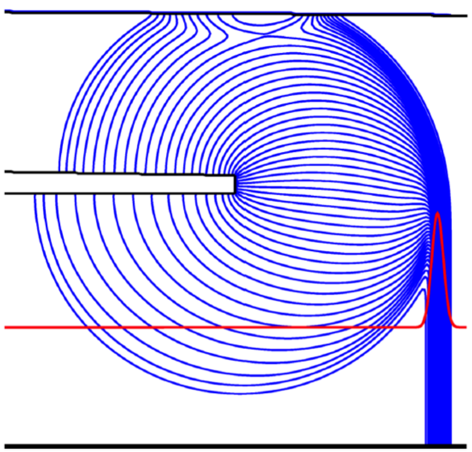

Our trapped unavoidable mode

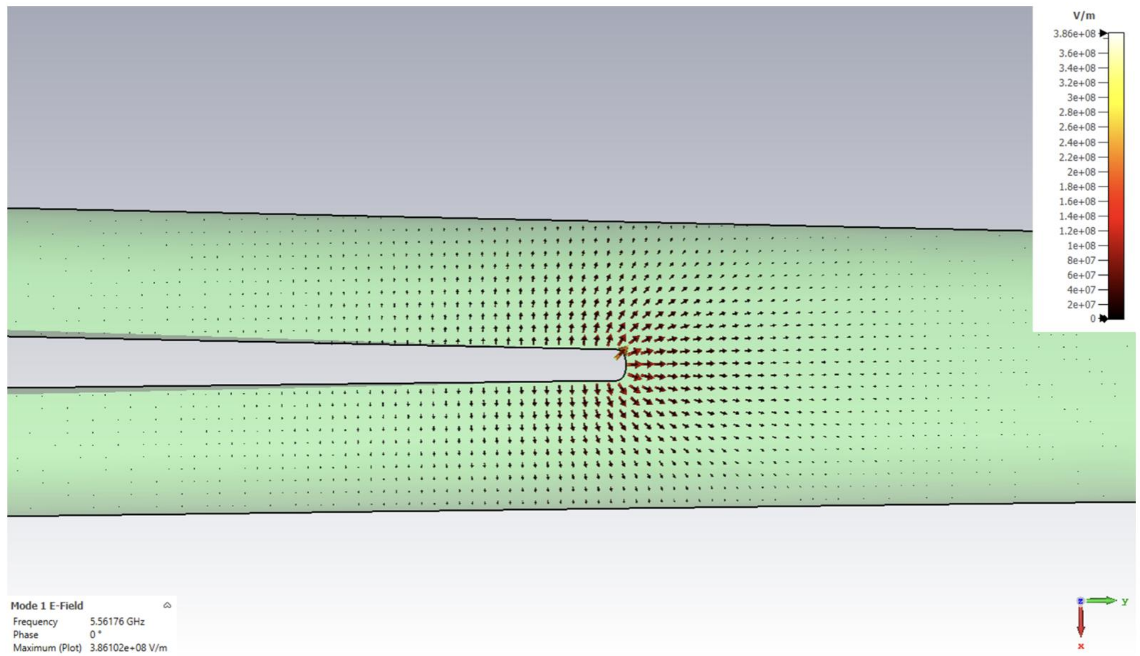

A. Novokhatski 10/06/23 12

FUTURE CIRCULAR COLLIDER FCC-ee MDI & IR mockup Workshop 16–17 Nov 2023 Laboratori Nazionali di Frascati

Trapped mode is part vertical, horizontal, and longitudinal: Hybrid mode.

FCCee IR bellows has HOM Losses

Central chamber has 1.5 Amp x 2 beams = 3 Amps of short length bunches!

Simplified model

What is important: the beam trajectory is not in the bellows center and the beam can easily excite transverse modes

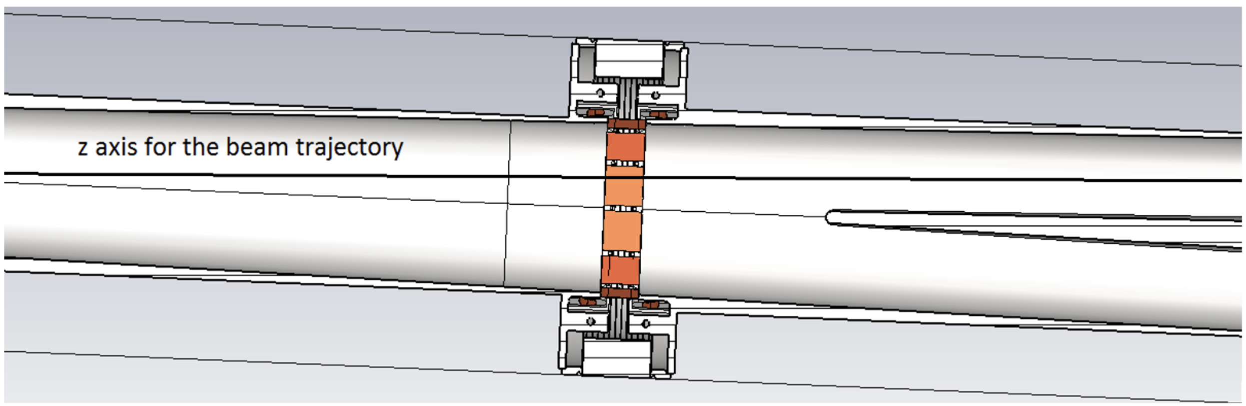

Unfortunately, the simplified model had thick springs, and we did not find any excited fields

HOM Modes in IR bellows design

We decrease spring thickness to 1mm and found a lot of trapped modes inside the bellows cavity

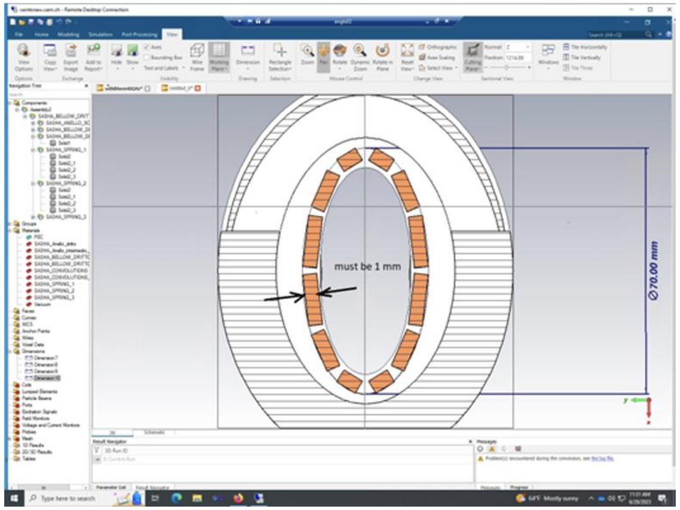

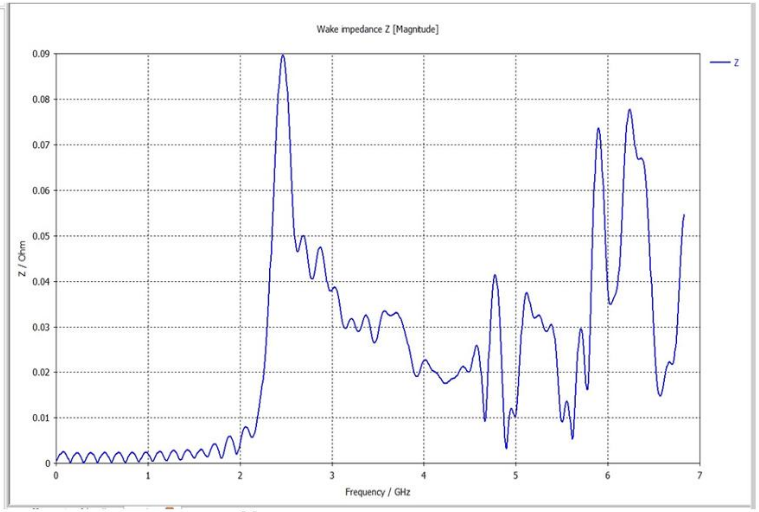

Bellows spectrum

A new "simplified" model is needed to get more or less real results

SuperKEKB beam impedance to study beam instabilities

SLAC

Impedance modeling – Vertical

σ_z=6.0 mm

Pre-LS1 (D06V1: ±2.9 mm)

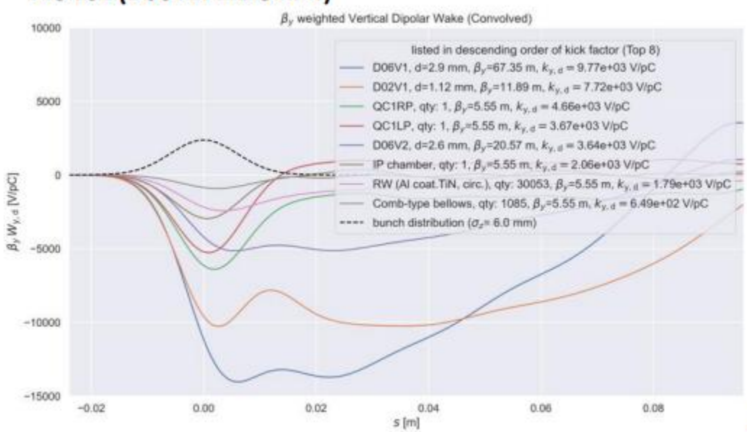

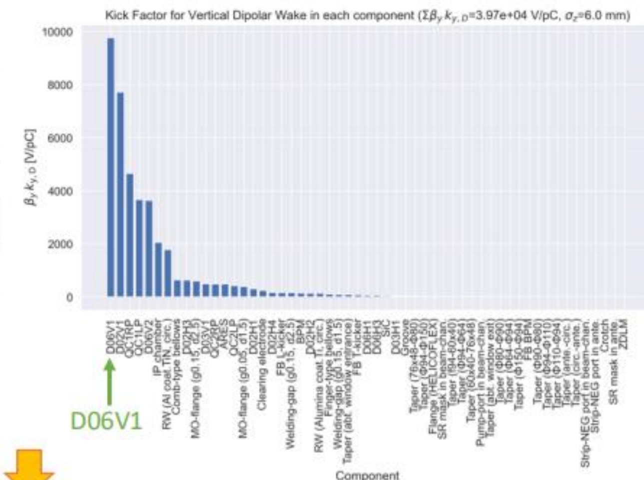

Post-LS1 (D06V1: ±8.0 mm, D05V1: ±3.8 mm)

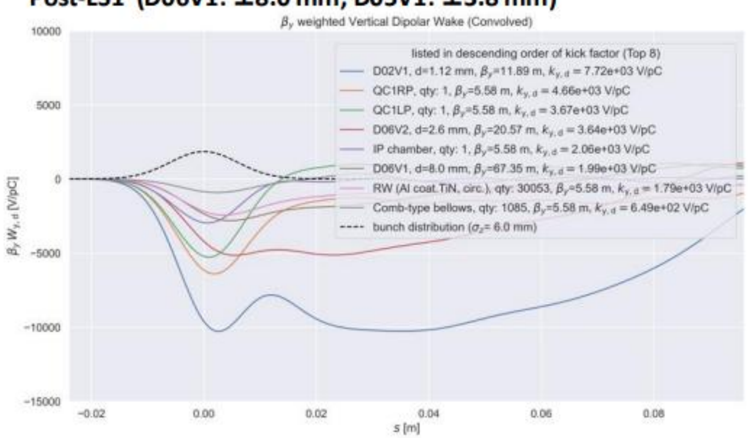

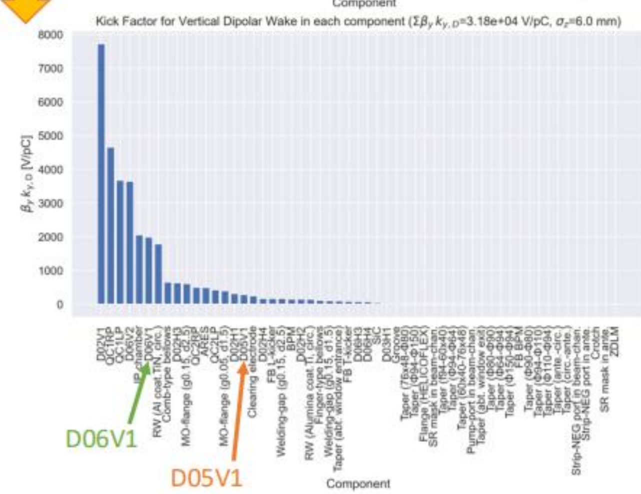

Vertical collimator

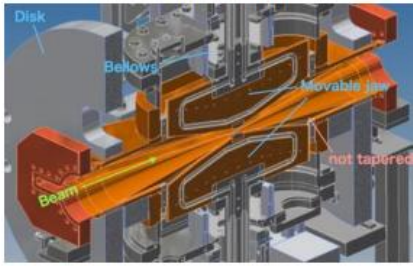

Tapered beam-pipe with BPM in final focusing magnet (QC1)

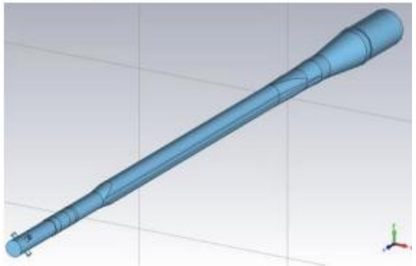

Beam-pipe around interaction point (IP chamber)

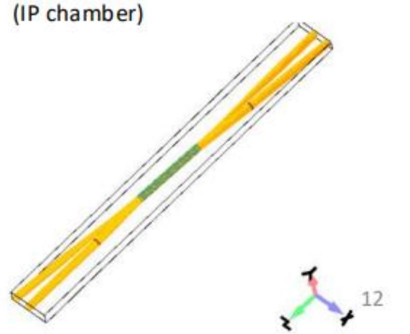

12

Polarization and Energy Calibration

Expected precision

Uncertainty	m_Z (keV)	Γ_Z (keV)	$\sin^2\theta_W^{\rm eff}$ ($\times 10^{-6}$)	$\frac{\Delta\alpha_{\rm QED}(m_Z^2)}{\alpha_{\rm QED}(m_Z^2)}$ ($\times 10^{-5}$)	m_W (keV)
	Observable				
Absolute	100	2.5	–	0.1	150
Point-to-point	14	11	1.2	0.5	50
Sample size	1	1	0.1	–	3
Energy spread	–	5	–	0.1	–
Total $\sqrt{s}$-related	101	12	1.2	0.5	158
FCC-ee statistical	4	4	2	3	180

How to?

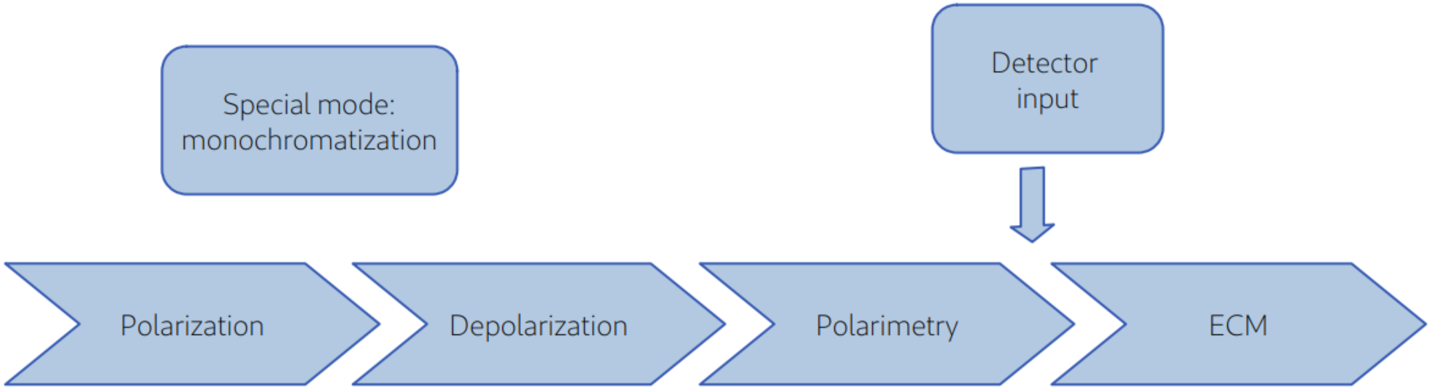

Beam polarization measurement near the IP

SLAC

$$\vec{e} + \vec{\gamma} \rightarrow e + \gamma$$

Dave Gaskell JNAL

Compton polarimetry basic design

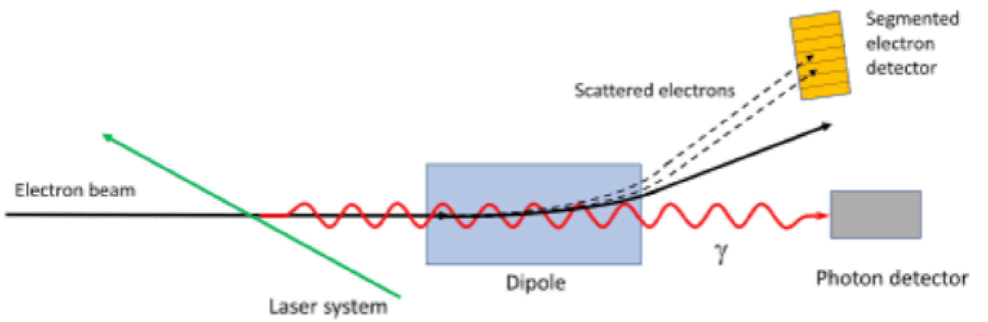

- The technique of measuring the polarization of a stored beam used by all current machine designs is to Compton scatter a laser beam of photons off a beam bunch and then collect the backscattered gammas and off-energy beam particles (either electron or positron) in detectors
- In order to collect the scattered particles (gamma and e/p), the stored beam must go through a bend magnet after passing through the laser IP
- The beam is deflected from the gamma trajectory and the lower energy electrons are over-bent and can be collected in a detector that is outside of but very close to the stored beam envelope (Beam-Stay-Clear)

Sources of Background in the MDI area

Luminosity backgrounds

- **Incoherent Pairs Creation (IPC)**: Secondary e^-e^+ pairs produced via the interaction of the beamstrahlung photons with real or virtual photons during bunch crossing.
- **Radiative Bhabha:** beam particles which lose energy at bunch crossing and exit the dynamic aperture

Single beam backgrounds:

- **Generic Halo Losses:** high rate of beam losses in the IR coming from halo (transverse or longitudinal) being diffused by the collimators after lifetime drop
- **Synchrotron Radiation** from upstream magnets
- **Beam-gas** (elastic and inelastic scattering)
- Compton scattering on **thermal photons**
- **Injection** backgrounds

Comprehensive collimation systems

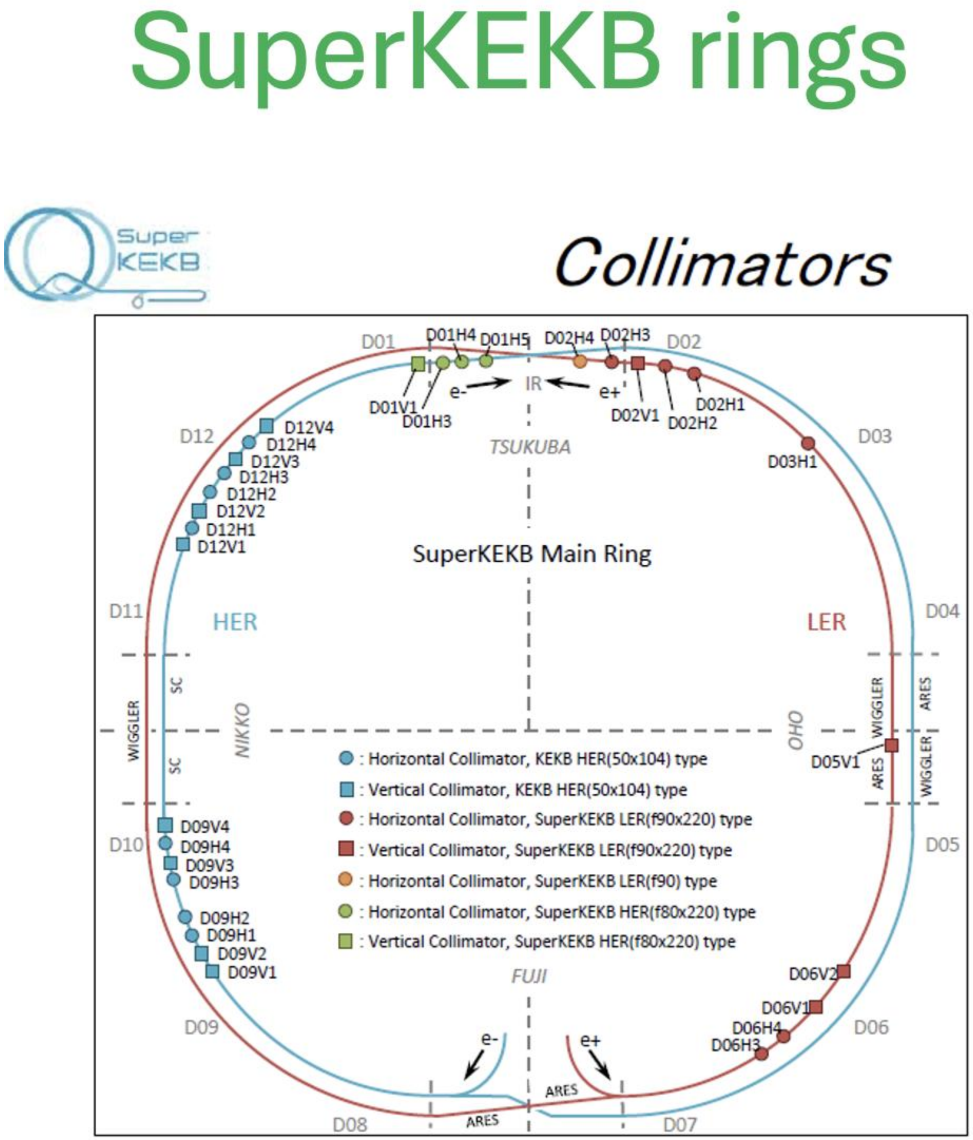

Radiative Bhabha's in SuperKEKB IR

SLAC

KEKB radiative Bhabhas

- KEKB had no close bending magnets and hence did not see much of a radiative Bhabha background initially
- The outgoing beams do get a strong bend from the off-axis orbits in the quads making a radiative background that was seen as the luminosity increased

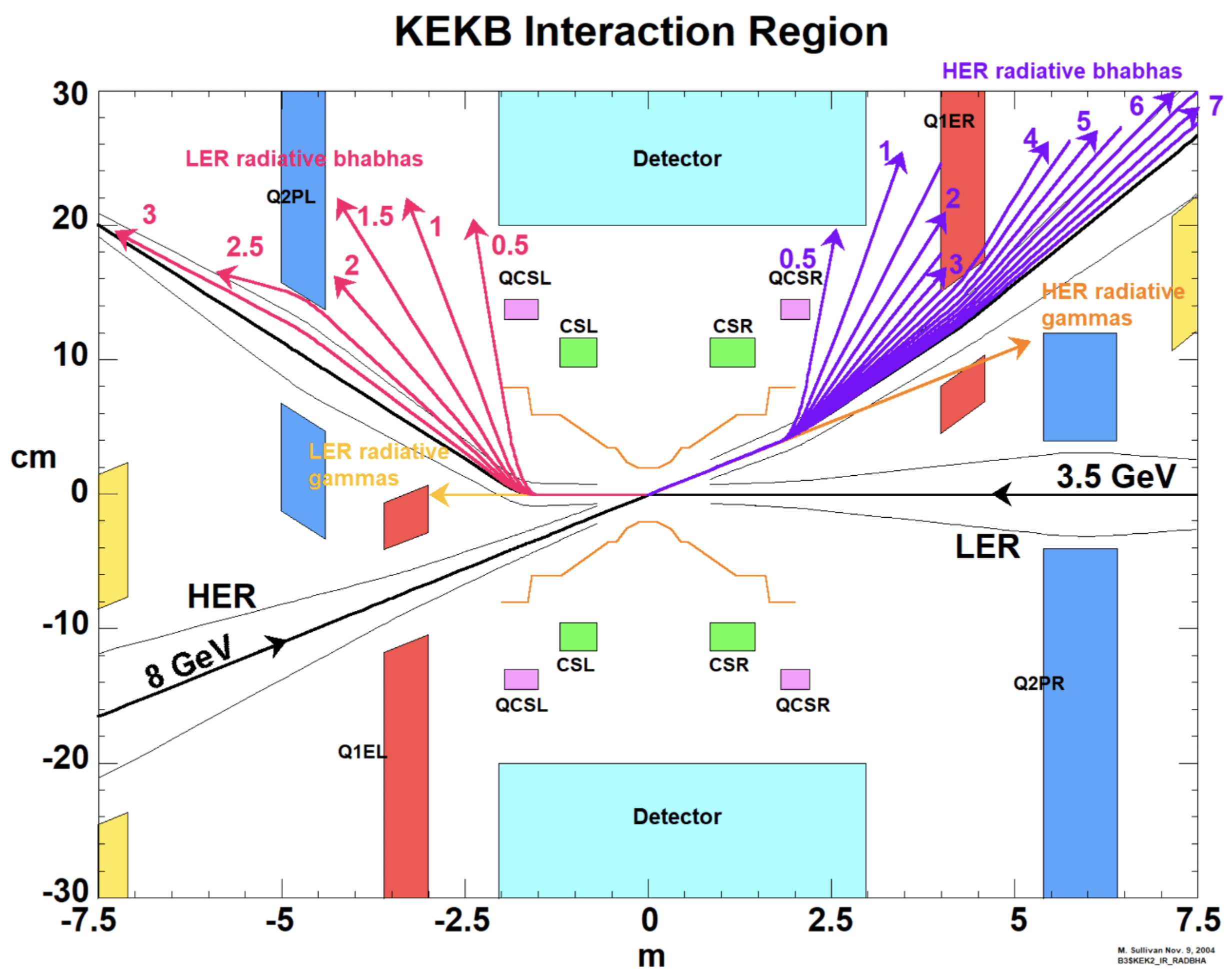

SLAC

Dedicated background study in April, 2024

- Heuristic fit of different background components

Preliminary

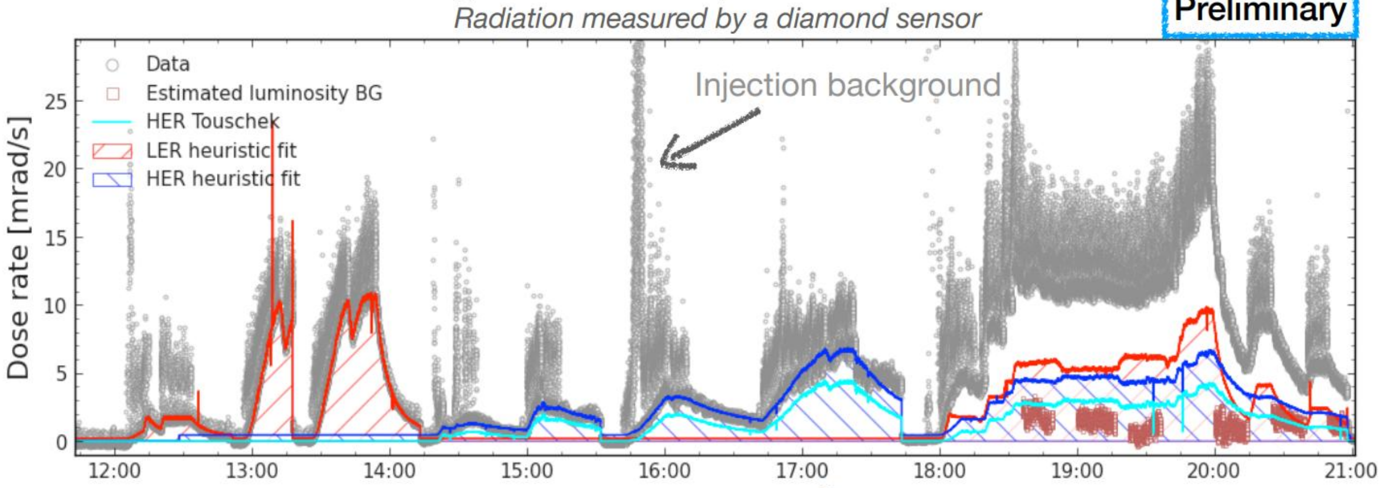

$$\mathcal{O}_{\mathrm{pedestal}} = \mathrm{D} \qquad \mathcal{O}_{\mathrm{Touschek}} = \mathrm{T} \times \frac{\mathrm{I}^2}{\mathrm{n_b}\sigma_{\mathrm{x}}\sigma_{\mathrm{y}}\sigma_{\mathrm{z}}} \qquad \mathcal{O}_{\mathrm{beam-gas}} = \mathrm{B} \times \mathrm{I}\bar{\mathrm{P}}_{\mathrm{eff}}$$

- Constants:
  - Detector pedestal D, background sensitivities (T, B)
  - Base pressure P_0 and the dynamic pressure coefficient dP/dI

$$\bar{\mathrm{P}}_{\mathrm{eff}} = 3\mathrm{I}(\mathrm{d}\bar{\mathrm{P}}/\mathrm{dI})_{\mathrm{CCG}} + \bar{\mathrm{P}}_{0,\mathrm{CCG}} = 3\bar{\mathrm{P}}_{\mathrm{CCG}} - 2\bar{\mathrm{P}}_{0,\mathrm{CCG}}$$

Cold cathode gauge (**CCG**) to measure gas pressure

https://arxiv.org/pdf/2302.01566

JH | SuperKEKB/Belle II backgrounds | Qingyuan Liu, March 5, 2025 qingyuan.liu@hawaii.edu 7

PEP-II Synchrotron Radiation Fans

PEP-II IR SR fans

HER SR fans

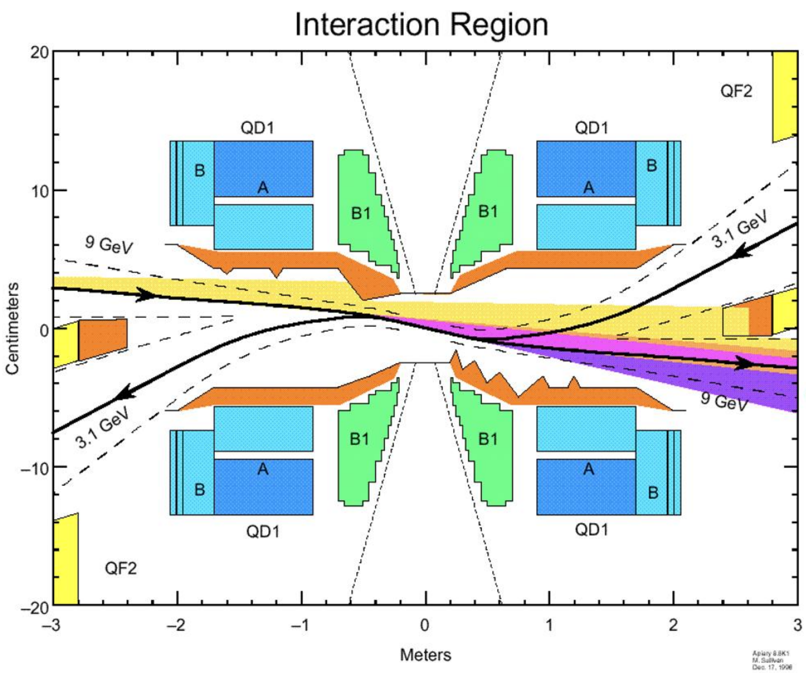

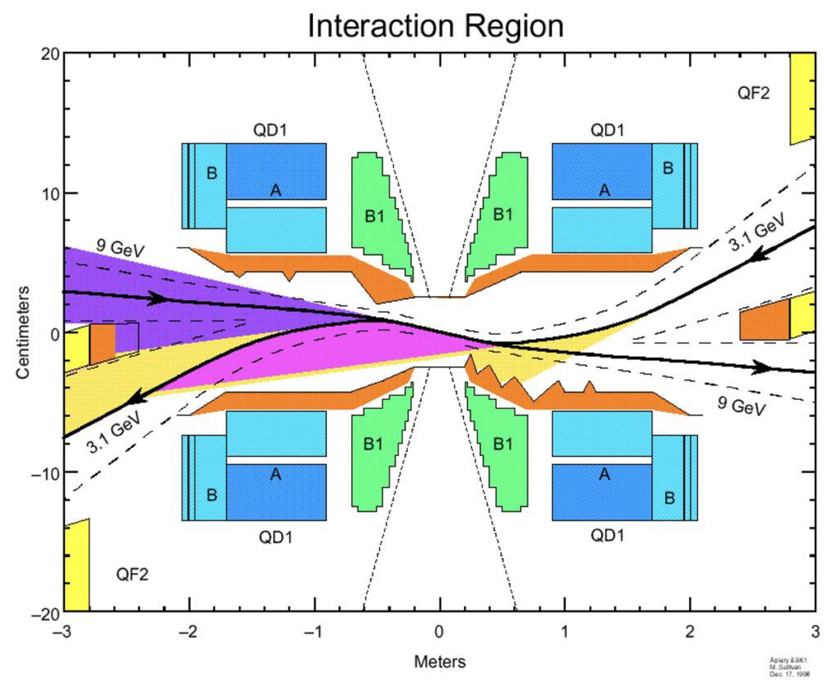

LER SR fans

This intense outgoing and overlapping fan from the B1 magnets intercepted the beam pipe wall from 10-20 m away and was a noticeable source of neutrons

SR scattering from FCCee Mask Tips (M. Sullivan)

SLAC

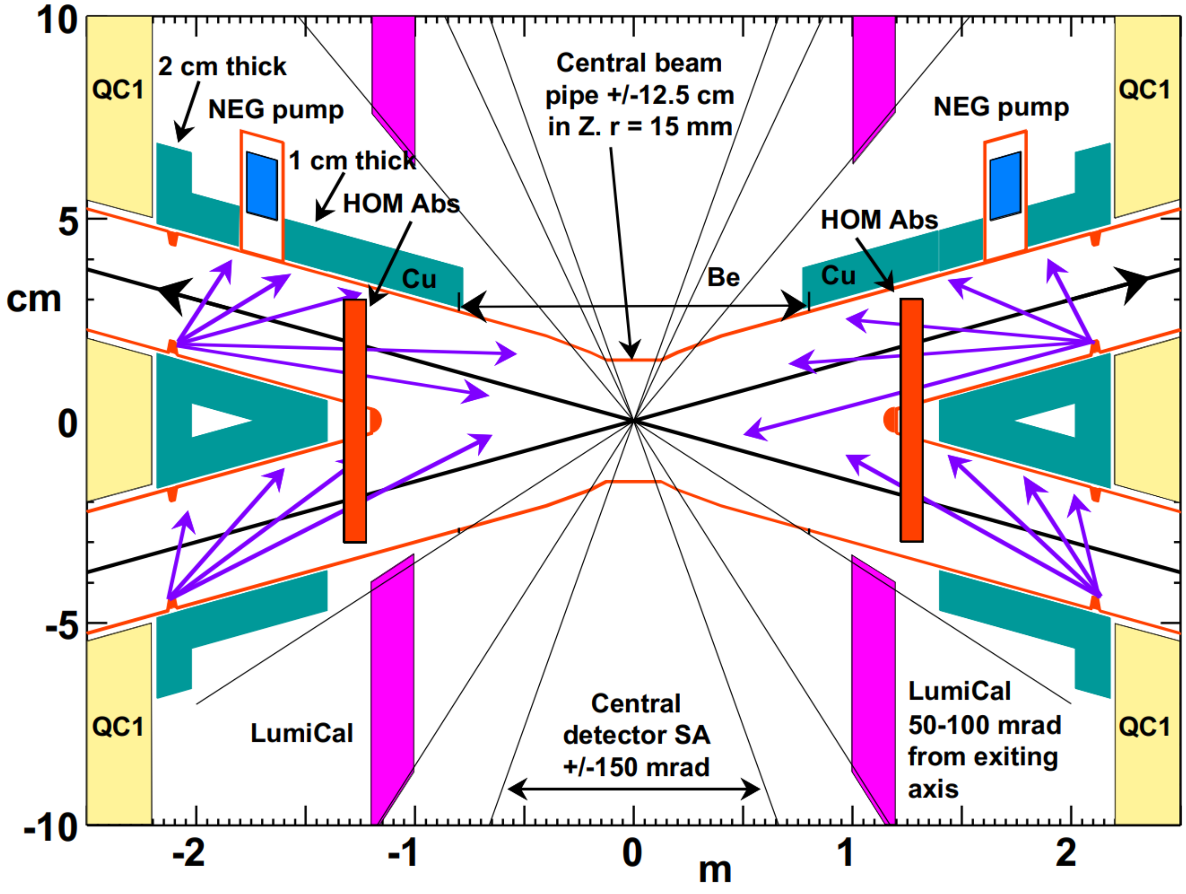

2.1 m mask dimensions

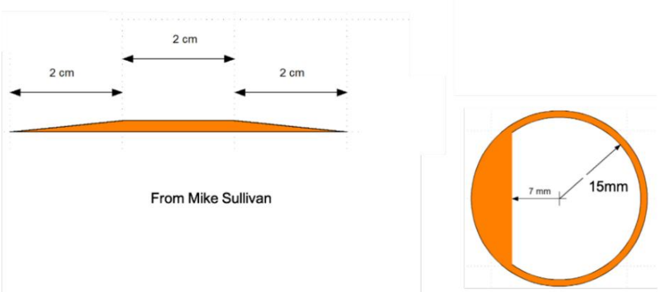

Background sources

- Single Beam
  - Touschek Scattering
  - Beam Gas Scattering(Elastic/inelastic)
  - Beam Thermal Photon Scattering
  - Synchrotron Radiation
- Luminosity Related
  - Beamstrahlung
  - Radiative Bhabha Scattering
- Injection(Not Considered yet)

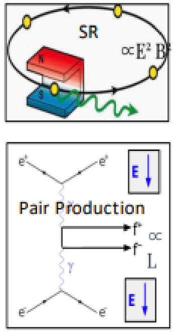

Photon BG

A. Natochii

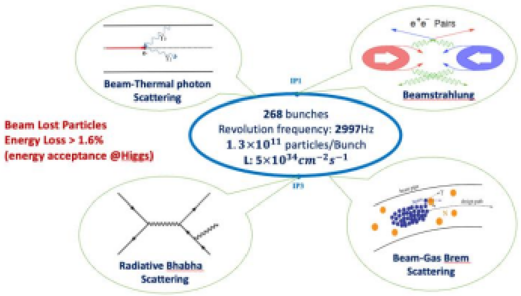

Beam Loss BG

A. Natochii

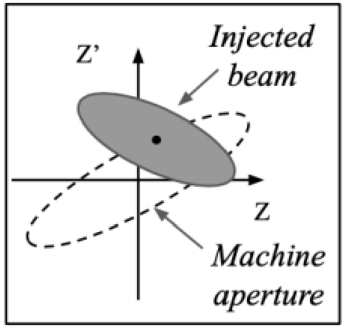

Injection BG

Background	Generation	Tracking	Detector Simu.
Synchrotron Radiation	BDSim/Geant4	BDSim/Geant4	
Beamstrahlung/Pair Production	Guinea-Pig++		
Beam-Thermal Photon	PyBTH[Ref]		
Beam-Gas Bremsstrahlung	PyBGB[Ref]	SAD	CEPCSW/FLUKA
Beam-Gas Coulomb	BGC in SAD		
Radiative Bhabha	BBBREM		
Touschek	TSC in SAD		

- One Beam Simulated
- Simulate each background separately
- Whole-Ring generation for single beam BGs
- Multi-turn tracking(200 turns)
  - Using built-in LOSSMAP
  - SR emitting/RF on
  - Radtaper on
  - No detector solenoid yet

FCC-ee Machine Detector Interface

upcoming talk:
M. Boscolo on FCC-ee MDI

Compact region common at the 4 working point energies

- Cooled AlBeMet162 IR chamber
- Detector acceptance $100\,mrad$
- Beam pipe separation at $\sim 1.5m$
- $L^* = 2.2m$ $\rightarrow$ QD0 **inside the detector**
- Local coupling compensation **-5T anti-solenoid**
- **Carbon Fibre tube** for support and installation of IR chamber, LumiCal and vertex detector

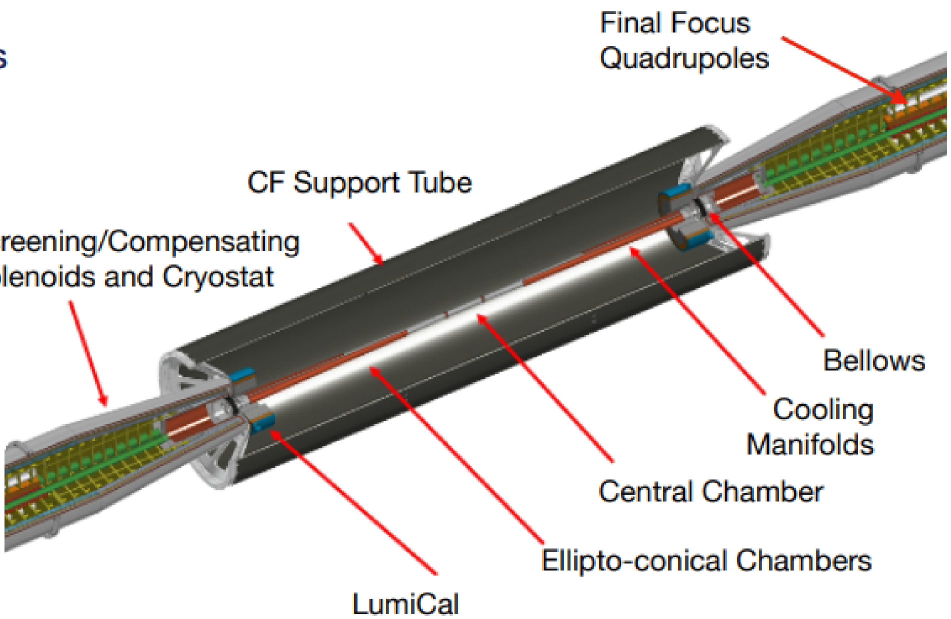

Many different MDI elements in the IR can be source of **scattering** or **secondary production**.
Accurate modelization in the simulation framework is necessary to estimate backgrounds and design shieldings.

Key4hep MDI modelization

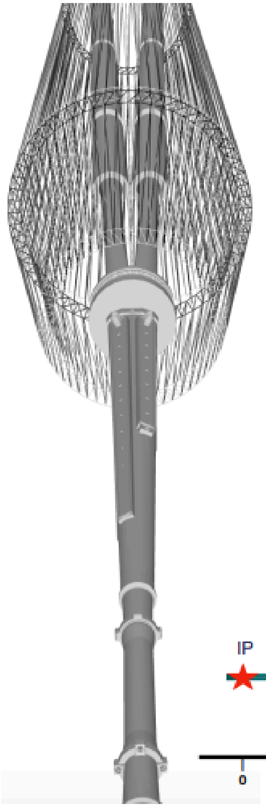

Engineered CAD model of IR beam pipe imported in **Key4hep**.
- Double-layered central section for paraffine cooling
- **Cooling manifolds** for ellipto-conical chambers implemented
- Bellows
- Beam pipe **separation region** profile congruent to impedance studies
- Tungsten **SR masks** after final focus

Compensating and Screening solenoid cryostats
Final Focus Quadrupoles simple equivalent material model

Future upgrades:
- IR carbon fiber **support tube**
- **Remote vacuum connection** flanges

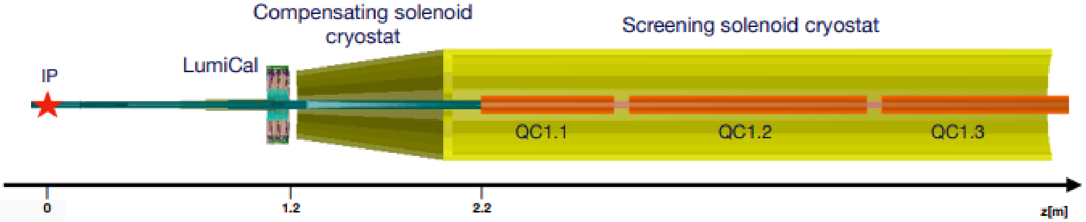

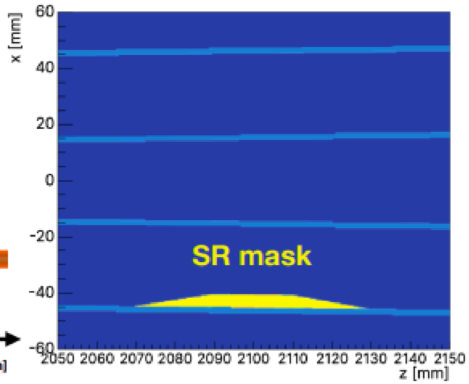

Direct observation of background spectra

The Beamstrahlung spectra should reach down to optical wavelengths.

Another possibility is to use glassy carbon screens (super light weight) to monitor Beamstrahlung photons in the optical range.

To be evaluated: the quantity of visible photons generated by Beamstrahlung.

And the BS to SR radiation levels with IP shielding against SR.

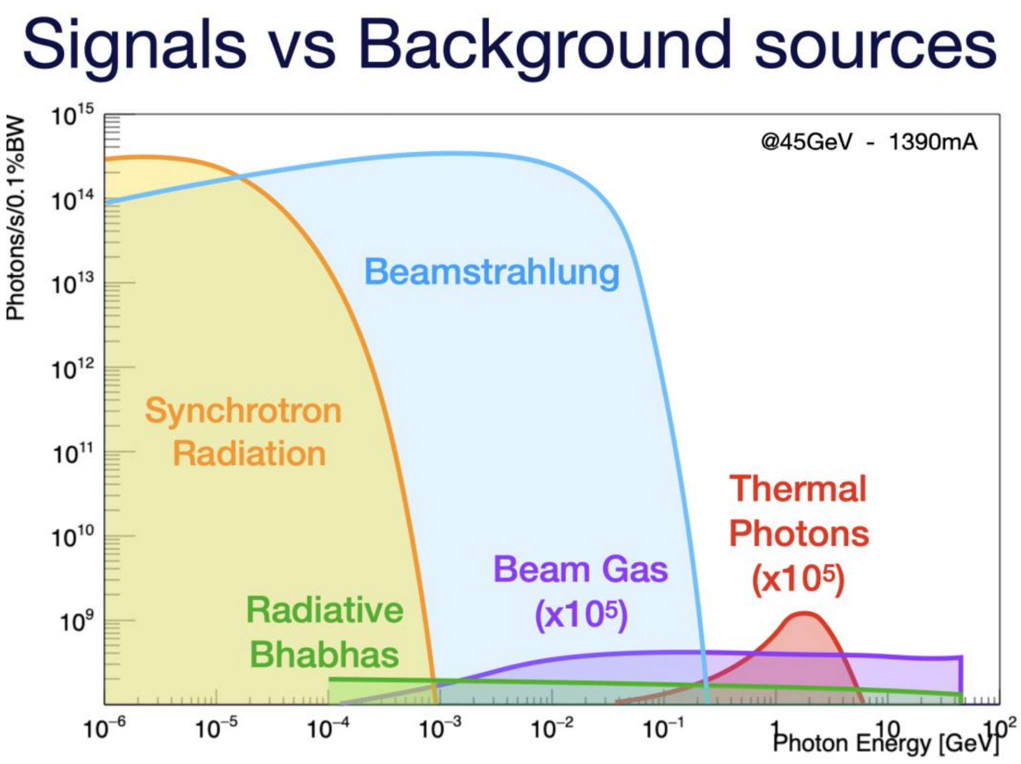

Large tails on beam shape due to Beamstrahlung

Beamstrahlung

Equilibrium energy distribution

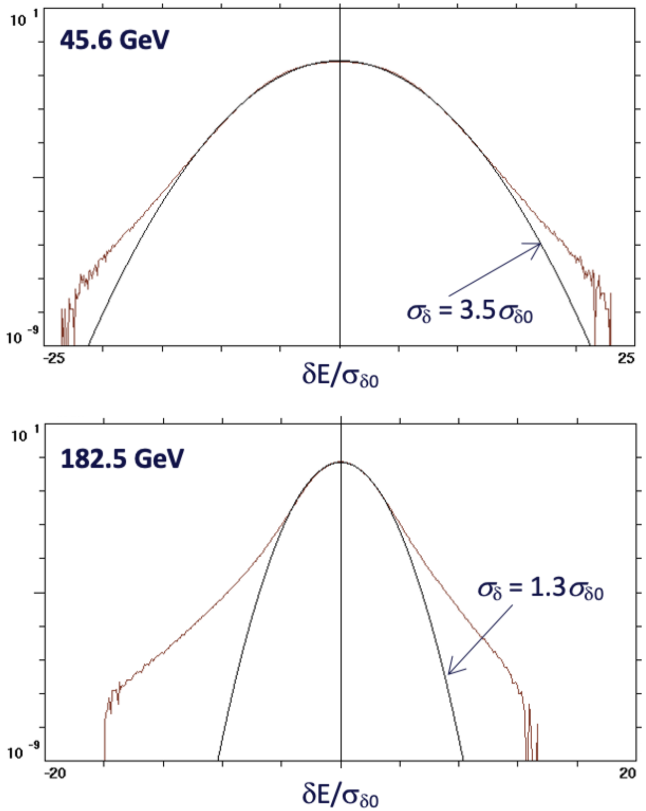

- The factor of increasing the energy spread is higher at low energies. The explanation is that it depends on the ratio of the bending radii in the arcs (SR) and in the IPs (BS).
- For low-energy colliders, ρ_{min} at the IP can be even smaller, but the effect of BS is negligible there, since the arc radius is much smaller than in the FCC.
- At 45.6 GeV, the energy loss due to BS is ~0.31 MeV per IP, compared to ~37 MeV in the arcs due to SR.
- Long tails at ttbar are produced by single emitted BS photons. Here the ratio u_c/σ_δ is important, which grows with γ.
- For asymmetry of the tails, an important parameter is the damping factor during the period of synchrotron oscillations. Therefore, asymmetry grows with γ.

Momentum acceptance determines the maximum allowable critical energy of BS photons, which in turn is proportional to ξ_y (and hence luminosity).

Beamstrahlung Radiation Spectrum

Beamstrahlung radiation Characterisation

The photons are emitted **collinear to the beam** with an angle proportional to the beam-beam kick.

This radiation is extremely intense **O(100kW)** and **hits the beam pipe** at the end of the first downstream dipole.

The generator for the beamstrahlung radiation is **GuineaPig++**

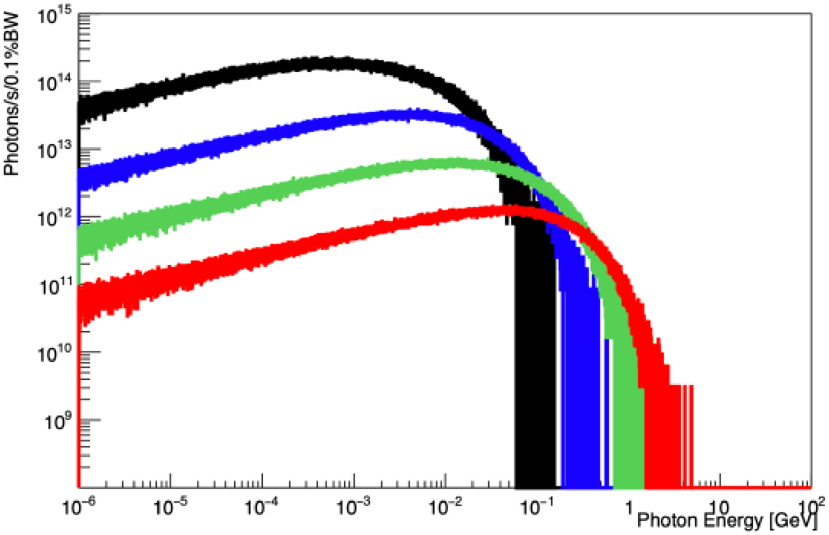

	Total Power [kW]	Mean Energy [MeV]
Z	370	1.7
WW	236	7.2
ZH	147	22.9
Top	77	62.3

M. Boscolo and A. Ciarma, "Characterization of the beamstrahlung radiation at the future high-energy circular collider" Phys. Rev. Accel. Beams **26**, 111002

Beam Synchrotron Radiation in FCCee IR

FCC | eeFACT 2025 - Tsukuba 05/03/2025 | Andrea Ciarma | INFN LNF | 16

Synchrotron Radiation

K. André

SR is the **main driver** for FCC-ee MDI and lattice design

- **Asymmetric bend** to mitigate SR coming from upstream magnets
- Characterization of the radiation using **G4 based tool BDSim**
- Tungsten **SR collimators and masks** to protect the IR

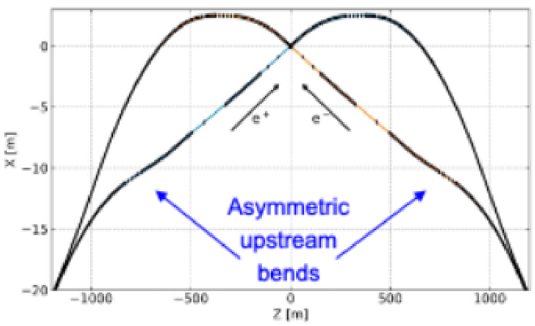

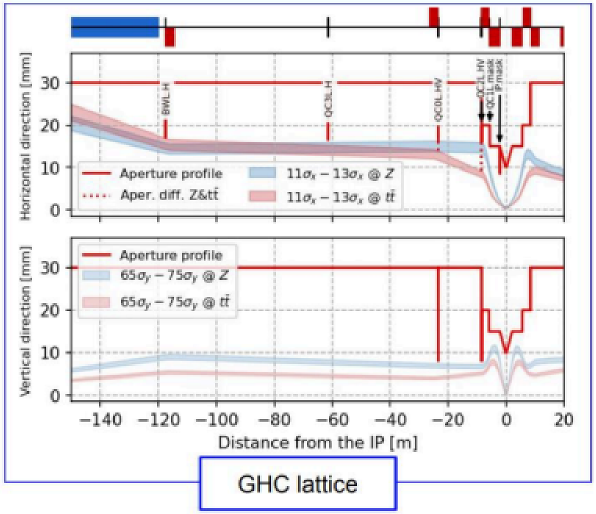

SR Background coming from the **beam core** particles is **completely shielded** thanks to the **tungsten masks**.

Other contributions currently under study are:

- **beam halo** particles
- non zero closed orbits
- top-up **injection**

Characterization of this background is essential for **dedicated shielding** design.
First tracking in key4hep ongoing for **occupancy calculation**.

Zero degree: Straight Ahead Detector

Optical line to monitor a scintillating screen on the extraction line.

- Could be inserted at low intensity for IP tuning procedures
- Heat deposition study: Monte Carlo simulation of particle matter interaction.
- Cooling system for the screen?
- The study will define the accessible range of bunch-charge (Beamstrahlung at the IP / heating the screen)
- Positioning: Be as far as possible from IP (dilution) and not to close from the dump (radiation background).

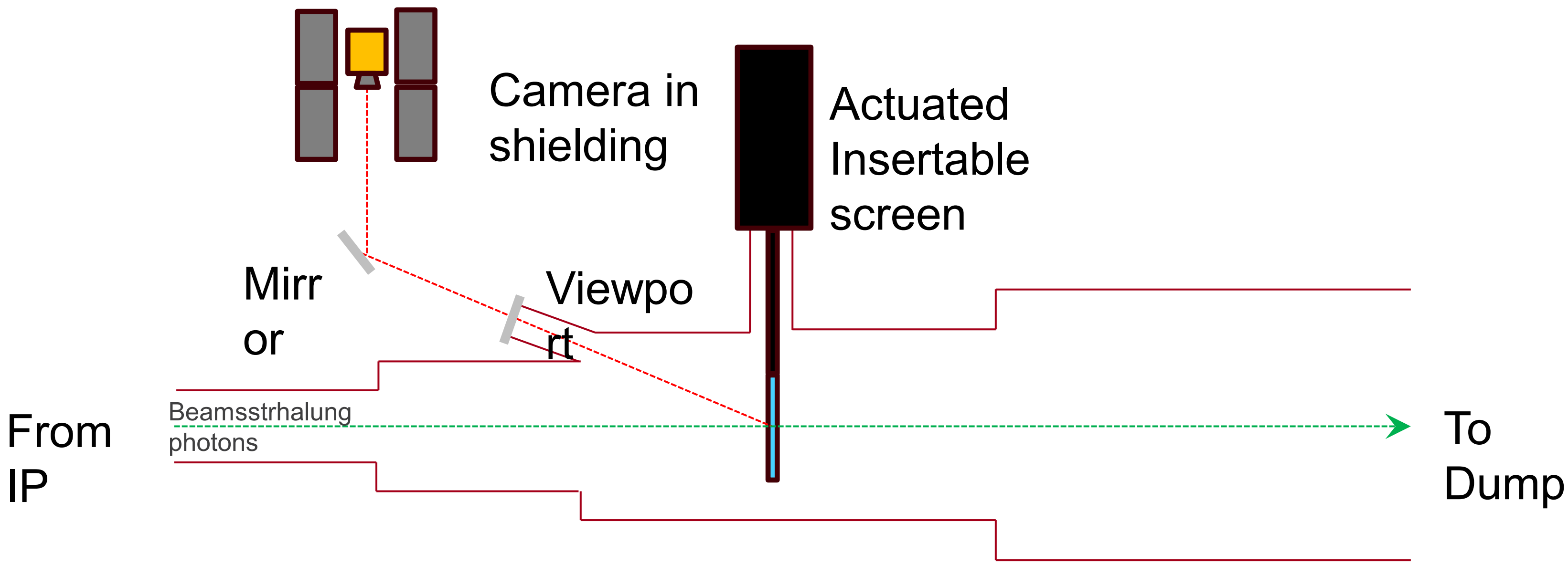

Beam gas scattering

Beam-gas Losses from multi-turn

G. Broggi

First multi-turn tracking in **X-Suite** using **beam-gas elements** based on lattice pressure profile.

Dominant contribution: **inelastic beam-gas** (Bremsstrahlung)

➡ Next step: tracking in Key4hep for occupancy estimates

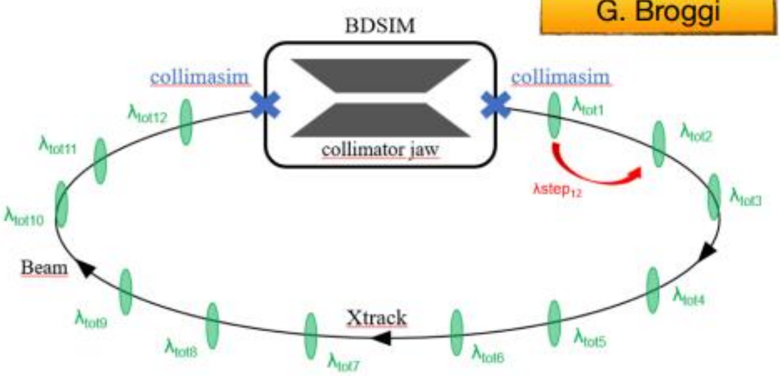

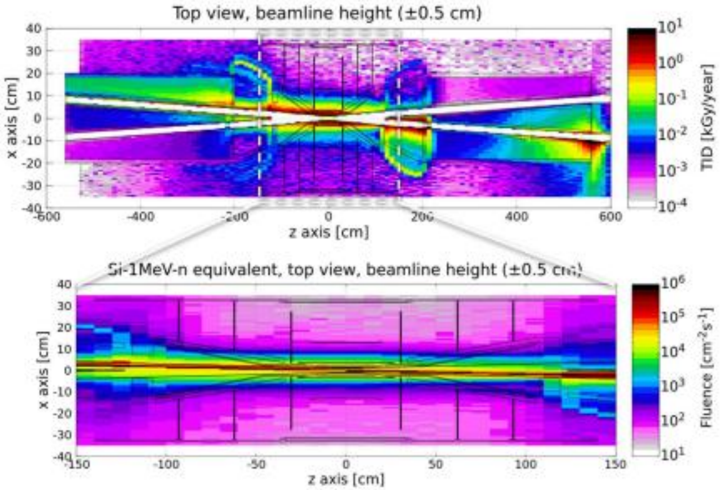

A. Frasca

Beam-gas Losses in IR

Local beam-gas losses in the IR studied also with FLUKA.

- Geometry includes both beam lines, SR masks and collimators, MDI elements, IDEA detector.
- particles generated from 500m upstream the IP
- first loss maps for e^- and photons
- Total Ionizing Dose below kGy/year

Secondaries from MDI elements

A large contribution of backgrounds in the studied sub-detectors comes from **secondaries** generated by low-Pt particles hitting the **beam pipe separation region**.

Large production of **photons** $< E_\gamma > \sim 15 MeV$ (bremsstrahlung, e+ annihilation), plus **pairs** and **photoelectric** from the surrounding materials.

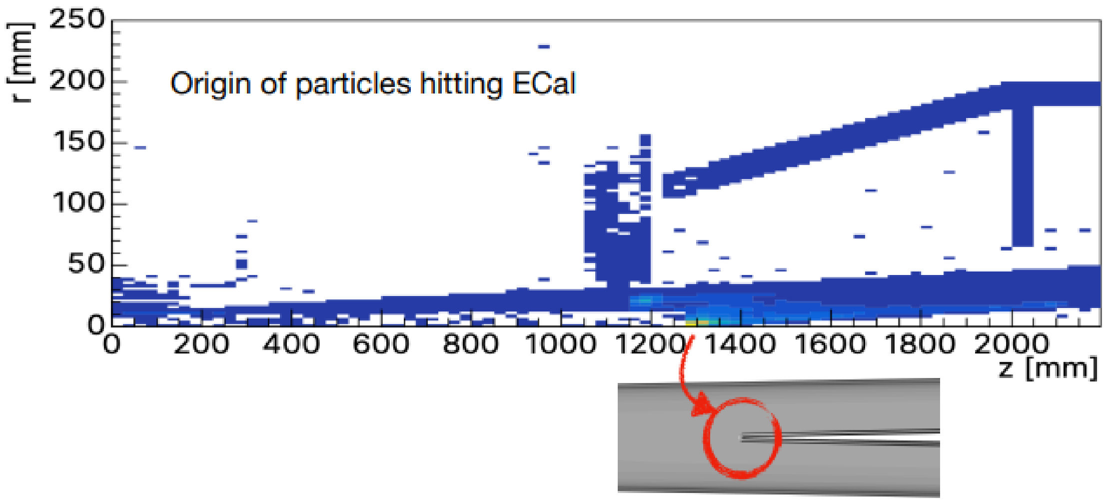

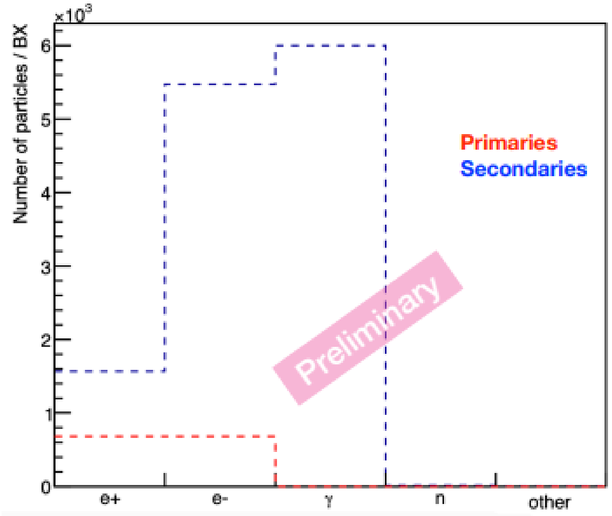

Radiative Bhabha Impact on IR Accelerator Quadrupoles

Simulated a realistic FFQ geometry

- water-cooled beam pipe in SS
- magnets modelled as layers of Al and coils (NbTi+Al+Cu mixture)

Estimates based on BBBrem+GuineaPig

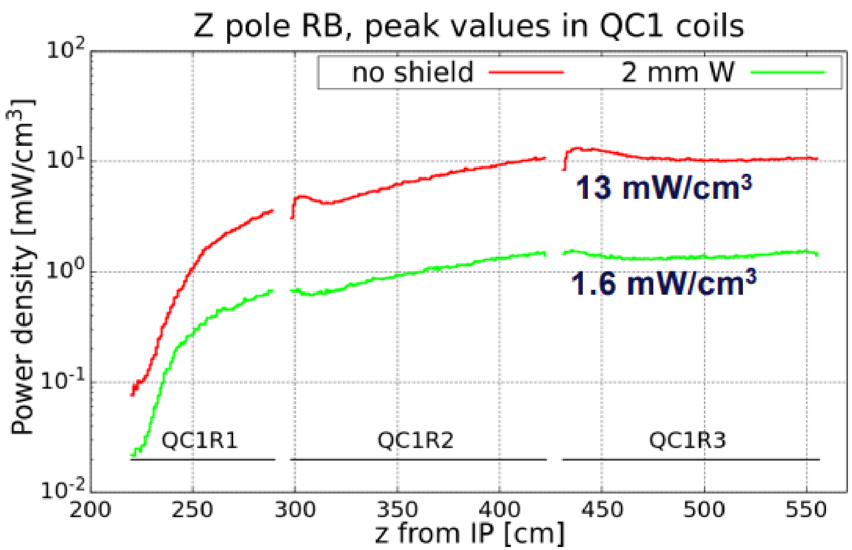

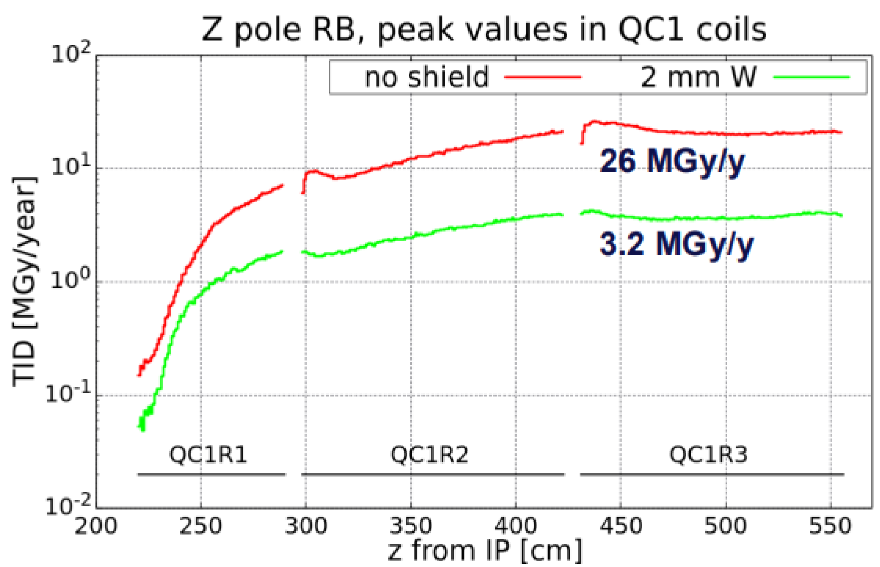

Courtesy of Alessandro Frasca

(May not be up to date)

Thank you for your participation!

Many FCCee topics to study!

FIN

Questions?